

Integration of Multijunction Absorbers and Catalysts for Efficient Solar-Driven Artificial Leaf Structures: A Physical and Materials Science Perspective

Thomas Hannappel,* Sahar Shekarabi, Wolfram Jaegermann, Erich Runge, Jan Philipp Hofmann, Roel van de Krol,* Matthias M. May, Agnieszka Paszuk, Franziska Hess, Arno Bergmann, Andreas Bund, Christian Cierpka, Christian Dreßler, Fabio Dionigi, Dennis Friedrich, Marco Favaro, Stefan Krischok, Mario Kurniawan, Kathy Lüdge, Yong Lei, Beatriz Roldán Cuenya, Peter Schaaf, Rüdiger Schmidt-Grund, Wolf Gero Schmidt, Peter Strasser, Eva Unger, Manuel F. Vasquez Montoya, Dong Wang, and Hongbin Zhang

Artificial leaves could be the breakthrough technology to overcome the limitations of storage and mobility through the synthesis of chemical fuels from sunlight, which will be an essential component of a sustainable future energy system. However, the realization of efficient solar-driven artificial leaf structures requires integrated specialized materials such as semiconductor absorbers, catalysts, interfacial passivation, and contact layers. To date, no competitive system has emerged due to a lack of scientific understanding, knowledge-based design rules, and scalable engineering strategies. Herein, competitive artificial leaf devices for water splitting, focusing on multiabsorber structures to achieve solar-to-hydrogen conversion efficiencies exceeding 15%, are discussed. A key challenge is integrating photovoltaic and electrochemical functionalities in a single device. Additionally, optimal electrocatalysts for intermittent operation at photocurrent densities of 10–20 mA cm⁻² must be immobilized on the absorbers with specifically designed interfacial passivation and contact layers, so-called buried junctions. This minimizes voltage and current losses and prevents corrosive side reactions. Key challenges include understanding elementary steps, identifying suitable materials, and developing synthesis and processing techniques for all integrated components. This is crucial for efficient, robust, and scalable devices. Herein, corresponding research efforts to produce green hydrogen with unassisted solar-driven (photo-)electrochemical devices are discussed and reported.


1. Introduction: Artificial Leaf Approaches Utilizing Efficient Semiconductor Configurations as Light Absorbers

Solar energy is one of the few CO₂-free and abundant energy sources that have the potential to replace fossil fuels in the near future. However, due to the intermittent nature of solar irradiation, efficient technology is required to stabilize the energy supply. One intriguing option is to store solar energy in the form of chemical bonds by “artificial photosynthesis,” that is, the direct conversion of sunlight into chemical fuels.^[1–4] The simplest chemical fuel with the highest gravimetric energy density is molecular hydrogen. The applications of H₂ as an energy carrier are diverse because it can be either directly combusted or converted into electric power by a fuel cell. Furthermore, a wide variety of gaseous and liquid fuels with a higher volumetric energy density, such as methane, methanol, or even diesel and gasoline, can be synthesized from H₂ and CO₂ by standard chemical pathways. Hydrogen therefore

T. Hannappel, S. Shekarabi, A. Paszuk
Institute of Physics
Fundamentals of Energy Materials
Technische Universität Ilmenau
Gustav-Kirchhoff-Straße 5, 98693 Ilmenau, Germany
E-mail: thomas.hannappel@tu-ilmenau.de

W. Jaegermann, J. P. Hofmann
Surface Science Laboratory
Department of Materials and Earth Sciences
Technische Universität Darmstadt
Otto-Berndt-Straße 3, 64287 Darmstadt, Germany

E. Runge
Institute of Physics
Theoretical Physics I
Institute of Micro and Nanotechnologies MacroNano
Technische Universität Ilmenau
Weimarer Straße 25, 98693 Ilmenau, Germany

 The ORCID identification number(s) for the author(s) of this article can be found under <https://doi.org/10.1002/solr.202301047>.

DOI: 10.1002/solr.202301047

serves as a base ingredient for any chemical fuel, as depicted in **Figure 1**. However, more than 96% of all hydrogen^[5] used today is produced with fossil fuels. Our vision of solar-driven hydrogen production, possibly combined with CO₂ capture

R. van de Krol, D. Friedrich, M. Favaro
Institute for Solar Fuels
Helmholtz-Zentrum Berlin für Materialien und Energie GmbH (HZB)
Hahn-Meitner-Platz 1, 14109 Berlin, Germany
E-mail: roel.vandekrol@helmholtz-berlin.de

M. M. May
Institute of Physical and Theoretical Chemistry
University of Tübingen
Auf der Morgenstelle 15, 72076 Tübingen, Germany

F. Hess
Institute of Chemistry
Technische Universität Berlin
Strasse des 17. Juni 124, 10623 Berlin, Germany

A. Bergmann, B. Roldán Cuenya
Department of Interface Science
Fritz-Haber-Institute of the Max-Planck-Society
14195 Berlin, Germany

A. Bund, M. Kurniawan
Electrochemistry and Electroplating Group
Technische Universität Ilmenau
Gustav-Kirchhoff-Straße 6, 98693 Ilmenau, Germany

C. Cierpka
Institute of Thermodynamics and Fluid Mechanics
Technische Universität Ilmenau
Am Helmholtzring 1, 98693 Ilmenau, Germany

C. Dreßler
Institute of Physics
Theoretical Solid State Physics
Technische Universität Ilmenau
Weimarer Straße 32, 98693 Ilmenau, Germany

F. Dionigi, P. Strasser
The Electrochemical Energy Catalysis
Materials Science Laboratory
Department of Chemistry Chemical Engineering Division
Technische Universität Berlin
10623 Berlin, Germany

S. Krischok, R. Schmidt-Grund
Institute of Physics
Technical Physics I
Institute of Micro and Nanotechnologies MacroNano
Technische Universität Ilmenau
Weimarer Straße 32, 98693 Ilmenau, Germany

K. Lüdge
Institute of Physics
Theoretical Physics II
Technische Universität Ilmenau
Weimarer Straße 25, 98693 Ilmenau, Germany

Y. Lei
Institute of Physics
Applied Nanophysics
Technische Universität Ilmenau
Unterpörlitzer Straße 38, 98693 Ilmenau, Germany

P. Schaaf, D. Wang
Institute of Materials Science and Engineering
Materials for Electrical Engineering and Electronics
Institute of Micro and Nanotechnologies MacroNano
Technische Universität Ilmenau
Gustav-Kirchhoff-Straße 5, 98693 Ilmenau, Germany

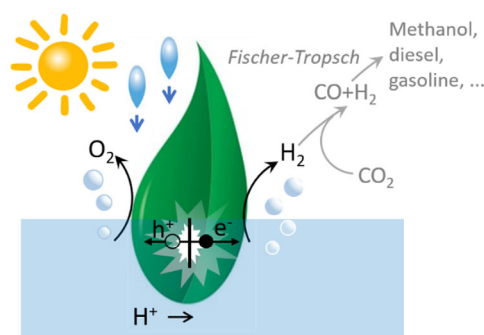


Figure 1. Direct solar-driven water splitting is the least complicated yet nontrivial (photo-) electrochemical reaction that provides a basis for all “solar fuel” technologies.

and conversion, would enable a gradual transition toward a sustainable and renewable energy economy.

The concept we will review is the production of “green” hydrogen using direct-unassisted photoelectrochemical (PEC) conversion of water into hydrogen and oxygen with functionalized and catalyst-modified semiconductor device structures. This is an attractive, feasible, and adaptable approach without CO₂ emissions during operation and use.^[6–10] Compared to wire-connected photovoltaic (PV)-powered electrolysis, this integrated approach offers several advantages. First, for planar monolithically integrated device structures without using light concentrator arrangements, typical current densities are 20–100 times lower than for PV- or wind-powered electrolysis. This significantly reduces the demand on the catalyst, allowing the use of Earth-abundant catalyst materials, and offers an advantage over polymer electrolyte membrane (PEM) electrolyzers, which so far depend entirely on expensive Pt- and Ir-based catalysts for hydrogen and oxygen evolution, respectively. Clearly, there is a trade-off to be made between operating at high current densities versus being able to use abundant materials. Second, the direct approach makes efficient use of solar heat, normally a “waste product,” to further enhance the electrochemical (EC) reaction kinetics.^[11,12] Moreover, the efficiency of a semiconducting light absorber decreases with increasing temperature; direct contact of the absorber with the liquid phase facilitates heat transfer, cooling down the semiconductor and increasing its performance.^[13,14] In addition, the integration of light absorption and electrolysis into a single device may significantly reduce

W. G. Schmidt
Department of Physics
Theoretical Materials Physics
University of Paderborn
33095 Paderborn, Germany

E. Unger, M. F. Vasquez Montoya
Department Solution Processing of Hybrid Materials & Devices
Helmholtz-Zentrum Berlin für Materialien und Energie GmbH
Hahn-Meitner-Platz 1, 14109 Berlin, Germany

H. Zhang
Institute of Materials Science
Technische Universität Darmstadt
Otto-Berndt-Straße 3, 64287 Darmstadt, Germany

the total system costs (although this may be offset by the need to collect gas-phase products over larger areas).

One of the main challenges in designing efficient PEC cells is generating a voltage large enough to drive the EC reactions. Under standard conditions, the thermodynamic voltage required for water splitting is 1.23 V. An additional overpotential of 0.4–0.6 V is needed for sufficiently fast EC reactions, even when facilitated by appropriate catalysts for the hydrogen and oxygen evolution reactions (HER and OER, respectively). Thus, a total photovoltage of at least ≈ 1.6 V is needed under operating conditions, that is, at photocurrent densities exceeding 10 mA cm^{-2} . This means that the open-circuit voltage (photovoltage without current flow) needs to be at least 1.8 V. While there are semiconductors that can deliver such high photovoltages, very few of them are stable in water. Well-known exceptions are SrTiO₃ and KTaO₃, both widegap (>3 eV) materials that absorb only the small UV part of the solar spectrum.^[15] In fact, after more than 45 years of intense international research efforts, not a single material has been found that can provide the required photovoltage, is stable in water, and absorbs an appreciable amount of visible light.^[9,16]

A solution for this scientific dilemma is the development and application of PV structures that exceed the Shockley–Queisser limit of single-absorber material, using so-called third-generation concepts.^[17,18] The most advanced devices are based on multi-absorber structures, in which each subcell absorbs light of a different spectral range of the incident sunlight, and the total photovoltage is the sum of the individual photovoltages generated within each subcell (compare **Figure 2**). These so-called “tandem” devices make optimal use of the solar spectrum and can, theoretically, deliver energy conversion efficiencies well above 25% for solar water splitting.^[6,19–21] The need for multi-layer absorbers in PEC water splitting devices has first been discussed in the early work of Nozik and Bockris.^[22,23] In 1998, Khaselev and Turner demonstrated the first monolithic multi-junction PEC device with a solar-to-hydrogen (STH) efficiency exceeding 10% in their seminal paper in Science.^[24] Their device was based on a surface-modified GaInP photocathode that was connected via a tunnel junction to a GaAs solar cell to provide sufficient photovoltage for water splitting. With a reported STH conversion efficiency of 12.4%, it was considered the (unofficial) efficiency benchmark in the field for more than 15 years.

This scientific benchmark by Khaselev and Turner also illustrated two of the main technological challenges for the development of high-efficiency PEC devices: long-term stability and competitive costs. The cells showed severe photocorrosion within the first hours of operation, which was exacerbated by the highly concentrated and UV-rich illumination that was used. Poor stability would be an issue for any PEC device but is especially detrimental for epitaxially grown III–V semiconductors due to the high materials and processing costs. In the following years, further work was presented on silicon-based multijunction thin-film absorbers and on III–V-based multijunction cells.^[25–27] A breakthrough in public awareness of this approach was achieved in 2011 with the use of a cobalt phosphate layer on a silicon-based triple-junction solar cell that served simultaneously as a protection layer and as an efficient OER catalyst at near-neutral pH conditions.^[28] This “artificial leaf,” reported by Nocera et al. achieved an STH efficiency of $\approx 5\%$.^[28] Further efforts using modified and

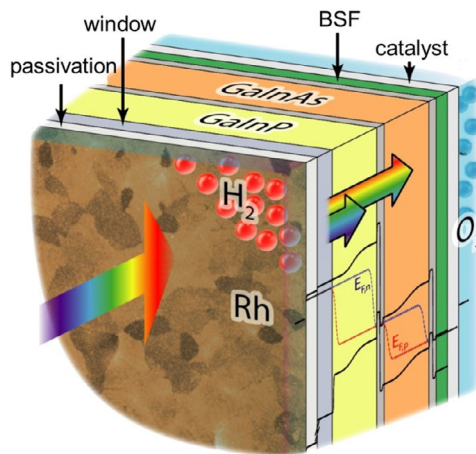


Figure 2. Schematic diagram of a dual-junction tandem photoelectrode for unassisted water splitting based on III–V absorbers modified with interfacial films and electrocatalysts. Essential functional layers are labeled: 1) the subcells of the tandem absorber, GaInP, and GaInAs, see Section 6.1, 2) two of the selective contacts for electrons and holes, so-called window layer and BSF,^[447] respectively, see Section 5.3, 3) the passivation layer for chemical and electronic passivation, see Section 4.2, and 4) the catalyst layer, see Section 4.3. Reproduced with permission.^[30] Copyright 2018, American Chemical Society.

improved contact, passivation and protection layers, in particular also by the groups of Jaegermann and Hannappel, resulted in thin-film silicon-based and epitaxial III–V-based tandem devices with STH efficiencies up to 10%^[29] and 19%,^[30,31] respectively. An alternative approach is to use a metal oxide as a top absorber in a tandem device. Metal oxides show superior chemical stability compared to other materials classes and offer a wide variety in key materials parameters, such as bandgap and band positions. Many oxides show bandgaps in the range of 1.6–2.1 eV, which spans the range of optimal values for a top absorber in a tandem device.^[6] The main challenge for oxides is their relatively poor semiconducting properties. One of the best-performing oxides is p-type cuprous oxide, Cu₂O, for which photocurrents up to 10 mA cm^{-2} (at 0 V vs reversible hydrogen) have been reported. The surface of bare Cu₂O photocathodes is reduced to metallic Cu under hydrogen evolution conditions, but TiO₂ protection layers have been successfully used to achieve >100 h stability.^[32] Also, BiVO₄ photoanodes have shown stable performance of up to 1000 h^[33,34] and were used in several tandem-based water splitting devices with reported STH efficiencies up to 8.1%.^[35–38] There may be new compounds with beneficial properties among the unexplored oxides or chalcogenides that will emerge in the future.

In this review, we do not aim to provide a comprehensive and exhaustive citation of all the work which has been published in recent times on different artificial leaf approaches. We will focus on our concept and discuss buried junction multiabsorber cells as they promise to lead to competitive artificial leaf approaches in their conversion efficiency, but also in their perspectives to technologically applicable devices. For these reasons, we will specifically address the research needs and efforts that need to be considered for such an approach. At first we will shortly

introduce promising semiconductor devices (Section 2), before presenting the key challenges in a schematic table comparing traditional approaches with the innovations needed for more efficient devices (Section 3). We used this table as a guide in structuring our review: In Section 4 and its subsections, we will present a general introduction into the most relevant research fields. Afterward, in Section 5, selected key challenges, which the authors have contributed to in their previous work and are familiar with, will be presented in great detail to provide new insights. Some specific case studies following the buried junction multiabsorber approach will be given in Section 6, before we will end with some thoughts about additional but not yet thoroughly studied long-term approaches in Section 7. Finally, we will end with our major conclusion (Section 8) on the future expectations and perspectives of research on “artificial leaves”.

2. Promising Semiconductor Device Configurations

Because of the long-term and still increasing scientific, technological, and societal interest in artificial leaf devices, which address the direct conversion of solar light into high-energy chemicals to be used as fuels, an extremely large number of papers and reviews have been published on this topic. We cannot summarize them here even if we limit ourselves to PEC systems for water splitting. Therefore, we will preferentially cite only those contributions relevant for systems based on buried junction multiabsorber cells and will not discuss the more classical approaches based on wide-bandgap single-junction systems.

Many different semiconductor-based PEC configurations and final technological implementations have been summarized in literature.^[39–41] We will concentrate here on the central conversion steps (light to H₂) of the PEC devices which covers 1) the PV action of light absorption, electron hole pair generation, and charge carrier separation; 2) the charge carrier transfer at external interfaces to contact/catalyst layers; and finally 3) the EC water splitting reactions, that is, the oxygen and HER. Two main configurations (see **Figure 3**) with different strengths and weaknesses will be considered: In one setup (right panel), two series-connected absorbers are connected via a wire to a counter electrode, with the HER occurring at the functionalized surface of the bottom absorber and the OER occurring at the counter electrode. This configuration is often used for fundamental studies but may be integrated into mechanically integrated systems in the future (the shown arrangements use already tandem cells as PV components). In the other setup (left panel), the cathode and the anode are active surfaces of the same monolithic structure. An important aspect of both designs shown in **Figure 3** is extensive engineering of the interface of the light absorber, which features a contact layer (resulting in the formation of a buried junction) and the functionalization of the buried junction with passivation layer(s) and cocatalysts.

A much simpler junction can be made in the form of a semiconductor–electrolyte contact, as shown in the left panel of **Figure 4**. For such a junction, the idealized Schottky-type behavior is usually assumed, and the contact potential difference, that is, the difference between the Fermi level of the semiconductor and the EC potential of the electrolyte (which is often

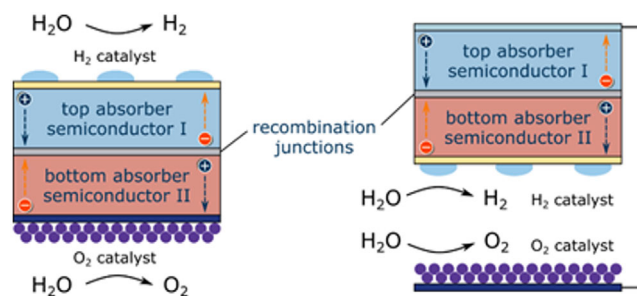


Figure 3. Schematic representation of two possible configurations of PEC tandem cells for water splitting. The left configuration most closely resembles a true “artificial leaf” and ensures easy separation of the reaction products, while the right configuration (wired configuration) is less likely to be limited by mass transport in the electrolyte and light scattering by the evolving gas bubbles. Both configurations are illuminated from the top; other device configurations do exist and may also be considered depending on the choice and arrangement of the absorbers. Reproduced and modified with permission.^[363] Copyright 2024, Elsevier.

determined by the presence of a redox couple), results in electronic charge displacement between the bulk and the surface of the semiconductor. This leads to the formation of an internal electric field and, therefore, a built-in voltage (for details see, e.g., refs. [42–44]). For nonequilibrium conditions induced by applied potentials or illumination, the literature often considers only changes in the relative positions of the Fermi level within the semiconductor to the changing redox couple, for example, the corresponding band bending. The change in band bending under illumination is then considered to be equivalent to the operative photovoltage. In fact, the splitting of the Fermi level can exceed the pre-existing built-in voltage in the dark, that is, the band bending in the dark, significantly, and the photovoltage generated in the semiconductor by illumination is thus not limited by band bending or the built-in voltage in the absorber.^[45] For junctions with additional passivation and metallic cocatalyst layers, similar conditions hold assuming idealized conditions. How such idealized semiconductor electrodes behave in their EC performance for nonequilibrium conditions has recently been discussed, for example, by Peter.^[46] It should, however, be noted that such idealized conditions are usually not observed for most semiconductor electrodes either forming direct contacts to the electrolyte or also after applying additional passivation/contact/electrolyte layers. These changes are due to additional electronic defect states formed at and across the phase boundary. These will be involved in charge transfer and often lead to charge carrier trapping during contact formation and under nonequilibrium conditions.^[44,47,48] These additional electron states (surface and interface states) are responsible for many of the deviations from the expected idealized behavior observed for most semiconductor (photo)electrodes. As we will discuss in more detail, a detailed understanding of such defect states, their passivation, and charge transfer dynamics is a key to design efficient devices. This is true for solid-state PV devices as well as for PEC devices. We already emphasized that PEC devices and their performance are more complex to understand and optimize than PV systems, because their defect electronic states at the surfaces and

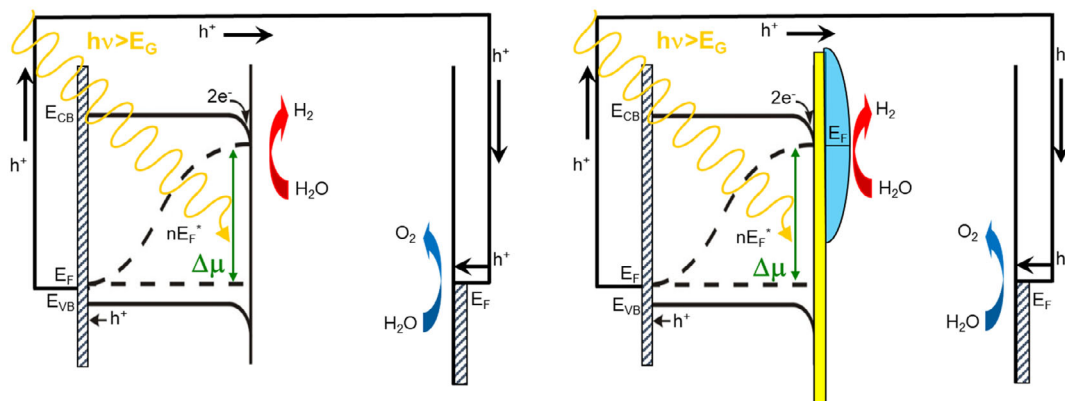


Figure 4. Idealized PEC semiconductor cathodes (single-absorber layer) for H₂O splitting under illumination (left: intimate semiconductor/electrolyte contact, right: semiconductor/passivation layer/metallc cocatalyst/electrolyte contact). The photovoltage given by the difference of EC potential ($\Delta\mu$) of the electron–hole pairs under illumination must be large enough to overcome the redox potentials including overpotential contributions of HER and OER. Adapted and modified with permission.^[48] Copyright 2016, Springer.

interfaces are usually modified during their application in contact with the electrolyte. The complexity increases significantly due to the catalyst adaption and the catalytic reactions, where many of the passivation/cocatalyst material structures are also semiconducting in nature, such as most oxides.

It should be noted already at this stage that defect states will lead to losses of both photovoltage and photocurrent and that the positions of the band edges in operation depend on surface orientation (different for different crystallographic faces), surface reconstruction, adsorbates, and charged defect states. Finally, the EC double layers also affect the contact potential distributions and modify the surface/interface dipoles already in the dark but may additionally vary during operation under nonequilibrium conditions. These modifications will shift the electron affinity and thus the band-edge positions of the semiconducting absorber layers. Also, the space–charge layers (band bending) will be affected. Furthermore, such effects may also modify the relative energetic positions of the passivation and contact layers as well of the cocatalysts. A more detailed discussion of such effects in PEC devices can be found in literature.^[44,48] However, such deviations strongly influence solid-state devices, such as alternations from idealized behavior observed in metal semiconductor Schottky junctions or semiconductor heterojunctions due to interfacial defects.^[49,50] High-performance devices will only be obtained when proper engineering strategies have been developed to fully control the nature and concentration of these defect states. This has motivated us to follow buried junction approaches in our own research as will be discussed in more detail (in particular in Section 6) and to focus on these in this review.

3. Key Challenges on the Way to Efficient Water Splitting: State-of-the-Art and Beyond

Any efficient water-splitting device using PEC approaches, which can compete in efficiency with nonintegrated PV-powered electrolyzers, must use a PV component with a conversion efficiency

similar to efficient solar cells and an electrolyzer component with low overvoltages. In addition, the coupling of the two systems must avoid additional losses due to unfavorable transfer of the EC potential of the electron–hole pairs (photovoltage) and of the photocurrent from the PV component to the cocatalysts. To achieve these goals, a number of materials and device-related challenges must be addressed and overcome: 1) designing and developing optimized absorbers, especially to be used for multi-junction absorber stacks; 2) passivating and protecting them with thin electronic and chemical passivation layers using preferentially solid surface layers; 3) functionalizing these intimate contact layers with suitable HER and OER catalysts; 4) investigating and optimizing the spatial structures of the used materials and their combination; and 5) integrating all these components into highly efficient and stable devices.

These challenges are schematically illustrated in the tandem device structure presented in **Figure 5**, which we consider representing the most promising prospective configuration for an efficient PEC device. The presented arrangement is a general scheme of an optimal tandem device structure for water splitting with all the essential and critical functional layers, problems, and challenges. Each part and issue is a matter of research and development, thorough analysis, and optimization. It is inspired by the record PEC devices applying III–V multiabsorber cells.^[31,32]

As first condition to achieve high conversion efficiencies, semiconducting absorber materials must be identified, which have already proven solar cell conversion efficiencies close to their expected theoretical maximum. Proven competitive solar cell performances have been reached so far only with a rather small number of semiconductor absorber materials including Si, III–V semiconductors, halide perovskites (HaP), and a few chalcogenides. Their properties as well as their advantages and disadvantages for PEC applications will be discussed in the next section and in Section 6 in more detail.

An inherent and major challenge for PEC devices with a semiconductor/liquid junction is the large loss of photovoltage that is typically observed at semiconductor/liquid junctions. This reduces the efficiency of the device and is one of the main factors

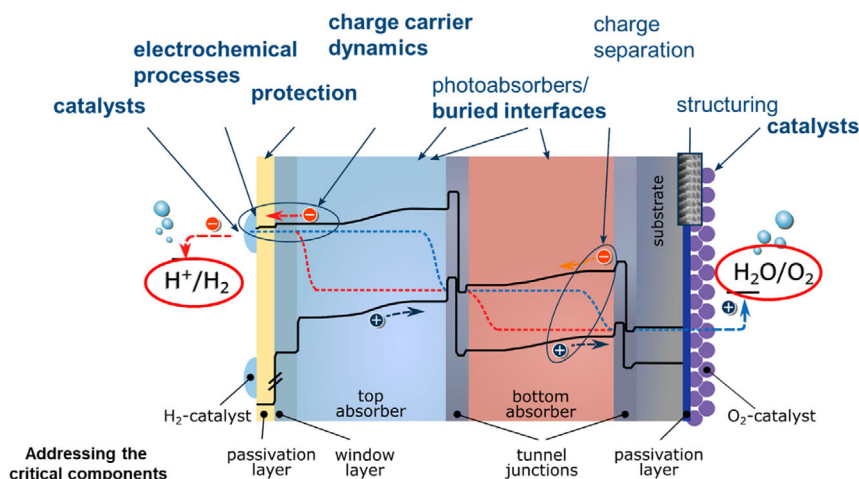


Figure 5. Scheme of an artificial leaf in a tandem PEC device structure; the needed research challenges of absorbers/catalyst device integration (top row) address crucial components and/or courses of action in the device structure, which must be investigated, understood, and optimized in order to develop an efficient and stable direct solar-driven water photoelectrolysis device. The operational photovoltage must be available at the terminal contacts. The figure does not necessarily reflect the architecture of the device structure, which can be very different such as Figure 3, right panel. Reproduced with permission.^[448] Copyright 2023, Elsevier.

that currently limit the overall efficiency. Photovoltage losses are generally attributed to the presence and formation of defect states in the bulk of the absorber, such as lattice defects, or polaron states in oxides,^[47] or to the presence of surface and interfacial bandgap states that are formed at critical interfaces either upon immersion in water or under the conditions at which the OER/HER reactions take place.^[42,51] These defects lead to interfacial recombination losses affecting the relevant key performance indicators of any PV or PEC devices, such as photovoltage, photocurrent, fill factor (FF), and therefore, must be neutralized. Various passivation strategies have been explored, ranging from additives in the electrolyte to the deposition of thin passivation layers. These efforts have thus far achieved only limited success, which is partly due to a lack of detailed understanding of the structure and electronic properties of solid–liquid interfaces. A more successful approach can therefore be expected in the fabrication of suitable heterocontacts (buried junctions).^[48] Charge separation in such systems takes place at interfaces between the semiconductor materials and the solid contact layer, and no longer at the solid–liquid interface, hence named “buried” junction. Benefitting from many decades of research in solid-state PV, there is now a limited number of semiconductors from which substantial photovoltages can be extracted using solid-state contacts.^[52] However, such junctions have not been proven in metal oxide semiconductors (MOS), which are appealing because of their chemical stability.

Furthermore, the practical viability of any water-splitting technology ultimately depends on two main factors: the leveled cost of hydrogen production (LCOH) and the net primary energy balance over the entire life cycle of the system.^[53] Both aspects have been studied in depth, and the overall conclusion of these studies is that the STH efficiency is the most important factor that determines both the LCOH and the net primary energy balance. Several studies have estimated and compared the maximum STH efficiencies that can be achieved with optimized

single-absorber systems and tandem systems.^[53–55] With a target operational photovoltage of 1.8 V, the minimum needed to drive the HER and OER at sufficient rates, maximum efficiencies well over 25% seem possible.^[10] Such efficiencies will only be reached with tandem junctions. Today, many demonstrations of bias-free solar-driven hydrogen production consist of solar cells that are electrically coupled to electrolyzers with external wires. In such systems, the necessary photovoltage is generated either by a (conceptually straight forward) series connection of several PV cells or by use of an electronic DC–DC converter. Here and in the following sections, we consider this a “nonintegrated” approach, where the active surfaces of absorber and electrolyte contact are not the same. While the nonintegrated approach may be viable, it has several disadvantages. One is the high balance of systems (BOS) costs that are associated with the packaging, sealing, and wiring of three separate devices (PV cell, electrolyzer, DC–DC converter). The second disadvantage is the high current densities at which commercial electrolyzers operate. While their compact design offers the possibility to produce hydrogen at elevated pressures, the use of noble metals, such as platinum and iridium, cannot be avoided in current PEM electrolyzer technology. One could argue that alkaline electrolyzers can work at high current densities and do not require noble metals, but they are fundamentally incompatible with solar energy since they photocorrode under intermittent operation.^[56–58] The third disadvantage is the unavoidable solar heating of the PV cell, which can lead to operating temperatures of 60–80 °C and efficiency losses upward of 10%.^[59]

The PEC (“integrated”) approach offers opportunities to avoid these disadvantages. First and foremost, the 50–100 times lower current densities in PEC devices ($\approx 20 \text{ mA cm}^{-2}$) compared to electrolyzers strongly reduce the demand on the HER and OER catalysts and will enable the use of nonprecious materials such as Fe and Ni. Having an integrated device may also reduce the BOS costs (although the need to collect product gases

over larger areas may present new challenges). Finally, the unavoidable solar heating of the device has now turned into an advantage since the solar heat is automatically transported away from the absorber toward the solid–liquid interface where it enhances the kinetics of the EC reactions.^[12] Thus, the integrated approach is expected to offer advantages over the nonintegrated technologies. Based on the considerations above, an integrated multijunction tandem arrangement must be scrutinized as the feasible optimum solution for an efficient H₂-generating PEC cell and we will therefore discuss such arrangements as the central research direction of this review.^[9,48,60,61]

The challenges outlined above are highly interdisciplinary in nature and require breakthroughs in the development of novel absorber materials, passivation and contact layers, electrocatalysts, device integration, and a deep fundamental understanding of the physics and chemistry of solid–solid and solid–liquid interfaces and of the involved transport processes. Based on recent developments in the field, a focused effort is needed to eliminate the remaining bottlenecks and achieve the main objectives of

complex challenges, which are summarized in **Table 1** as a comparison of the state-of-the-art approaches to the major innovations needed in future research activities.

The routes toward innovation presented in Table 1 will contribute to the development of competitive PEC devices. Although PEC generation of hydrogen has already been demonstrated successfully on a lab scale, the large-scale production poses significant extra challenges and is not yet economically competitive with the production of hydrogen from fossil fuels. While many of the challenges are technical in nature and require clever engineering solutions, there are also a number of fundamental challenges that need to be addressed. Examples are lacking insights into the elementary charge transfer and EC reaction steps, incomplete understanding of the origin of efficiency losses, poor control over the interfacial reactivity, and stability of solid–solid and solid–liquid interfaces. These are exactly the challenges where major breakthroughs are needed for practical application of (P)EC water splitting systems, as summarized in Table 1. In addition, the research efforts on these topics will also

Table 1. Comparison between the state-of-the-art and major innovations to be envisaged as essential research targets, as will be explained in more detail in chapter 4.

Aspect	State of the art	Innovations needed
Photoabsorbers, see Section 4.1	<ul style="list-style-type: none"> • Single-junction photoelectrodes that deliver insufficient photovoltage and/or photocurrent • Huge losses due to suboptimal use of the solar spectrum • Only few multijunction devices with high STH efficiencies (Ge/III–Vs), costly and rarely studied • Few materials with photovoltages close to theoretical maximum 	<ul style="list-style-type: none"> • Multiabsorber structures that enable operational photovoltages and sufficient photocurrents for unassisted PEC water splitting with efficiencies >15% • Overcoming present efficiency limitations based on improved understanding of the fundamental effects involved • Significantly enhanced photovoltages for several materials classes
Interface energetics, see Section 4.2	<ul style="list-style-type: none"> • Semiconductor/electrolyte and semiconductor/catalyst junctions suffering from Fermi-level pinning, interfacial recombination, insufficient charge carrier separation • No general interface engineering concepts for PEC available 	<ul style="list-style-type: none"> • Novel buried junction concepts that enable breakthroughs in efficiency • Advanced knowledge-based design of semiconductor/passivation/catalyst layers • Separation of functionalities in terms of bandgap engineering
Electrocatalysts, see Section 4.3	<ul style="list-style-type: none"> • Dominant use of noble metal containing electrocatalysts • No specific alignment of electronic states for efficient multielectron charge transfer • Device lifetime limited by detachment of catalysts 	<ul style="list-style-type: none"> • Electronically matching electrocatalysts with robust deposition • Resource-optimized electrocatalysts operating at typical PEC currents
Charge transfer at PEC interfaces, see Section 4.4	<ul style="list-style-type: none"> • Marcus–Gerischer model of electrochemical interfacial charge transfer • Charge transfer processes and involved electronic states across the multilayer semiconductor/electrolyte junction not well understood • Surface states only characterized by their energy level 	<ul style="list-style-type: none"> • Chemical and electronic specificity aids the understanding of charge transfer processes • Control of charge carrier separation and charge transfer across adjusted interface junctions • Surface states identified by their chemical nature
EC transport issues, see Section 4.5	<ul style="list-style-type: none"> • Diffusion limitation in the concentration boundary layer • Bubble adherence blocks active electrode surface • Limited electrode surface area 	<ul style="list-style-type: none"> • Active flow control for enhanced mass transport and fast bubble removal • Superaerophobic electrodes for passive fast bubble removal <ul style="list-style-type: none"> • Increased surface area by nanostructuring • Multiscale models for combined description of gas bubble dynamics and ion diffusion in nanostructured interface
Novel experimental techniques, see Section 4.6	<ul style="list-style-type: none"> • Analytical techniques mostly based on preuse, post operando approaches <ul style="list-style-type: none"> • Characterization mostly based on EC studies • Need for chemical and molecular information about identity and kinetics of intermediate species involved in HER and OER • Understanding and design of transport processes of the chemical reactants and products 	<ul style="list-style-type: none"> • Cutting-edge in situ and operando experiments with structural, chemical, and electronic sensitivity including synchrotron studies • TR experiments and theoretical studies on all relevant timescales • Establishing link between electronic structure and chemical speciation at solid–liquid interface <ul style="list-style-type: none"> • Analysis of the two-phase fluid flow at the electrodes and characterization of the mass transport at the gas–fluid interface and near the electrode

provide a deeper understanding of the interrelation between key material properties, novel strategies to synthesize semiconductors with the desired properties, and concepts for the integration of the promising components into highly efficient devices.

Gaining fundamental knowledge will also lead to benefits in various related, topical research fields such as tandem PV cells, water electrolysis, solar cell architectures, semiconductor development, and fuel cells, particularly in understanding and tailoring the materials and interfaces of functional devices that need to be modified, for example, with protection layers, contact layers, and/or electrocatalysts, as depicted in Figure 5.

4. Relevant Research Fields and Essential Innovations Needed

In the following of this section, we will delve into four key research areas that are relevant to the development of PEC devices. Within each field, we will identify critical research needs and propose innovative approaches.

4.1. Advanced Photoabsorbers and Photovoltaic Structures

The choice of appropriate absorber materials is a key issue for the realization of efficient water splitting PEC devices. In general, the performance of the PV component of the used device structure is also the key for the STH efficiency (as it may be deduced by the possibly solar-to-electric (STE) power conversion efficiency, which may be tested with reversible redox couples). In general, the STH efficiency will be even smaller due to additional losses in the coupling of the PV to electrolyzer component and the EC overvoltage and transport losses. Selecting appropriate absorbers becomes even more challenging when semiconductors are required to be suitable for usage in tandem junctions due to, for example, necessary matching or adaptation of lattice constants. The material's criticality aspects must be considered as additional boundary condition when large-scale applications will be within reach (addressed in Section 7.2). There is long-lasting discussion on the most promising strategy in semiconductor selection, reflecting a divergence of opinions among researchers: Some emphasize material stability in the electrolyte as the most relevant criterion, while others, like us, initially prioritize the potential attainable PV conversion efficiencies. This preference is based on the availability of chemical passivation layers that can improve device stability.

As mentioned above, our approach aiming at excellent absorbers with passivation has been substantiated by achieving STH efficiencies of 10% and 19% with silicon and III–V-based materials, respectively.^[29,30] A summary of actual competitive STH efficiencies is provided in the PEC H₂ conversion efficiency table published by Ager et al.^[60] Due to the inherent drawbacks of current systems, including the limited STE efficiency of thin-film Si and the cost associated with epitaxial III–V tandems, there is a growing need to explore new materials and novel combinations.^[61] A recent exciting development in this field is the use of a novel class of absorbers, the HaP, in PV tandem devices. Currently, extensive research efforts are focused on silicon/perovskite tandem solar cells, resulting in noteworthy progress with reported STH efficiencies of 19.68% and 20.8% using

architectures, where only the silicon interface is exposed to the electrolyte,^[62] or the entire device is encapsulated in a quartz glass/epoxy design.^[63] Impressively, the pace of advancement in this area is exemplified by a recent recordbreaking STE efficiency of 33.9% in solar cell devices.^[64] These results clearly underline the fact that STH efficiencies are closely connected to PV efficiencies in STE. In a first estimate, the expected STH are given by the realized STE efficiencies reduced by the unavoidable losses due to overvoltage of the applied cocatalysts and additional losses due to the involved coupling process and chemical transport.^[42–44,46,65]

The challenge of limited stability in highly efficient absorber materials upon water exposure may be addressed with suitable protection layers. Several wide-bandgap metal oxides, such as TiO₂, SrTiO₃, Ta₂O₅, and NiO, combine reasonable optical transmission and good electronic conductivity with excellent chemical stability. NiO and TiO₂, in particular, have been used as chemically inert window layers for a variety of absorber materials, including silicon,^[66] III–V semiconductors,^[67] and less stable oxides and oxynitrides.^[68] For an extensive overview of thin-film protection layers for semiconducting photoelectrodes, the reader is referred to several reviews.^[69–71]

In conclusion, based on the results presented so far, we expect that thin-film-based multijunction absorber structures, which can be scaled up industrially, provide the most promising solutions for PEC-based artificial leaves. Besides III–V-based compounds, III–V-on-Si tandems, quantum structures, transition metal-based multinary oxides, and chalcogenides should be explored. Additionally, it is worth exploring new perovskite absorbers with optimum bandgaps for integration with Si. As an alternative, more stable novel wide-bandgap chalcogenide absorbers for integration with Si, such as defect-tolerant (alloyed) ZnTe and thio perovskite (e.g., BaZrS₃) absorbers with nonbonding band-edge states,^[72,73] may be considered. In addition, new materials must be screened for, and low-dimensional structures such as nanowire absorbers should be tested, see Section 7.1.

The wide-range tunable direct bandgaps, band offsets, and lattice constants of III–V semiconductor compounds and their superior quality and properties such as minority charge carrier lifetimes, mobilities, and doping capabilities are quite unique among semiconductor materials.^[74] The III-nitrides have been discussed to provide similar advantages as III–V-compounds without nitrogen, in particular bandgaps covering a very wide range. Moreover, most of them are stable at relatively high temperatures and harsh environments.^[75,76] This has been demonstrated by the successful accomplishment of III-nitrides on silicon-based tandem solar cells^[77] and nitride-based solar cells on free-standing GaN.^[78] Already small amounts of nitrogen incorporation enable lattice-matched growth of GaP_{0.98}N_{0.02} on Si(100) with suitable bandgaps for direct photoelectrolysis^[79] and increased stability toward the electrolyte.^[80] However, up to now, the obtained efficiencies have been relatively low, primarily attributed to various challenges and limitations. These include issues such as low minority charge carrier lifetimes and limited diffusion lengths, mainly arising from high and effective defect densities in the GaInN material. Consequently, the III-nitrides are currently not considered as suitable absorber materials, although their good thermal stability has been reported.^[75]

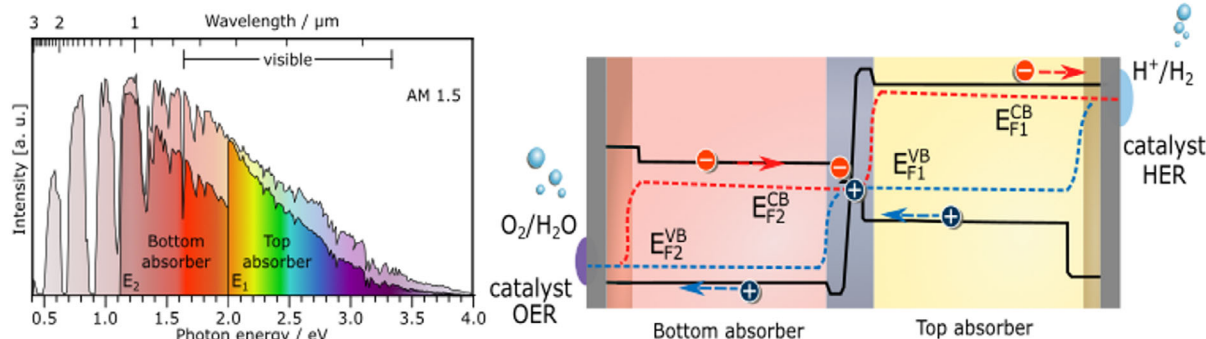


Figure 6. The initial two mandatory steps toward an efficient multijunction device for direct and nonassisted water splitting are (1) maximizing absorption and therefore exploitation of solar radiation and (2) its conversion into the adequate amount of free energy (equivalent to the photovoltage in operation V_{ph}^{op}). (Left panel) In a tandem structure with, for example, two absorbers, the different bandgaps allow each absorber to utilize complementary parts of the solar spectrum. For optimized bandgaps E_1 and E_2 , this results in equal numbers of photons for current matching, ultimately leading to the maximization of photocurrent, as illustrated in the right panel. Since the absorbers are connected in series, the total photovoltage is given by the sum of the EC potentials in each absorber, which in turn are determined by the difference between the quasi-Fermi levels of electrons in the conduction band (CB) and holes in the valence band (VB) in each absorber.

Nevertheless, they still might be useful as selective contacts or passivation layer due to their high stability (see Section 4.2).

For efficient devices, the exploration of suitable tandem absorber structures that optimize the utilization of the entire solar spectrum (see Figure 6 and 7) is essential. For this purpose, the absorbers must provide optoelectronic properties equivalent to good solar cells and supply a sufficient potential difference (photovoltage) needed as the driving force for bias-free water splitting. Thus, only multiabsorber cells are expected to split H_2O efficiently. However, so far, only limited research effort has been directed to identify and develop appropriate cost-effective absorber structures, which are able to generate the required (quasi-)Fermi-level splitting (photovoltages in operation $V_{ph}^{op} > \approx 1.6$ eV near the maximum power point) and prevent nonradiative recombination losses in order to obtain

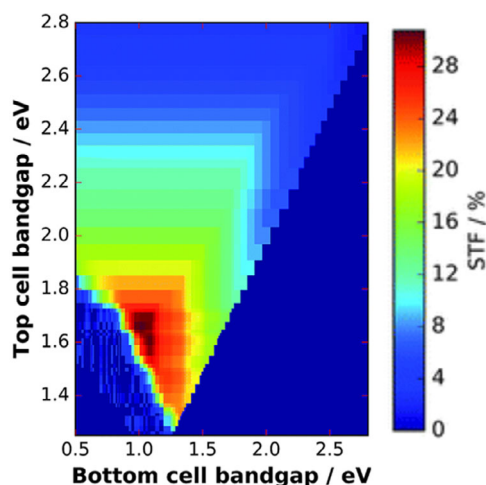


Figure 7. Theoretical STH efficiency limit for a two-junction tandem device at an EC load of $\Delta G = 1.43$ eV as a function of top and bottom cell bandgaps for AM1.5G. Reproduced with permission.^[6] Copyright 2017, Royal Society of Chemistry.

the maximum possible photocurrents. In an efficient absorber material, the diffusion lengths L_D of charge carriers must be large enough in relation to the thickness of the absorber d and the absorption lengths $1/\alpha$ (i.e., $1/\alpha \ll d \ll L_D$), with the absorption coefficient $\alpha(\omega)$. In a tandem, the currents of the different subcells and, thus, the exploitation of the solar spectrum must be matched to each other. A more detailed discussion on tandem configurations to be used in PV and PEC devices can be found in related literature.^[81] It should be noted at this point that a working PV or PEC device at optimized efficiency must be close to flat-band condition, as shown, for example, in Figure 6, and remaining band bending will hardly contribute to charge carrier separation.^[45,82]

Besides efficiency, costs are the critical criterion for economic success. The price depends on production costs and material costs, see Section 7.3. For traditional III-V tandem cells as an example, world-record efficiencies come with a substantial cost factor due to the epitaxial growth process via metal-organic vapor-phase epitaxy (MOVPE) systems. These cells are typically prepared on III-V or Ge(100) wafers, which are challenging to scale up in a cost-effective manner. As alternatives, scientific routes, novel materials, variations in their configuration, for example, using p-i-n structures and simple and less cost-intensive growth processes, should be considered. This is of course also of interest for III-V systems but may be easier to be realized with alternative promising absorber materials such as perovskites, novel thin-film chalcogenides, and oxides.

An alternative to significantly reduce the costs is to use Si(100) as a substrate and the active bottom cell. Such a combination of III-V top absorbers with the Si(100) bottom absorber into a two-junction device enables STH efficiencies close to the optimum of over 25% (compare Figure 7).

Therefore, a lot of work focuses on surface preparation of Si(100) surfaces as well as the involved heterointerface for low-defect GaP/Si(100) epilayers. The main challenge during the growth of the III-V materials on Si(100) is to avoid antiphase domains (APDs) which originate at the substrate. In addition, lattice mismatch between the epitaxially grown layer and the

substrate generally introduces crystalline defects in the bulk. In order to avoid APDs as well as other defects in the III–V layer, a precise preparation of atomically well-ordered substrate surface and the control of the III–V/substrate heterointerface is required. Specifically, double-layer atomic steps at the Si(100) surface are a crucial prerequisite to avoid APDs in the III–V epilayers.^[83]

In such an approach, the required thickness of the III–V absorber could be reduced by applying multiple quantum wells (MQWs)^[84] or vertical III–V semiconductor nanowires.^[85] As another alternative to reduce the costs, complex metal oxides, metal–HaP, and chalcogenides are of interest for the top absorber for thin-film tandem structures in order to reach scalability. Initially, the envisaged materials can also be explored separately, as a separated but connected photoabsorber before they are integrated into different tandem device structures, for example, thin-film tandems, epitaxial layers, 2D quantum, or 3D nanostructures. Of course, the development of novel materials can be accelerated by high-throughput (HTP) density functional theory (DFT) calculations.

From the theoretical point of view, in addition to the physical processes at the interfaces, designing solar absorbers entails both mechanistic understanding and quantitative evaluation of the optical absorption, charge conduction, and carrier dynamics in the bulk materials.^[86] For instance, the first challenge is the accurate evaluation of the bandgaps, where different flavors of DFT-based methods including specific functionals to account for strongly correlated systems (DFT + U), self-energy effects (DFT-GW), or exchange interaction (DFT Heyd–Scuseria–Ernzerhof [HSE]-06) can be applied but should be benchmarked in order to make reasonable predictions.^[87] The optical absorption efficiency can then be evaluated based on the spectroscopic limited maximum efficiency criterion.^[88] However, it is challenging to quantitatively evaluate the charge transport and carrier dynamics properties, which are mostly driven by electron–phonon and electron–defect interactions. For instance, the mobility of electrons and holes is usually estimated by the effective masses, whereas electron–phonon interaction and electron–defect scattering have not been widely evaluated, though reliable methods have been developed.^[89] Moreover, the formation energies and charge transition levels of various possible defects should be systematically evaluated.^[90] Correspondingly, various dynamical processes, such as nonradiative recombination, can significantly limit the number of free charge carriers available to induce electrical current, which limits a solar cell’s power conversion efficiency. Thus, a systematic consideration of the underlying radiative, nonradiative, and Auger processes based on the electronic structure and defect states is indispensable,^[91] in particular a quantitative assessment of the relaxation and recombination processes in the ultrafast regime.^[92]

From the materials point of view, although the industrial processes on engineering Si and III–V semiconductor-based absorbers are pretty mature,^[93] there is still a strong impetus to design tandem solar absorbers which are nontoxic, only contain Earth-abundant elements, and are easily integrable into developed devices for optimal efficiency. For instance, hybrid HaP^[94] as represented by CH₃NH₃PbI₃ exhibit high absorption coefficients and defect tolerance, as well as long carrier diffusion lengths, leading to promising PV efficiency for single-junction^[95] and tandem^[96–98] STH applications.^[99] Nevertheless, such materials

suffer from poor stability and contain toxic Pb. Two strategies to go beyond is either to study Ge- and Sn-based compounds with various organic cations (which, however, usually have even lower stability than lead HaP) or to search for double perovskites A₂BB’X₆ (e.g., inorganic perovskite^[100] like Cs₂AgBiBr₆ with a bandgap around 2 eV^[101]). Nevertheless, there is still no consistent designing principle for further improvement of their efficiency by playing with the A-cations.^[102] Interestingly, the emergent low-dimensional perovskite compounds exhibit improved stability with enhanced quantum confinement effect.^[103] Thus it seems worthwhile to systematically tackle the relationship between the versatile structures^[104] of hybrid HaP and their multifunctional properties in particular as PV absorbers. For such 2D perovskites, it is found that the magnitude of the bandgaps is mostly determined by the thickness of the inorganic layers,^[105] which offers a possibility to tailor their properties for tandem absorber applications. Last but not least, as exemplified by CdTe and CIGS, chalcogenides are known to be good PV/tandem absorbers, as there are many of known compounds with nearly optimal bandgaps.^[106] Therefore, there is a strong impetus to implement an efficient screening methodology and evaluate the performance of the known and possibly unreported stable compounds as tandem absorbers. To date, however, no efficient use of chalcogenides in STH PEC applications has been demonstrated.

To design tandem absorbers with proper bandgaps and associated properties, HTP DFT calculations have been extensively performed.^[107] For instance, there are many predictions of possible candidates of Pb-free inorganic compounds with enhanced stability.^[107] Those predictions already lead to the successful experimental synthesis of Cs₂InAgCl₆ with a wide bandgap.^[108] Nevertheless, there are still several essential challenges to be addressed. First, most of the HTP calculations are done with cations of the *s*⁰/*s*² electronic configurations.^[72,73,109–114] The corresponding optical transitions take place between the *s*–*p* orbitals with weak absorption onset due to the large dispersions of the *s/p* bands. The small effective masses of carriers in such bands can lead to larger mobility, but whether this results in an enhanced overall performance is still an open question.^[115] Materials with *d*-orbitals involved in the optical transitions have also been proposed to be good absorbers, like CuTaS₃^[116] and FeS₂.^[117] Therefore, an interesting question is to systematically characterize such semiconducting materials with partially/fully filled *d*-shells as optically active absorbers as well. Furthermore, the current theoretical predictions either rely on the known compounds or are constrained by limited characterization on the thermodynamic stabilities of the target materials. For instance, the formation energies of multinary chalcogenides with limited structural variations are usually evaluated with respect to a few typical binary compounds,^[110–112] whereas systematic evaluation of the phase diagrams is rare. Thus, the predicted candidates may not be stable and more stable compounds might be overlooked. For the future, it is interesting to go beyond the most common crystal structure prototypes, as demonstrated for ABX₃^[118] and ternary^[119] chalcogenides. Last but not the least, most of the theoretical calculations performed so far focus on characterizing the bulk properties particularly for single-junction solar cells, whereas two absorbers with bandgaps within (0.8 and 1.2) and

(1.5 and 1.9) eV with proper band alignment at the interfaces are needed for promising tandem adsorbers.^[31]

HTP virtual screening can significantly accelerate materials design. However, due to the inherent complexity (i.e., composition, crystal structure, and derived properties) of materials, it is still challenging to perform exhaustive combinatorial calculations on a vast compositional chemical space and structural phase space. In this regard, machine learning can not only be applied to perform statistical forward inference to map out the structure–property relationships^[120] but can also be incorporated with experimental knowledge^[121] to guide materials developments and explorations even at the industrial scale.^[122] Importantly, machine learning often provides a decent solution to implement a robust multiscale simulation platform, for example, machine learning interatomic potential bridging accurate DFT calculations and large-scale atomistic simulations,^[123] which can be used for efficient predictions of crystal structures for hybrid organic–inorganic compounds.^[124]

4.2. Interface Band Structure and Chemical and Electronic Passivation

For enhancing the stability and durability of PEC devices, suitable passivation and protection layers for semiconducting absorbers in artificial leaf devices must be developed. Passivation layers are also required to mitigate the influence of electronic defect states in the bandgap that can act as recombination centers and reduce the photocurrent or “pin” the Fermi level and limit the photovoltage. Strategies are needed that electronically neutralize these states and ensure proper energetic alignment of the photoabsorber with the contact material. For this purpose, strongly chemically interacting adsorbates, ultrathin reaction layers, and/or thin passivation layers can be applied (compare **Figure 8**). Additionally, charge-selective contacts are needed that maximize the quasi-Fermi-level splitting (photovoltage) by controlling the charge transport directions and the prevention of charge carrier losses due to interfacial recombination at the contacts. The passivation layers, which may possibly also work as contact layers, must be adapted for an isoenergetic charge transfer to the cocatalysts.

Surface passivation is specific for any applied semiconductor and must be developed specifically, for example, for III–V semiconductors, HaP absorbers, novel chalcogenide semiconductors, or metal oxide absorbers. To achieve effective passivation and

contact formation, an in-depth understanding of the chemical and electronic structure of the interface between the absorber and passivation/protection/contact/co-catalyst layers is essential. As already mentioned above, the additional layers between the absorber and the catalysts are needed to efficiently fulfill the following functions: 1) to passivate the absorber surface electronically and chemically; 2) to define the energy converting contact; and 3) to transfer the charge carriers. For this purpose, one or more layers may be needed to realize the desired properties. For obtaining the desired properties of the interlayer and contact phases, the exposure and deposition to reactants and surface layers must be optimized, which turns out to be a complex challenge. Therefore, advanced surface science methods must be applied to study the synthesis steps and the obtained properties in detail (see also Section 5.5). For example, the exposure of interfaces to water and oxygen must be investigated in a controlled fashion to study favored adsorption sites using atomic force microscopy (AFM) or scanning tunneling microscopy (STM), whereas structural changes can be deduced from low-energy electron diffraction or reflection anisotropy spectroscopy.^[125–127] The influence on the electronic structure can be studied by X-ray photoelectron spectroscopy (XPS), ultraviolet photoelectron spectroscopy, and inverse photoelectron spectroscopy as well as scanning tunneling spectroscopy.^[128] Additionally, the quasi-Fermi-level splitting in the material can be estimated from photoluminescence (PL) spectroscopy.^[129] Guided by electronic structure calculations (DFT), the formation versus passivation of defect states at the surfaces and interfaces of the absorber materials, the modification of interfacial dipoles, as well as doping of the intermediate layers must be adjusted to optimize the energetic alignment. The structure and dynamics of the water molecules at the interface to the passivation layer can be studied by ab initio molecular dynamics. Candidate materials for the passivation layers are usually specifically adjusted metal oxides (TiO₂,^[130] HfO₂,^[131] Ga₂O₃,^[132] BaSnO₃^[133]) and group III binary, ternary, and doped nitrides,^[134] which can be deposited in a highly controlled, layer-by-layer fashion using atomic layer deposition or molecular beam epitaxy. For example, the interaction of hydrogen, oxygen, and water (also in the presence of alkali atoms) has been investigated (see, e.g.,^[135–139]).

Ohmic loss is another issue to minimize. The electrical conductivity of, for example, TiO₂ passivation layers can be enhanced by surface defect engineering. In addition, the adhesion between the passivation layer and catalyst can thereby be modified.^[128] These and other factors can have a positive or negative influence on charge carrier transfer from the absorber to the reactive outer interface between the catalyst and electrolyte.

In addition, the coordination state of the catalysts can be tailored by the surface defect states of the passivation layer for further improvements of the catalytic performance. To study the effects of the solid–solid contact on the phase formation of the electrocatalyst active surface, which is commonly observed during application with the aim of minimizing interfacial performance losses, the electronic and chemical interfaces between protection layers and often semiconducting multinary oxide electrocatalyst thin films must be investigated. Because changes of the electronic structure of the interface can occur at various stages of the growth process, in situ and in system studies might

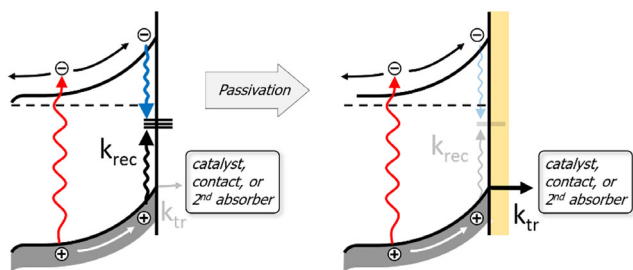


Figure 8. A passivation layer (right) can neutralize recombination at surface defects (left). Adapted with permission.^[249] Copyright 2017, Royal Society of Chemistry.

prove valuable tools to deduce the needed insights into the passivation behavior.

Thicker passivation layers can also serve to protect the absorbers against photocorrosion^[140] and at the same time directly provide the contact layer.^[30,130,140–142] Chemical passivation (protection) layers need to be optically almost transparent, electronically conducting or allow tunneling for either electrons or holes, and must show excellent chemical stability. Extended PEC stability measurements need to be combined with charge transfer studies by EC impedance spectroscopy (EIS),^[143,144] open circuit, potential step, linear polarization measurements, as well as DFT calculations. Finally, postmortem analysis should be applied using transmission electron microscopy (TEM), scanning electron microscopy (SEM),^[145] and AFM^[146] to develop a better understanding of degradation pathways and suitable passivation/protection strategies. In addition to processes in neat water, also corrosion mechanisms at acidic conditions need to be understood. Free energy profiles for the degradation mechanism (with and without ions) can be calculated by a combination of ab initio molecular dynamics simulations and enhanced sampling techniques such as meta dynamics.

4.3. Novel Electrocatalysts and Electrochemical Structures

The chemical reactions at the solid/electrolyte interface are a major kinetic bottleneck in the overall operation of water-splitting devices. Some state-of-the-art Earth-abundant catalysts for HER and OER are promising candidates with regard to their stability, kinetic overpotential, and current density.^[147,148] However, the integration of the catalysts into an artificial leaf device faces additional challenges compared to conventional EC devices, as illustrated in **Figure 9**. The catalysts must be coupled in an effective way to reach high STH efficiencies and enable practical fabrication procedures of PEC devices especially of tandems with high durability.^[149] To realize efficient charge transfer, the catalysts must be electronically and structurally coupled to the underlying layer.^[150] In doing so, the electronic levels of the catalyst must be correctly aligned with the passivation layer sandwiched between the multiabsorber and catalyst.^[82,151] Catalysts are needed to accelerate a reaction and lower the

required overpotential. First insights into the interplay between energetic alignment of catalysts and relevant support materials are already available.^[152–155] These need to be deepened to elucidate the interplay between catalyst, intermediate functional layers, and semiconductor on a fundamental level, as schematically indicated for different arrangements in **Figure 9**. Relevant parameters include, but are not limited to, the atomic and electronic structure, morphology, and the type of interaction (such as chemical bonding type and charge redistribution) between catalyst and support.

Besides good electrocatalytic properties, high active surface areas and high stability under intermittent conditions and elevated temperatures while minimizing or avoiding light absorption are required in the integrated device. To address these unique challenges in artificial leaf catalysts, the development of flexible catalyst platforms consisting of multinary oxides, single-atom catalysts, subnanometric cluster catalysts,^[156] and organic–inorganic hybrids supported on nanostructured or grafted contacts and passivation layers are needed.^[157] Among these approaches, organic–inorganic hybrids such as Ni-based layered double hydroxides (LDHs) organomineral hybrids are expected to be very promising as they might combine the high catalytic activity of Ni(Fe)-based LDHs^[158] with the structural tunability offered by the organic ligand.^[159] As a precondition, the electronic structure of the layer sequence across the interface, which is often unknown in devices studied so far, must be elucidated. While the valence and conduction states of the involved materials are often well understood, much less is known about surface, interface, and defect states in the bandgap. Catalyst platforms like doped multinary oxides,^[160–162] advanced materials based on LDHs,^[163] or metal complexes with substituted ligands^[152,164] enable the tuning of energy levels, catalytic properties, and stabilities. Correspondingly, new catalysts composed of nonprecious, preferentially Earth-abundant elements, must be developed for HER and OER, while optimizing their interaction with the support and charge transfer properties. The long-term goal is to effectively suppress nonradiative charge recombination, minimize Ohmic potential drops across interfaces, and to promote fast interfacial solid–liquid charge carrier transfer. The key objective of an integrated catalyst design is to optimize

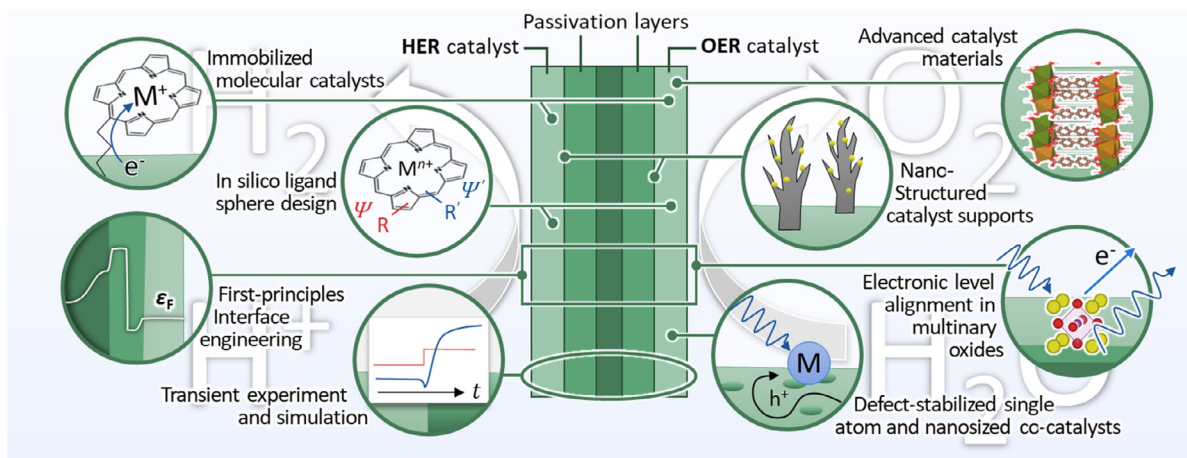


Figure 9. Schematic overview of different catalyst classes and arrangements as well as related research topics.

the electronic and structural interaction for different types of catalyst–support combinations. In situ and operando characterization in well-defined model catalysts has to be complemented by state-of-the-art computational methods, quantum chemistry, and theoretical spectroscopy to achieve a mechanistic understanding and to establish structure–function–stability relationships in these integrated catalysts.

Both immobilized molecular and inorganic crystalline materials depicted in Figure 9 have shown great potential as catalysts coupled to a tandem PEC device. Moreover, organic–inorganic hybrid materials joining molecular motifs with inorganic layers have recently been reported as highly active and stable catalysts for the dark OER^[160,165–168] highlighting another flexible, tunable catalyst platform as a potential light-driven water-splitting catalyst. Mechanistic studies of catalytic reactions can be accomplished by state-of-the-art operando and in situ spectroscopic experiments in model catalysts and interfaces. In situ and operando experiments addressing charge transfer kinetics at the interfaces, electronic band alignment, and transient behavior must be complemented with theory regarding catalyst and interface design, as well as data analysis on the atomic level. In this context, a hierarchical nanocomposite architecture is a relevant strategy to overcome the limitations of 2D semiconductors toward a 3D catalyst and to achieve high-performance stable materials.^[169–172] On selected passivation layers loaded with catalysts, studies on the alignment of the electronic levels and possible structural changes of the catalyst can be carried out. By manipulating the interface effect between different active materials (with the same catalytic function), one can design and fabricate multicomponent catalysts (coupling a HER catalyst with other HER catalysts or coupling an OER catalyst with other OER catalysts) to achieve enhanced catalytic performance.^[170]

4.4. Absorber–Catalyst Integration and Device Engineering

Once promising materials for the PV, catalyst, and electrolyzer components have been identified, two further essential steps toward the overall goal of realizing efficient and durable artificial leaf devices will be taken: 1) the integration of the materials into multijunction photoelectrodes; and 2) the integration of these photoelectrodes with supporting components into working devices (the related general references have already been presented above and detailed references will be cited in Section 5).

The first step, that is, the integration of absorber structures, passivation layers, and electrocatalysts must lead to stable multijunction photoelectrodes. Incompatibilities of materials and in the processing of materials for such composite photoelectrodes have received little attention in the field so far, but must be considered at an early stage. Studies of interface formation need to be performed following the development of the applied reaction and processing conditions to find appropriate surface and interface engineering strategies. Here, the characterization needs to be carried out before and after preparing the interfacial layers and preferably under in situ synthesis and operation conditions. For an improved understanding and knowledge-based development and adjustment of the interface formation, the processes at the absorber/passivation/catalyst interfaces need to be studied in their temporal development, at all timescales with TR

spectroscopy (see Section 5.4). This includes photophysical charge carrier dynamics from sub-ps to ns as well as slower charge carrier transfer and mass transport processes involving chemical reactions with and within the electrolyte at timescales ranging from microseconds to seconds and even at slower timescales. A key aspect for further improvements must be the ability to correlate the (ultra-)fast timescale of photophysical processes, which involve the formation of specific localized electronic states and the storage of minority charge carriers therein, to the much slower reaction processes of electrochemistry. The design of adjusted coupling schemes associated with chemical changes at the surface during operation needs therefore to be studied with recently developed ambient pressure hard- and soft X-ray spectroscopy capabilities at synchrotron facilities providing these unique new capabilities such as BESSY II (see Section 5.5). All these studies on system integration and device engineering must be complemented with theoretical calculations and simulations. These reach from the macroscopic level using, for example, multiphysics codes for the coupled solution of Maxwell's equations and transport equations^[173,174] down to DFT-based electronic structure calculations and ab initio molecular dynamics on the atomic scale.

Microscopic theoretical modeling, typically based on DFT, is essential for understanding the charge trapping and charge transport across the various interfaces and inhomogeneities of the devices and their respective optimization. It also helps to understand the influence of most importantly defect formation and dipolar double-layer potential drops on interfacial processes and improve our understanding how catalyst/support interactions and (photo)corrosion mechanisms affect electrocatalytic activity and device durability.

As an example, we show in **Figure 10** the orbital character of an interface state that forms a GaInP/AlInP(001) junction. Within hybrid DFT, this state is a bound interface state at the (0.5,0.5,0) point of the interface Brillouin zone (BZ), around 0.1–0.2 eV below the VB maximum.^[175] It corresponds to phosphorous states with *p* character. The character and energy of this state

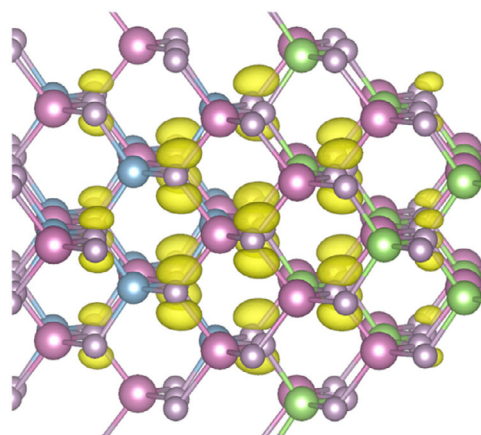


Figure 10. Orbital character of a bound GaInP/AlInP interface state, blue, green, violet, and small balls indicate Al, Ga, In, and P atoms, respectively. Reproduced under terms of the CC-BY license.^[175] Copyright 2021, The Authors. Published by Wiley.

and its impact on the charge transport depend sensitively on the stoichiometry and atomic structure of the interface.^[175,176]

Another example, where DFT yields detailed insight into a microscopic process, is light-induced degradation, which is well-known for boron-doped silicon PV cells.^[177] Light-induced degradation is to be expected for PEC as well. In the silicon case, the $B_{Si}Si_i$ defect with an interstitial Si close to a substitutional B becomes unstable when negatively charged, that is, at large minority charge carrier concentrations under strong illumination. It converts spontaneously from a shallow defect to a deep defect, leading to increased nonradiative recombination.

While ballistic transport calculation^[178] provides often a good starting point for a qualitative understanding of charge transport; quantitative agreement with measured data can typically only be achieved by taking the coupling between the charge carriers and vibrations as well as polaronic effects into account. For example, in the case of the organic semiconductor P3HT, it was found that high-frequency molecular vibrations with strong coupling constants are found to reduce the hole mobility considerably at room temperature.^[179]

Excited-state potential surfaces, calculated, for example, with constrained DFT,^[180] allow to calculate the structural^[181] and electronic dynamics of excited interfaces^[182] and give access to the dynamics of transport relevant phenomena like polaron formation and polaron hopping.^[175,176,178-183] Again, information such as this can be used directly in the materials design.

4.5. Transport Issues in EC Devices

When addressing real devices and their scale-up, the multijunction photoelectrodes must be integrated with supporting components, such as membranes, into scalable, robust, and efficient artificial leaf devices.^[184] For devices larger than $\approx 1 \text{ cm}^2$, mass transport limitations in the electrolyte become increasingly important. Even in concentrated electrolytes, pH gradients are difficult to avoid and can lead to efficiency losses and degradation. Absorbers made of microperforated membranes, perforated solar absorbers, and/or forced electrolyte flow can mitigate the effect of pH gradients and ensure efficient product separation. For designs where light passes through the electrolyte, the optimization strategy here also depends on the bottom photoabsorber: As this will be typically of a lower bandgap in the order of 1.1 eV or below, it will suffer from infrared absorption of the electrolyte. This implies that electrolyte layers on top of a photoabsorber for a configuration as sketched in panel (a) of Figure 12 need to be thin. This, however, increases losses from mass transport and pH gradients. Numerical modeling that includes solar spectrum, photoabsorber configuration, as well as reactor geometry is therefore required to find suitable configurations.^[185] Bubble management may be needed to avoid optical scattering losses, while reactor sealing and downstream product purification become important at higher technology readiness levels (TRLs).

As far as mass transfer is concerned, the efficiency in the final PEC device is governed by three contributions: the boundary layer, the bulk electrolyte, and the membrane. Herein, the most critical part is the boundary layer between the electrode and electrolyte. The transport processes within this region are dominated

by diffusion of reactive or ionic species into and from the catalytic surface. Mass transfer limitations caused by the boundary layer are minimized if the PEC device is operated under strong acidic or alkaline electrolytes because concentration gradients are suppressed and the processes at the electrodes are enhanced due to the high educt concentrations. However, the electrode and catalyst materials are in general not stable under these harsh conditions. Therefore, multiion buffered solutions are most likely to be used as electrolyte at near-neutral pH.

Figure 11 shows a schematic representation of the electrode/electrolyte surface for HER in the presence of gas bubbles. The processes are nicely described by Angulo et al.^[186] The HER on the electrode results in concentration gradients that may limit the mass transport to the surface and through the electrode. When the gas molecules in the liquid electrolyte reach a high enough saturation level, nanobubbles are formed spontaneously, typically at nanoscale surface defects. Eventually many of these nanobubbles coalesce and form a larger bubble that is fed by a carpet of the nanobubbles. The evolving gas bubbles will additionally block the active electrode area and cause local distortions in the electric field and the concentration distribution. This concentration and/or temperature gradients may further induce a Marangoni flow at the gas interface depending on pH and electrolyte.^[187-189] When the buoyancy force is larger than the capillary forces, the bubbles will lift off and produce a flow in their wake. This flow may enhance mixing at the electrode surface^[190] and thus largely influences the concentration gradient. The knowledge of these processes is currently still limited, but the large impact has been shown in several studies.^[186,191]

In future PEC systems, strategies such as stirring or the generation of an external flow may prove necessary in order to minimize concentration gradient/polarization. If the electrodes are larger and vertically aligned, the rising bubbles will drive by themselves a larger convection that can be further enhanced using Lorentz forces by external magnetic fields.^[190,192] This stirring effect may also improve the efficiency of the whole system.

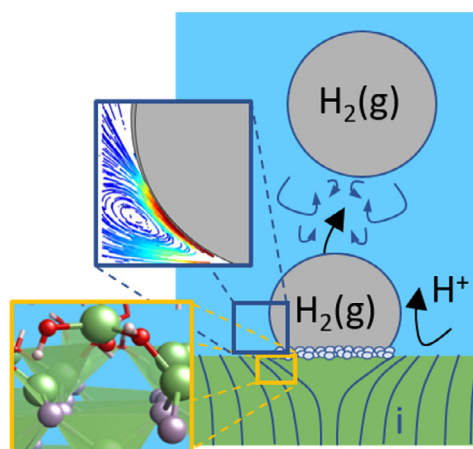


Figure 11. Schematic representation of the hydrogen evolution at the surface. The reaction on the electrode results in concentration gradients that may limit the mass transport to the surface. The evolving gas bubbles will block the active electrode area and cause local distortions of the electric field. Concentration and/or temperature gradients may further cause a Marangoni flow at the gas interface.

External convection, on the one hand, does reduce ionic concentration gradients, but it also leads to the transport and mixing of hydrogen and oxygen. Since gas separation is a fundamental requirement in a PEC device, it is crucial to consider the addition of ion-exchange membranes that possess excellent capabilities in both ion conduction and gas separation. On the other hand, external-induced flows or stirring facilitate the removal of gas bubbles (see, e.g.,^[193]), which can also limit the overall mass transport.^[187–189] Gas bubble removal can also be enhanced by a careful design of the electrode morphology and functionalization, for example, hydrophilic coatings to the electrode surface can improve wetting properties, reduce bubble adhesion, and enhance reactant transport.^[171,194] Nanostructuring of the photoelectrodes increases the catalytically accessible surface and is an important design concept for the development of efficient PEC devices. These advantages must be carefully balanced against the possible limitations of mass transport imposed by hierarchical nanostructures. Ion diffusion is significantly impeded when the nanochannels are blocked by gas bubbles, and the desired increase in the active surface area through nanostructuring also increases the interactions of the ions with the electrode surface and may reduce their mobility.

To avoid significant ionic resistance losses in the bulk electrolyte, the design of reactor architectures should minimize the ionic path length, including, for example, the placement of the catalysts and the ion-exchange membrane.^[184] The migration length of the ions should be shortened to reduce the ionic resistance losses in the bulk electrolytes. This is particularly important for devices that operate at high current densities.

Membranes for efficient PEC device have to fulfill two different properties: high ionic conductivity and low gas permeability. Membranes with a balanced interplay between these two functionalities are still under development.^[184]

For the conduction of hydroxide ions, polybenzimidazoles (Aemion) or polymeric anion-exchange membranes (AEMs) (Sustanion, Fumatech-FAA3) are commercially available state-of-the-art materials.^[195] The AEM generally consists of a (positively charged) quaternary ammonium head group and a polymeric (e.g., polyaryl or polyether) backbone. Also imidazolium, pyridinium or quaternary phosphonium groups are possible positively charged head groups.^[196–198] For proton conduction, Nafion (and similar compounds such as Aciplex, Fumasep) are the most important commercially available materials.^[199] These compounds are polymeric perfluorosulfonic acids. Their nanostructure is composed by ion-conducting domains embedded in a semicrystalline matrix.^[200–202] Alternative proton conductors are, for example, sulfonated polystyrene membranes incorporating an aliphatic-backbone or polyimide-based membranes.^[203,204] While Nafion was developed in the 1960s, efficient AEMs have only been the subject of intensive research for a much shorter period of time. Both polymeric proton and hydroxide ion conductors combine a hydrophobic backbone with hydrophilic head groups (e.g., sulfonic acids or quaternary ammonium groups), resulting in microphase separation and the formation of water-filled channels in the single-digit nanometer range for ion transport. Proton and AEMs were mainly developed for applications in fuel cells or

electrolyzers. Despite significant similarities between the membrane requirements of electrolyzers and PEC devices, there are still important differences in the design of efficient membranes. While electrolyzer systems operate in the $A\text{ cm}^{-2}$ range, the current densities of PEC devices can range from a few $A\text{ cm}^{-2}$ to several 100 A cm^{-2} . For low current densities of PEC devices, the use of AEMs, with an order of magnitude lower conductivity compared to Nafion, is much more feasible, as the ideal thickness of the membrane is not only determined by its conductivity. Gas permeability and current density must also be taken into account. For a detailed discussion, see ref. [184]. The main disadvantage of the Nafion membrane for fuel cell applications is the limitation of the operating temperature to below $200\text{ }^{\circ}\text{C}$ (as residual water in the nanopores is a prerequisite for proton conductivity). AEMs for alkaline water electrolysis suffer mainly from limited stability under alkaline operating conditions. Membrane degradation is particularly enhanced when the membrane nanochannels are not fully hydrated.^[205] For PEC applications, these drawbacks are less important since each part of the membrane is in contact with the electrolyte and operating temperatures are below $100\text{ }^{\circ}\text{C}$. However, due to the slow degradation of perfluorinated compounds in nature, PFAS-free alternatives to Nafion are desired. Current materials under investigation are, among others, quaternized poly(arylene perfluoroalkylene)s (QPAFs)^[206] or poly(*m*-triphenyl carbazolyl piperidinium)^[207]-based AEMs for hydroxide conduction or sulfonated polyphenylene-based polymers (e.g., SPP-TFP-4.0-PVDF)^[208] and aromatic graft polymers^[209] for proton conducting membranes. In general, promising candidates are block-copolymer membranes with multifunctional domains, polymer blends where conducting and gas-impermeable materials are provided to achieve balanced transport. Future research should also focus on semicrystalline ion-conducting polymers, as the gas permeability of the membrane decreases significantly with increasing crystallinity of the polymer matrix (as has been shown for Nafion^[210]). This is achieved by two microscopic phenomena: an increased tortuosity due to the increased volume fraction of the crystallites and a reduced water uptake of the ionic domains due to the stiffening of the surrounding matrix. In addition to the gas permeability, these changes also affect the ionic conductivity, which must be taken into account in the targeted development of membranes with balanced gas permeability and ionic conductivity.

For PEC water splitting, many electrocatalysts, which are used to drive the HER, show the lowest overpotentials in acidic media, while nearly all Earth-abundant catalysts used to drive the OER at low overpotential are only stable under alkaline conditions. Therefore, it may be ideal to use in PEC devices membranes that should separate two different regions with different pH values. A bipolar membrane would allow the cathode to operate under acidic conditions and the anode under alkaline conditions.^[211,212] This is possible because a bipolar membrane is an ion-exchange membrane, consisting of a cation-exchange layer and an anion-exchange layer, allowing the generation of protons and hydroxide ions via a water dissociation mechanism.

Addressing mass transfer limitations in the boundary layer, the bulk electrolyte, and the membrane in a unified/

holistic approach requires innovative device architectures and multiscale, multiphysics modeling to guide the design process.^[174,213,214] In addition, harmonized protocols for performance and stability benchmarking will have to be established, as these are not yet firmly established in the field.

4.6. Surface and Interface Characterization: In situ and Operando Studies

An important research element for an improved understanding and tailored engineering of device structures is the investigation of fundamental properties of solid/solid and solid/liquid interfaces with in situ/operando techniques. The ability to interrogate these interfaces and investigate interfacial processes under realistic operating conditions represents an experimental challenge in (photo-)electrochemistry. A summary of different techniques to be applied for such studies may be found in the literature.^[112,117,118] A detailed atomistic analysis of working interfaces is a necessary prerequisite to develop strategies for controlling EC charge transfer reactions. Figure 22 highlights specific opportunities in the utilization and advancement of in situ and operando tools.

The application of different in situ spectroscopic techniques enables the direct observation of interfacial processes of the reactive electrode surface to the electrolyte in combination with the standard EC characterization techniques. The relevant experimental (in some cases very recently developed) techniques include optical spectroscopy,^[215] X-ray and UV-based spectroscopy of core levels and VBs,^[216–218] X-ray scattering^[219] and diffraction,^[220] local probe imaging techniques such as in situ EC liquid TEM, or STM.^[221,222] These can be complemented by TR experiments such as two-photon photoemission (2TPPE),^[223] TR ellipsometry, and IR spectroscopy.^[224] Such methods are targeted to understanding EC surface reactivity starting from the atomic level, while a bridging of different domain of characterization methods is currently rarely pursued. Currently, there is no research on correlating electronic structure features observed in interfacial X-ray spectroscopy with chemical, particularly molecular, composition at the reactive interface analyzed by techniques like vibrational spectroscopies. Challenges connected to this aspect are the spectroscopic discrimination between reactive species and spectator species at the EC interface and the low interface concentration of reactive intermediates, calling in for signal enhancement strategies like resonance spectroscopies or surface enhancement via plasmonic approaches such as surface-enhanced IR or Raman spectroscopies (SEIRAS or SERS). The same holds true for a correlation of such spectral or structural information in time and space over the multiple involved time and length scales ranging from fs-s and sub-nm to mm. While EC surface science has focused in the past on single-crystal surfaces, it is important to go beyond and broaden investigations to more realistic complex EC interfaces, of course realizing that some methods do require well-defined (single crystalline) starting structures in order to benchmark studies and to assign the observed features. Generally, the interaction of the semiconductor absorber interface with and without applying passivation layers and/or electrocatalyst as promoters/inhibitors should be studied. Passivation layers, for instance, serve as

inhibitors against semiconductor corrosion but may reduce conduction and change energy-level alignments. This necessitates a comprehensive analysis of their impact. Designed in a smart way, such passivation layers could bring functionality for catalyzing the desired EC reactions at the solid–liquid interface. The interplay of all experimental outcomes deduced from the different characterization techniques shall be applied to study the chemical bonding at EC interfaces as the basis for an understanding of structure–reactivity relationships and mechanistic reaction pathways.

For more specific details on advanced and novel approaches in EC surface science, which has been applied by the authors of this review, the reader may refer to Section 5.5.

5. Selected Scientific Key Challenges on Electronic Structure and Reaction Dynamics of Photoelectrodes

To achieve the ambitious goal of fabricating PEC cells for direct and efficient STH conversion, we must develop device designs that enable us to approach theoretically feasible performance levels. We will therefore focus our discussion in this section on the central components of the photoelectrode and the involved scientific key challenges. These are: 1) EC surface reactivity and interface formation; 2) electronic alignment of involved energy states (to promote appropriate interfacial charge carrier transport); 3) selectivity of contacts (promoting desired vs. undesired electron reactions); 4) charge carrier dynamics (coupling the fast semiconductor electron dynamics with slow EC reaction rates); and 5) complexity of interfaces (as a consequence of loss-minimized coupling processes). Research efforts must combine complementary scientific disciplines as is described in more detail in the following subsections.

5.1. Challenge No 1: EC Surface Reactivity and Interface/interphase Formation

The performance reached in (P)EC energy conversion is determined by the controlled and kinetically optimized charge transfer of electrons/holes to electrolyte species at the solid/electrolyte interface. There are a number of factors, which need to be considered for contact formation and the kinetics control of preferred versus unwanted side reactions depending on the solid-state physical properties of the electrodes, the electrostatic arrangements of reactants across the double layers, as well as from mass and charge transfer. For PEC energy conversion via light-driven splitting of H₂O, the photovoltage provided by the optimized PV component (a tandem cell) must be transferred without severe voltage and current losses to the catalyzed HER and OER reactions. As already mentioned in the introductory part of our review, most of the theoretical concepts consider idealized semiconductor/electrolyte contacts without considering specific surface or interface electronic states (surface or interface states). However, as is evident for most, if not all, investigations of photoelectrodes in contact to H₂O that are used in artificial cells, there are always new electronic surface/interface states formed at the solid/electrolyte or solid/cocatalyst or

solid/passivation layer/cocatalyst interface. Those states must be considered for describing contact formation and even more charge carrier transfer under operation.^[51,225–227] As a consequence, the overall contact potential distribution cannot simply be described only in terms of Marcus–Gerischer theory or the Butler–Volmer approach, but novel combined theoretical approaches are needed depending on the number and position of possibly formed surface/interface states (see e.g.,^[228,229]). These new states are specific for any system under investigation and depend on the materials involved, their pretreatment, and operational conditions affecting reactive sites and intermediates of multielectron transfer reactions. When transition metal oxides come into play either as photoelectrodes or as cocatalysts, the occupation of defect states in the bandgap of the solid material, for example, formed by localized d-states, can change during operation, with consequences for the electronic structure, charge recombination, and transfer reactions due to the formation and involvement of the modified interphase arrangements. These desired or undesired charge rearrangements might occur between all of the possibly involved electronic states in all components, including the VBs, CBs, defect states, and electrolyte (compare **Figure 12**).

For this reason, emphasis must be put on an atomistic characterization and understanding of surface reactivity. This involves electrocatalytic activity which refers to the rate of conversion of water to either hydrogen gas or oxygen gas. Additionally, attention must be given to stability, examining potential corrosion phenomena at the interface. This interface encompasses the semiconductor, the chemical passivation, electronic properties of formed or applied junction layers, and the electrolytes (see^[225,230,231]). The complex interplay between the interrelated compositional, structural, electronic, and electrostatic boundary conditions required for the PEC reaction of H₂O to H₂ or O₂ is for most cases still an unsolved scientific and technological challenge.

To ensure optimal synergy between the light absorber and the customized catalyst, it is essential to have precisely adjusted, immobilized, and interface engineered absorber–catalyst or absorber–passivation/contact layer(s)–catalyst, as well as

catalyst/electrolyte junctions. A detailed analysis of the structure, chemical composition, interfacial reactivity, and interfacial energy alignment (Figure 12) depending on the applied deposition and processing steps, and EC reaction conditions can provide design rules for functional layers and electrocatalysts.

For a full understanding of the theoretical concepts of solid-state device structures of buried junctions describing the contact formation between possibly involved absorber/contact/catalyst layers, knowledge of solid-state semiconductor contact formation is needed in addition to EC concepts for the discussion of absorber/electrolyte and catalyst/electrolyte interfaces.^[50,232,233] Additionally, it must be considered that depending on synthesis conditions and surface/interface layer materials' properties, reactive components may interdiffuse crossing the layers during synthesis and application of the converter structures, which will lead to severe modifications of the properties.

Therefore, a specific problem but also a promising design perspective lies in the fact that under operation conditions the catalyst layers as well the interface may adopt the nonequilibrium conditions due to the trapping of charge carriers, leading to energetic double-layer potential shifts across inner and outer interfaces. Such surface layer charging or discharging processes may be advantageous or detrimental depending on the induced potential shifts of the trapped charge carriers and their energetic position at the EC junction (see, e.g.,^[225,230,234,235]).

In summary, the scientific and technological aim must be to transfer the achieved photovoltage and photocurrent of the PV component to the electrocatalytically active surface layer(s)/electrolyte interface without loss of voltage or current and with proper adjustment across the outer EC double layer. We are convinced that for most absorber materials, a buried junction structure must be considered, which either may be formed due to surface reactions under operational conditions or which is due to specifically designed and preprocessed contact layer arrangements at least including cocatalysts. The overpotential for catalytic reactions should be reduced as much as possible, for example, by increasing the catalytic surface area. Additionally, side reactions such as corrosion must be hindered by optimized interface energetic conditions to improve the long-term stability

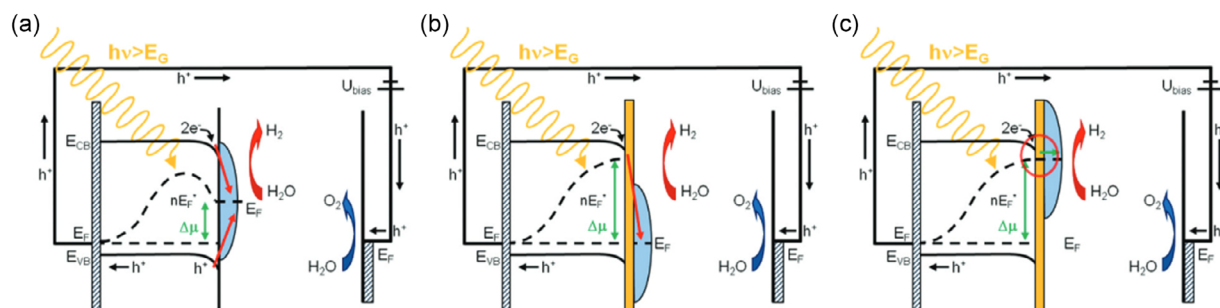


Figure 12. Energetics at the EC interfaces for a p-type semiconductor photoelectrode with a) directly deposited metallic HER electrocatalyst (with high work function, e.g., Pt) leading to small photovoltage and low photocurrent at the maximum power point due to Fermi-level pinning and b) with electrocatalyst deposited on a thin, insulating wide-bandgap passivation layer. c) Using adjusted MOS/metal–insulator–semiconductor (MIS) junctions. In the case of (a,b), a loss of photovoltage is due to Fermi-level pinning or electron transfer to the high-work function catalyst, respectively. High conversion efficiencies are expected for case (c) due to an optimized MOS/MIS layer with a degenerately doped charge carrier-selective contact layer (n+ oxide, n+ semiconductor layer) and Fermi-level alignment of the semiconductor and electrocatalyst close to the CB minimum. Reproduced under terms of the CC-BY license.^[128] Copyright 2020, The Authors, Published by De Gruyter.

of functionalized multijunction photoelectrodes. The impact of small ions (such as H^+ , OH^- , K^+ , SO_4^{2-}) on the electrolyte/photoelectrode interface must be studied in addition to gain insight into 1) how the ions affect the water structure at the interface and how they can significantly enhance corrosion mechanisms; and 2) how the mobility of the ions is affected due to interactions with the interface.

5.2. Challenge No 2: Electronic Alignment of Involved Electronic States

The formation of PEC interfaces in water-splitting cells and the device performance are very often described in terms of a simple and idealized semiconductor–electrolyte interface, in analogy to the ideal Schottky model of semiconductor–metal (Schottky) contacts.^[128,236] Under equilibrium conditions, the Fermi level in the semiconductor is aligned with the equilibrium redox potential of the electrolyte at these interfaces. Commonly, the photovoltage-induced shift of the quasi-Fermi level is considered under illumination by keeping the band-edge positions fixed, and the charge carrier transfer to the electronic states of the electrolyte is described in terms of the Marcus–Gerischer theory. Specific effects such as potential drops in the double layer, due to the charging of defect states or modifications of surface dipolar structures, are usually neglected and their values are widely unknown.^[237,238] Here, the formation, involvement, and dynamic charging of surface and interface states as well as changes of electron affinity due to modifications of the surface dipolar layers may occur and change the band-edge positions at the interface. Naturally, these electronic states are involved in charge carrier transfer reactions. However, the electronic density of states (DOS) distribution of intermediate and single charge transfer redox states of the electrolyte, when multielectron transfer reactions are considered, are not known for most cases as they may form additional (reoccupied) electronic trap states during operation^[239,240] The energetic alignment and the involved elemental transfer steps of charge carriers are even more complex in

cases, where metallic or oxidic cocatalysts are involved together with possibly formed or intentionally included interfacial chemical and/or electronic passivation layers (see **Figure 13**). This is the case for most junctions either formed unintentionally or designed in a controlled way using an engineering approach and these must be optimized for artificial leaf PEC devices. So far to the best of our knowledge high performance is only reached in electrochemically modified or synthesized buried junction device structures, including a number of often empirically designed interface engineering steps.^[21,48,128]

For an improved knowledge-based engineering of the PEC junctions, which possibly contain semiconductor–interlayers–cocatalyst/electrolyte junctions, the electronic coupling of the different layers must be understood and adjusted for efficient artificial leaf devices. For equilibrium conditions, this comprises 1) the band-edge positions; 2) the position of the Fermi level within the semiconductor; 3) the respective electronic levels of passivation phases (intermediate layers); 4) the possible formation and influence of interfacial pinning levels; 5) the energetic position of the Fermi level of the catalyst layer; and 6) the electronic states of the reactants (intermediates) in the electrolyte. For the relevant nonequilibrium conditions, the energetic situation is very often significantly modified. The flow of minority charge carriers may lead to a severe redistribution of the photo-generated charge carriers across the junction affecting the quasi-Fermi levels of electrons and holes in the semiconductor. In the interfacial layers and at the phase boundaries, existing defect states are reoccupied or new electronic states may form, which can also be expected for the cocatalysts. Additionally, in multielectron/proton transfer processes, the concentration and energetic position of intermediate states formed with the electrolyte must be considered, depending on possibly formed chemical bond formation of reacting species from the electrolyte with the solid surface. High conversion efficiency can only be expected when the quasi-Fermi levels of the semiconductor device are energetically aligned across the intermediate passivation layers to the active catalyst reaction sites. In operation, the quasi-Fermi level of electrons (or holes) must be in electronic

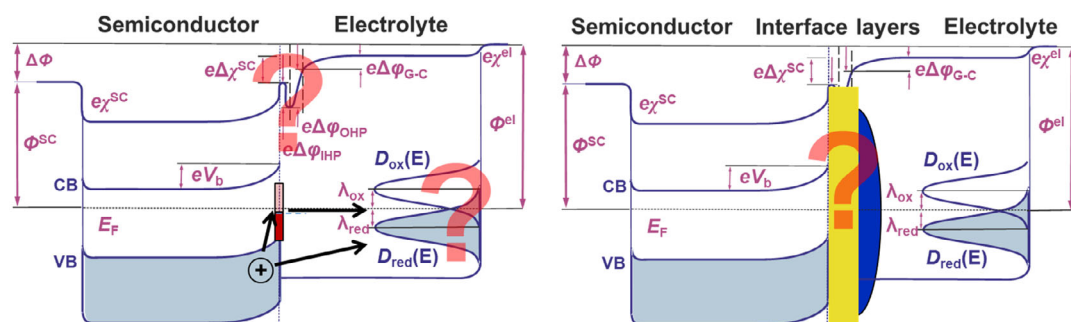


Figure 13. Schematic representation of contact formation at semiconductor–electrolyte junctions at equilibrium conditions and involved energy contributions (Φ : work function, $e\chi$: surface dipole potential, eV_b : band bending, λ : reorganization energies, $e\Delta\chi^{SC}$: semiconductor dipole, $e\Delta\phi_{IHP}$: inner Helmholtz, $e\Delta\phi_{OHP}$: outer Helmholtz, $e\Delta\phi_{G-C}$: Gouy-Chapman). Question marks highlight the unknown electronic properties with respect to band-edge position, interfacial defect states, and DOS of involved redox reactions. Left: Assuming only a semiconductor/electrolyte contact. Right: With involvement of a passivation layer and catalyst. The electrolyte DOS as shown is only valid for fast one-electron transfer redox couples and does not apply to multielectron transfer reactions involving bonding of intermediates to the electrode. Reproduced with permission.^[363] Copyright 2024, Elsevier.

alignment to the energetic position of the HER (OER) catalyst charge transfer states to enable low overpotentials (for metals defined by the Fermi level, for metal oxides, e.g., defined by the energetic position of charge transfer bandgap states). Thus, the answer to the question, which materials must be combined and which device structures and processing steps have to be chosen for an optimized performance, depends strongly on the electronic properties of all involved materials and interfaces.

5.3. Challenge No 3: Selectivity of Contacts

Functionalized heterointerfaces are the enabling building blocks in all kinds of modern semiconductor devices and play an essential role with regard to charge carrier selectivity, too. A big scientific challenge arises from the need to develop electron- and hole-separating contacts at different spatial positions of the envisaged device structure. Also for PEC cells, the contacts will vary in their function and design involving different homo or heterocontacts, from the one side containing the H₂ evolution electrode, via different types of internal contacts, finally to the interfacial contacts to the O₂ evolution electrode on the other side (see **Figure 14**). Here, electronic alignment and band structure engineering is mandatory to facilitate effective charge carrier separation and photovoltage sum-up at the internal selective contacts as theoretical^[45] and experimental work^[241] has shown. 2D heterojunctions at planar layer structures,^[45] axial,^[242] and radial heterocontacts^[243] in nanowires as well as point contacts have already been realized as charge-carrier-separating contacts. Such contacts must have high selectivity, while also prohibiting losses such as nonradiative electron-hole recombination or loss of EC potential due to nonadjusted electron energy states. The selective transport of electrons and holes to the two terminals of a PV-driven cell is often attributed to band bending or to electric fields, but in fact they are driven by the gradient of their EC potentials, that is, their gradients of quasi-Fermi levels^[38] as the highest conversion efficiency are only reached close to the open-circuit voltage. At charge-separating heterocontacts, selectivity is rather achieved by the different conductivities of different charge carrier species^[45] and/or different rates of reactivity arising from the electronic alignment and/or the electronic coupling at the heterocontact.^[241,244] Models therefore describe, see **Figure 14**, selectivity in a quantitative manner either by minority and majority charge carrier currents that are driven by concentration

gradients at the interface or by contact resistances for the two carrier types.^[245–247] High selectivity for electrons and holes is essential at the tunnel junction (**Figure 21** below), at different charge carrier-separating contacts (a-d, often referred to as window and back surface field, BSF) and for the catalytic reactions at the solid-liquid interfaces (a, d). The balance between selectivity and stability must be adjusted allowing both at the same time, and it is not known whether both demands can be easily decoupled. It seems evident that probably a sequence of different interface layers either composed of molecular absorbers or of solid-state contact layers must be designed and coupled to each other for the optimization of every junction included. The internal interface engineering but even more the interfacial coupling (electronic alignment) between the catalysts and photoactive components and/or supporting/passivation layers is not yet well understood. An insight that is already emerging, however, is the finding that the selectivity of a solid-liquid junction between a homogeneously doped semiconductor and the electrolyte alone does typically not lead to efficient charge transfer. This junction can be seen as a Schottky-like contact, and work on PV Schottky solar cells has shown that increased charge carrier recombination rates at such a junction from in-gap electronic states reduce the achievable photovoltage, as depicted in **Figure 15a**.^[247,248]

Selective contacts for PEC devices can be generated in a number of ways, using different material combinations. A prominent example is cobalt phosphate (CoPi), which was initially considered a cocatalyst on the photoabsorber BiVO₄, improving the overall water-splitting performance. Yet later, it was found that the improvement is largely due to a suppression of charge carrier recombination, hence serving as a charge-selective contact.^[249,250] For a homogeneously doped InP photocathode, PEC surface functionalization producing an n-doped oxide layer on top of the bulk absorber served as a selective contact, creating a selective p-n junction by intentional corrosion.^[251] Recent work on III-V tandems used AlInP-based window layers for creating the selective contact toward the liquid junction, increasing the stability of this highly reactive material either by an additional epitaxial layer^[252] or by dedicated corrosion.^[31] The latter approach results in a phosphate-rich layer as contact between the coelectrocatalyst nanoparticles and the top absorber. The layer is n-doped, resulting in a low contact resistance for electrons, but a high resistance for holes due to an offset in the VB. A generalized band diagram for a PEC device with suitable

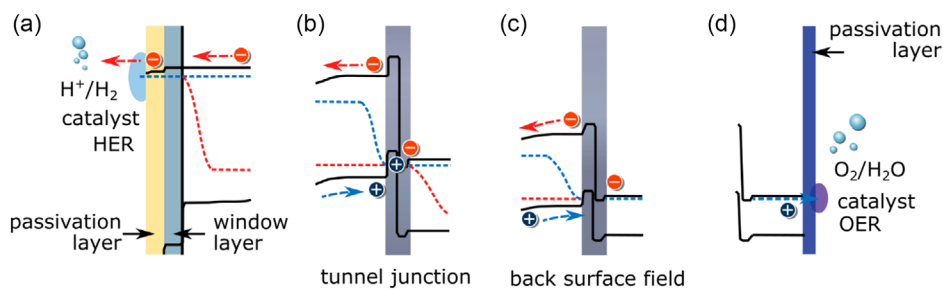


Figure 14. Different heterocontacts (for the design, compare **Figure 21**) acting as charge carrier-selective contacts at a) the PEC reaction and the so-called window layer, b) the tunnel junction and the surrounding charge carrier-selective contacts, c) the so-called BSF, and d) the EC catalytic reaction.

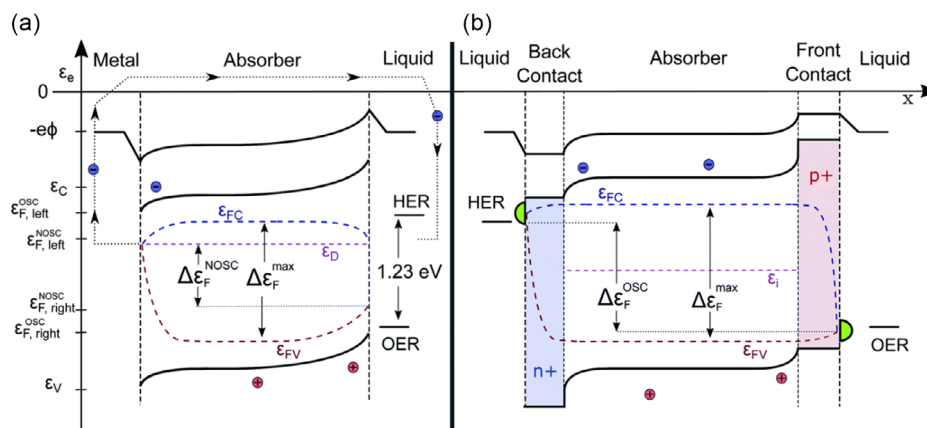


Figure 15. Band diagrams of single-junction PEC devices under illumination: a) n-doped absorber layer with a metal back and a liquid front contact. Surface recombination leads to voltage losses; therefore, the extractable energy per electron hole pair $\Delta\epsilon^{\text{NOSC}}_F$ is significantly smaller than $\Delta\epsilon^{\text{max}}_F$. For water splitting, an additional bias voltage would be necessary. b) Weakly doped absorber sandwiched between two additional contact layers added for optimization. The voltage losses are significantly smaller; therefore, the extracted free energy $\Delta\epsilon^{\text{OSC}}_F$ is closer to $\Delta\epsilon^{\text{max}}_F$. Green bubbles represent the electrocatalytic active sites of cocatalyst. In a multijunction device, the metal/back contacts have to be replaced by a tunnel junction to the bottom absorber. Reproduced with permission.^[247] Copyright 2022, Royal Society of Chemistry.

selective contacts is shown in Figure 15b, where an intrinsically doped (high-bandgap) absorber is sandwiched between two selective contacts, further modified followed by the catalysts for HER and OER, respectively. Yet it has to be noted that the selectivity of a contact can also show a dynamic behavior, either because corrosion (periodically) changes the charge neutrality level^[253] or illumination induces reactions that change the surface electronic structure.^[254] In principle an intimate semiconductor/electrolyte contact may also provide a carrier-selective contact. However, for such cases the surface of the semiconductor must provide efficient charge carrier transfer competing with recombination currents, which probably is hard to achieve as the multi electron transfer reactions lead to surface bond formation and thus to trapping of charge carriers at the surface which easily recombine before the next charge carriers will arrive.

Fundamental studies of the interfacial reactions at these charge carrier-selective contacts under realistic operating conditions are therefore the prerequisite for indispensable heterojunction engineering strategies and the design of the appropriate coupling between highly selective and active catalysts to the light harvesting device structure. The critical solid–liquid interface and especially the related dynamics of charge transfer across the EC contact must be thoroughly understood and properly designed. From a systems perspective, so far, understanding of how to build an assembly that will manage and balance the rates of photon absorption, charge carrier separation, and catalysis is limited. PEC device structures have already been theoretically modeled assuming idealized conditions and considering optimized PV converters.^[255] However, strong deviations from the assumed ideality are usually observed for not yet optimized solar cell arrangements when using novel absorber materials. The theoretical deduction of surface and contact engineering is challenging because modeling the interfacial electronic structure and dynamics based on existing theoretical approaches remains difficult. Therefore, the search for efficiently working selective contact is still an open challenge, which needs

strong improvements in understanding and knowledge-based engineering.

In the long run, the geometric arrangement of the PEC cells and the separation of the reaction products must also be taken into account when designing artificial leaf solar H₂ generators. Depending on the charge carrier dynamics in the PV component versus charge separation and transport rates to and within the electrolyte, differences in performance (recombination) and stability (competing corrosion rates) may occur.

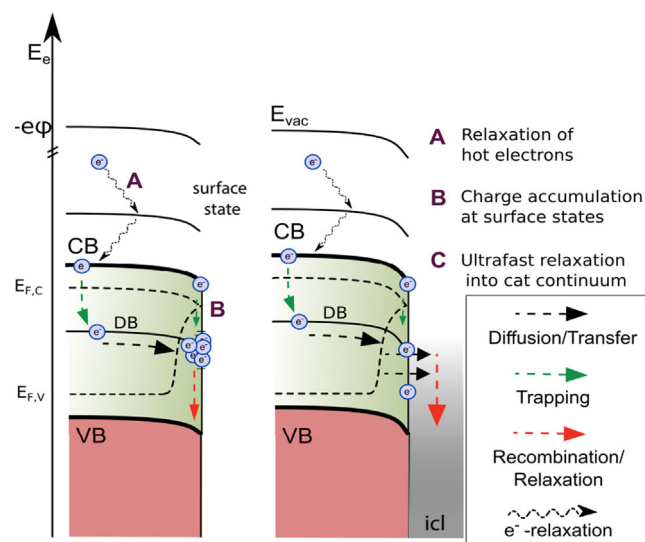


Figure 16. Charge carrier processes and pathways within the absorber/immediate contact layer (icl): excitation, trapping, separation, as well as recombination and thermalization occurring on timescales over several orders of magnitude. Reproduced under terms of the CC-BY license.^[223] Copyright 2019, The Authors. Published by Nature Communications.

5.4. Challenge No 4: Charge Carrier and Chemical Reaction Dynamics

The dynamics of charge carriers strongly influence the efficiency of any optoelectronic semiconductor device^[92,223,256–259] involving a variety of processes and pathways as illustrated in **Figure 16**. For the absorber and its immediate contact layer, excitation, trapping, separation, as well as recombination and thermalization of minority carriers occur on timescales, which vary over several orders of magnitude (fs to ms). One of the most demanding challenges is the understanding of the reaction dynamics of charge carriers of PEC cells. In particular, the large difference in the fast physical reaction dynamics of electrons and holes within the PV device compared to the rather slow chemical reaction rates in the PEC fuel formation and transport processes in the electrolyte must be understood and designed in a proper way to ensure the control of charge carrier reactions and to avoid efficiency losses. As a promising perspective, advanced design strategies of layered structures must be generated for the reduction of losses and the development of efficient devices. As already discussed above, the buried junctions needed may either be formed in contact with the electrolyte during operation or may be synthesized before contacting the electrolyte applying thin-film growth processes of overlayers. We will discuss first the research challenges related to the electron dynamics of the PV component before we address the challenges related to EC reaction rates.

5.4.1. PV-Related Electron Dynamics

In particular, the electronic alignment at interfaces and the presence of interface states represents a challenge and, at the same time, opportunities for suitable device designs (see discussion earlier). Knowledge about existing electronic states and how they are coupled to each other along with the timescale and prevalence of their electronic transitions are a prerequisite for a detailed understanding of the occurring processes. Subsequently, upon identification of the dominating pathways, specific tuning of the electronic structure by interfacial functionalization (formation of passivation and contact layers) may quench undesired electronic states or introduce desired ones, which will allow to stabilize the minority charge carriers to allow for slow charge transfer reactions and avoid fast recombination.

In this context, TR measurements of charge carrier dynamics and interfacial reactions are of utmost importance in the field of solar energy conversion, where nonradiative recombination needs to be suppressed, while carrier transport toward a selective contact should be dominating, and subsequent injection into acceptors or the contact layers should be efficient. Specifically in PEC cells for solar water splitting, photoexcited electrons not only need to reach the surface contact layer of the semiconductor absorber but also need to be injected into the electrolyte at a specific potential to drive the chemical reactions, while corrosion pathways should be suppressed. In addition, since there is a large temporal mismatch between the final PEC reactions with adsorbed H₂O or formed intermediates at the interface and the photogeneration and recombination processes in the semiconductor, strategies to bridge these time scales remain to be found.

Hence, a detailed understanding of the electronic structure and dynamics in the bulk and at semiconductor surface and interfaces and surfaces is of essential interest for the development of high-efficiency PEC cells. As a consequence, there is a need to develop and to apply in situ and operando characterization tools as well as theoretical simulation approaches, which are able to follow also nonequilibrium processes in working devices.

In order to complement the thermodynamic and steady-state insights, dynamic processes must be scrutinized including charge carrier dynamics in artificial leaf device structures and in particular at critical interfaces with different TR techniques and experimental setups. Promising TR optical spectroscopies are already available, which provide important information about the reaction kinetics.^[258,260–263] However, they must be complemented by structural-sensitive TR experiments such as X-ray diffraction^[264] and chemical-sensitive vibrational studies in chemically reactive environments such as wet chemical ambience to obtain information about the chemical speciation of reaction intermediates.

In this review, we will only shortly describe specific advantages and disadvantages of some of the applicable novel TR techniques. Most promising for the study of TR electron dynamics in the VB region are two-photon-photoemission (2PPE) experiments, as shown in **Figure 17**, which can provide information on energy-state occupation with time and energy resolution.^[92,265,266] Distinct challenges arise from the involved electron dynamics and reactivity at critical interfaces, in particular, near the solid–liquid and the internal solid–solid interfaces, including near-surface functional layers. Well-designed and defined contacts allow controlling photoinduced charge carrier dynamics in a way that 1) suppresses and minimizes nonradiative recombination; 2) enhances charge carrier transfer to occur through energy levels close to the band edges in order to sustain the generated photovoltage; and 3) avoids undesired side reactions, such as photocorrosion.

For optimization of the desired reaction and avoiding undesired losses, the energy–momentum–space carrier dynamics can be studied from photoexcitation until their final recombination in the OER/HER processes on different time- and energy scales, ranging from 10^{−13} to 10⁰ s and from meV to eV. One can employ a variety of both bulk and surface-sensitive

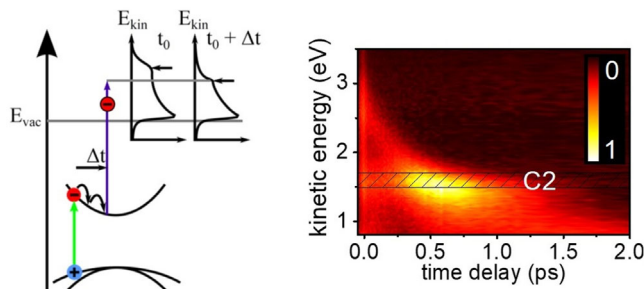


Figure 17. Capture of photoexcited bulk electrons into the surface state C2 of InP measured with tr-2PPE. Carrier accumulation appears as a bright yellow spot on the background of relaxing bulk electrons. Exposure to O₂ (not shown) passivates the surface; no carrier accumulation is observed. Reproduced with permission.^[265] Copyright 2015, American Physical Society.

techniques, combining experiment with theoretical calculations to obtain a conclusive picture of the interplay of individual dynamic processes in the photoabsorbers, the functional layers, the electrocatalysts, the electrolyte, and, above all, their coupling.

TRPL is an excellent, contact-free method to characterize the dynamic properties of minority charge carriers in semiconductor absorber materials and its PV suitability directly.^[258,267,268] In its application, the extraction of meaningful parameters involves different key ingredients: a suitable absorber structure such as a semiconductor double heterostructure, a state-of-the-art measurement setup, a kinetic model appropriate for the description of the sample behavior, and a general analysis method to extract the model parameters of interest from the measured TRPL transients.^[258] Specifically, the lifetime of minority charge carriers has already been studied in various semiconductor structures using TRPL, such as in MQW top absorbers and semiconductor nanowires,^[269–271] or to determine recombination rates and charge extraction processes in perovskite absorbers.^[157] TRPL measurements based on time-correlated single-photon counting and its analysis have been advanced,^[258] allowing for quantification of charge carrier-trapping kinetics at defect states. It is a fundamental approach to describe the intensity-dependent dynamics of an absorber structure using a coupled set of rate equations, which describe multiple TRPL transients all at once. While it is still necessary to obtain suitable measurement data and to choose a valid set of rate equations, state-of-the-art fitting procedures allow the reliable extraction of the different parameters governing the charge carrier recombination processes. The result of the fitting also provides an indication of the validity of the chosen set of rate equations. And in principle, TRPL can also be applied for in situ measurements of charge carrier dynamics in the PEC environment providing direct access to the crucial minority charge carrier recombination rates depending on the applied PEC conditions. Such measurements will ultimately guide synthetic protocols to minimize nonradiative charge carrier recombination at solid/solid and solid/liquid interfaces and develop a robust transfer method such that any laboratory around the world can perform PEC-relevant science research on well-defined samples. One can use TRPL to characterize the minority charge carrier lifetime of the pristine material and study, for instance, how the surface coatings modify the charge carrier dynamics and recombination. Here, the key point is to systematically tune the interfacial chemistry and energetics to maximize charge carrier lifetime in the absorber materials. Furthermore, the combination of transient photoconductivity techniques using TR microwave and TR optical pump terahertz probe spectroscopy^[260] complements the surface charge carrier dynamics and energetics by continuous and rather complete monitoring of the kinetics of thermalization, trapping, localization, and recombination of charge carriers in a variety of materials, such as metal oxides and perovskite photoabsorbers.^[272–274]

To ensure a semiconductor's suitability as an absorber material in a PV or PEC cell, it must facilitate the efficient transport of charge carriers toward the respective interfaces while minimizing resistive or recombination losses. Key parameters to assess are conductivity, mobility, and carrier lifetime.

TR microwave conductivity (TRMC) is a widely employed technique for investigating material properties,^[275] distinguishing itself from methods like Hall effect or time-of-flight

measurements, by operating without electrical contacts. This eliminates issues such as contact resistances, unintended doping, or unfavorable band offsets^[276] and also allows the examination of nanostructured samples that are initially difficult to study with contact-based methods.^[277,278]

TRMC serves a dual purpose: probing the complex conductivity (dielectric function [DF]) of materials in the GHz regime and conducting transient measurements to examine the propagation of photoexcited charge carriers. The method utilizes microwaves with relatively low energy, making them ideal for investigating interactions with free charge carriers within the CB and VBs, since band-to-band transitions do not generate additional charge carriers. Instead, the interaction between photogenerated charge carriers and the electric field of alternating standing microwaves is influenced by both the number of charge carriers and their mobility.

Extending into the THz regime enables the exploration of the conductivity response using three common methodologies in THz spectroscopy:^[279] Terahertz time-domain spectroscopy (THz-TDS) investigates the direct interaction of THz radiation with a material, finding various applications such as thickness determination of semiconductor layers, substance studies, or detection of drugs and explosives.^[280] The ability of THz radiation to penetrate weakly interacting materials facilitates measurements, where the pulse provides amplitude and phase data through a medium and is analyzed via Fourier transformation to assess the complex refractive index over its entire bandwidth. Pump-probe measurements (optical pump terahertz probe, OPTP) involve an additional pump pulse with a variable time delay, allowing the investigation of transient physical phenomena, including charge carrier trapping,^[281] surface and bulk recombination, etc.^[274,282,283] Analysis of the changing peak amplitude of probing THz pulses over time provides insight into the decay of photoconductivity within the sub-ps-to-ns regime.

TR terahertz spectroscopy and TR pump-probe spectroscopic ellipsometry (TSE) combine aspects of both THz-TDS and OPTP, analyzing frequency spectra for a photoexcited sample to determine (time-dependent [TD]) the complex refractive index of the material, facilitating the extraction of the complex mobility $\mu^b(\hbar\omega)$.^[284,285] Those techniques provide valuable information on charge carrier dynamics and material properties after optical excitation. However, those techniques are limited, measuring only the real or the imaginary part of the DF in a limited energy range, requiring Kramers–Kronig transformation and assumptions for reconstructing the complex DF as done before.^[286,287] To circumvent these established methods, fs-TSE^[288] is a unique tool that directly provides the transient complex optical response of a system after optical excitation of charge carriers. TSE offers resolution in the fs-to-ns timescales, allowing the probing of band structure, joint DOS and transition matrix elements, as well as dynamic phenomena such as charge carrier carrier and phonon scattering, excitation, and relaxation.

A TSE experiment consists of an ellipsometer component and a classical pump-probe system.^[288] It extends the well-established method of ellipsometry, which measures the change in polarization state of light after interaction with a sample and, thus, provides access to properties of thin films and material optical constants, which gives insights into the electronic structure of

materials, by introducing time resolution due to pulsed excitation of a sample and subsequent TR ellipsometric probing.

TSE can be also applied to study various properties of optoelectronic materials like Si, Ge, InP, GaP, ZnO, GaN, and perovskite oxides.^[286,289–293] After exciting a semiconductor with a high-intense laser beam, electrons and holes will occupy CB and VB band states, respectively. This will immediately, within some fs, cause bandgap renormalization (BGR) as expressed in the redshift of transition energies between VB and CB. Concurrently, transitions between now occupied states are Pauli blocked, causing reduction of absorption at the respective energies. Furthermore, the excess electrons and holes can be excited now by the probe light, allowing additional intra-VB and/or intra-CB transitions, reflected in increase of absorption at the respective energies.^[286] Also, directly after excitation, charge carriers spread within the entire BZ to energetically matching bands, causing also here Pauli blocking and/or new intraband transitions. When the material exhibits excitons, they are screened by the excited carriers, but may also form so-called Mahan excitons.^[286,294] In the following, the excited carriers will scatter among each other and with the lattice (phonons). This causes energy dissipation in the form of heat, which manifests in redshift of transition energies and also, relaxation of the carriers to band minima, observed as redshift of the Pauli-blocked absorption features. Coherent hot-electron-hot-phonon states can also occur and be stable over some ps.^[286] The hot electrons can propagate ballistically over several μm ^[289] and phonons can oscillate coherently.^[290] Finally, the system will relax back to

equilibrium either due to radiative or nonradiative carrier recombination within, depending on the material, some tens of ps (e.g., ZnO) or up to several ns (e.g., GaP).

Figure 18 illustrates the power of fs-TSE for bulk single crystals of the prototypical III–V material GaP. The dominant processes contributing to the transient DF difference $\Delta\varepsilon(\tau) = \varepsilon(\tau) - \varepsilon(\tau = 0)$ after a short, strong excitation are 1) absorption bleaching primarily due to Pauli blocking of filled states visible as negative $\Delta\varepsilon_2(\tau)$; 2) carrier density- and temperature-dependent BGR; 3) carrier scattering in particular from the CBM's Γ minimum to the L point; and finally 4) carrier recombination on the ns timescale. Detailed information on this processes is obtained by modeling the experimental $\Delta(\tau)$ data, for example, by a combination of a Tauc–Lorentz (TL) oscillator centered at $E_n(\tau)$ and with the bandgap energy E_G , Drude functions, and ε_1 offset to account for effects outside the measured spectrum range. The BGR can be obtained from $E_{G\text{-static}} - E_G(\tau = 0 \text{ ps})$ and the shift due to heat, in this case, from $E_{G\text{-static}} - E_G(\tau = 4 \text{ ns})$. Time-dependent relaxation of the carriers to the band extrema can be observed from the redshift of the main—negative—TL absorption peak at E_n , which approaches $E_{G\text{-static}}$ at large delay times, and the decreasing amplitude caused by the diminishing (oder fading) blocking of the transitions due to carrier recombination.

Scientifically interesting, but of little relevance for solar-driven water splitting, are TSE studies on changes of the band structure as a function of the excited carrier density. In contrast, theoretical carrier relaxation rates and nonradiative recombination rates as well as the study of nonequilibrium distribution via real-time

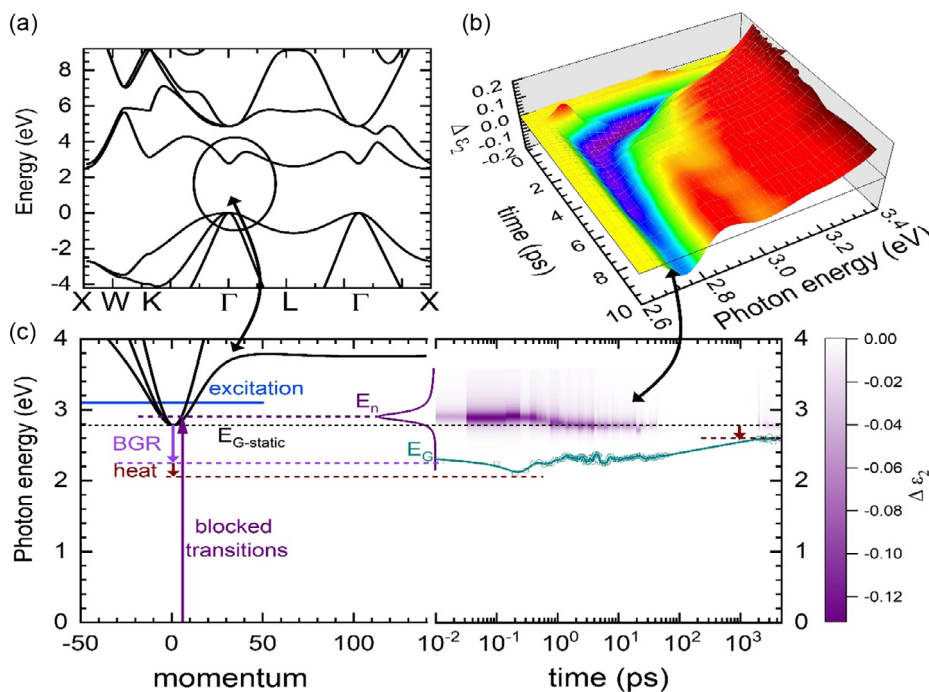


Figure 18. a) Calculated band structure with direct gap at Γ point. b) Change of the imaginary part $\Delta\varepsilon_2(\tau)$ of the DF obtained via TSE as a function of delay time showing blocked and enhanced transitions. c) Time evolution of the transition responsible for the strongest blocking seen in (b) as a violet feature is shown: Energy difference between the lowest CB and topmost VBs around Γ (left) as well as the assigned TL amplitude (violet shading and fit of the profile at $\tau = 0$ ps, right) as a function of time. The model-derived $E_G(\tau)$ and $E_n(\tau)$, the static bandgap energy $E_{G\text{-static}}$, as well as the excitation energy and energy shifts due to heat and BGR are indicated.

Boltzmann transport equation are important, as they are needed for modeling the PEC efficiency.

A particular challenge is OER, as at least four photons need to be absorbed before enough electrons for forming a single O_2 molecule are generated. A numerical description needs ideas from ab initio molecular dynamics, but possibly also from TD-DFT. Obviously, a deep understanding of HER at semiconductor or passivation layer surfaces is a good intermediate goal.

We mention that in situ spectroscopic ellipsometry has become a well-established method.^[295] In electrochemistry, it was applied to study, among many others, charge transfer processes at liquid–solid interfaces, chemical changes as well as formation of surface layers, and surface band bending under applied potentials (e.g.,^[296,297]). Recently it was applied in cyclic voltammetry studies in the OER regime of a mesoporous IrO_x film, where the volume fraction of the produced gas was obtained by ellipsometric modeling.^[298]

Whereas the preceding paragraphs addressed spatial homogeneous and mostly steady-state device operation, inhomogeneities within the device, scattering, and feedback effects as well as variations in the incoming light intensity will lead to additional effects and transient changes in the charge carrier occupations. Therefore, an effective dynamic modeling approach needs to go beyond the steady-state solution of the drift diffusion equations, in order to capture possible instabilities that decrease the efficiency of carrier transport. One possible modeling approach is the hydrodynamic Boltzmann equation, which describes the evolution of the moments of the electron distribution function as a function of space and time. For this approach, the space-dependent carrier relaxation times within every part of the tandem structure as well as the DF need to be known. TR measurement techniques such as ellipsometry or photoemission as well as TD DFT calculations can provide those material details and are crucial to form a consistent modeling approach spanning all the timescales relevant for carrier generation and transport. A subsequent characterization of the charge carrier dynamics as a function of device parameters can identify instability regions and will yield guidelines for optimization.

5.4.2. Electrochemical Reaction Dynamics

In addition to the absorption of sunlight in a semiconductor and the generation and transport of charge carriers (i.e., electrons and holes), the processes at the catalytic centers or the semiconductor/liquid interface and the bulk electrolyte are crucial for the efficiency of the overall photoelectric device. The latter includes the hydrogen and oxygen evolution process, the transport of neutral species (water and products in liquid or gaseous phase), and the transport of charged species. Multiphysics models aim to take all these processes into account. They have been and are used for modeling, simulation, and development of design criteria for PEC water-splitting systems.^[174,214] Using these multidimensional continuum simulation approaches, attainable device efficiencies could be predicted,^[20,299–302] operating conditions were screened,^[213,303,304] cell dimensions provided,^[305] and material and operating trade-offs compared and novel cell architectures and concepts evaluated.^[306,307]

Although devices are being quantitatively designed and implemented, various open questions remain for example regarding the incorporation of complicated physics (e.g., thermal effects and bubble formation). Very recent numerical studies start to bridge this gap and incorporate the effect of the microstructure of the electrode on the hydrogen gas evolution.^[308] The different electrode geometries investigated in this study are shown in **Figure 19**. The impact of gas evolution on the EC characteristics can mainly be broken into three phenomena: 1) a shift in the local reversible hydrogen electrode potential; 2) hyperpolarization; and 3) an increase in the solution resistance of the electrolyte. Chen and Lewis^[308] state that compared to planar electrodes, a microwire array structure reduces the impact of bubbles on the solution conductance, but the shift in the local reversible hydrogen electrode potential varies with distance from the actual electrode surface.

Figure 19 also illustrates that mass transfer and bubble formation are coupled at nanostructured interfaces. Efficient mass transfer of reactants to the electrode surface is important for efficient EC conversion rates, that is, bubble formation. However, (large) bubbles can block nanochannels and reduce the

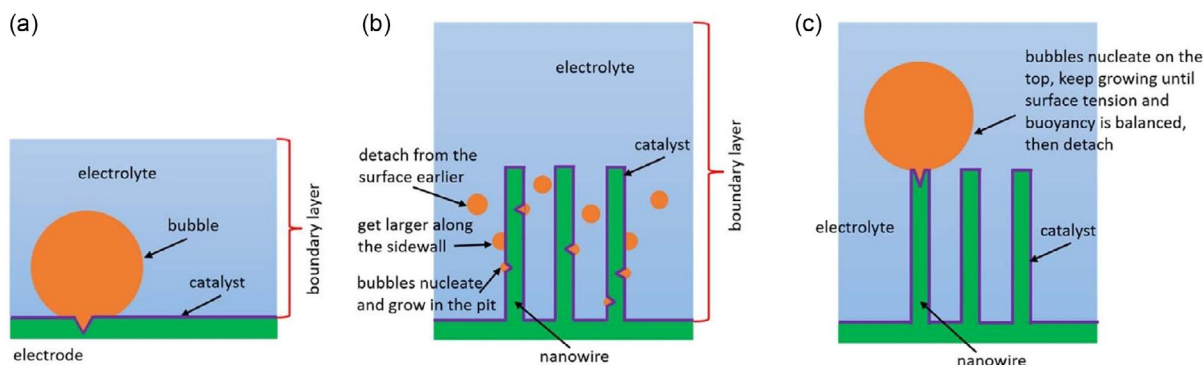


Figure 19. Schematic of three different configurations of a cathodic gas-evolving chamber: a) a planar photoelectrode configuration, b) a micro- or nanowire array electrode configuration where bubbles nucleate on the side of the wire, and c) a micro- or nanowire array electrode configuration where bubbles nucleate on the top of the wire. Reproduced with permission.^[308] Copyright 2022, IOPScience.

catalytically accessible surface area, which in turn limits conversion rates and mass transfer.

The design of the water-splitting device also affects mass transfer.^[184] In wired two-electrode systems with at least one photoelectrode, ionic resistance can be minimized by reducing the distance between the electrodes. In monolithically integrated wireless devices, the ionic charge carriers must migrate along the surface of the semiconductor and through the ionic conductor, that is, the electrolyte. The long migration paths can lead to higher Ohmic losses.^[309]

From an atomistic point of view, small ions such as H^+ , OH^- , K^+ , and SO_4^{2-} interfere with the interface between water and photoelectrode (boundary layer) in two different ways: 1) the ions affect the water structure at the interface and can significantly enhance corrosion mechanisms; and 2) due to interactions with the interface, the mobility of the ions is affected.

The individual techniques to study diffusion in the interface, corrosion, and gas bubble evolution are already well established. 1) Ab initio molecular dynamics can be used for the simulation of the atomistic structure and dynamics of the photoelectrode/electrolyte interface.^[310–318] For example, the dissociative or nondissociative water adsorption can be addressed. Free energy profiles for the removal of atoms from the surface can be calculated via enhanced sampling techniques such as metadynamics (see Figure 20). In Figure 20, free energy profiles of Ga dissolution under pH-neutral and acidic conditions are presented. Under pH-neutral conditions, Ga dissolution starts with the subsequent breaking of the two Ga–P bonds (with activation energies of 0.61 and 0.51 eV) and formation of a new bond with the nearest H_2O molecule (Figure 20a,b). In the last dissolution step, $Ga(OH)_3$ is desorbed from the surface into solution by breaking the remaining Ga–O bond. This step takes about 0.56 eV (Figure 20c,d). Under acidic conditions, the protonation of P atoms is likely, which weakens the structural Ga–P bonds leading to more stable intermediate states and considerably lower activation barriers. In ref. [319], it is found that after a subsequent

protonation of adjacent P atoms, the cumulative dissolution barrier drops down to 0.48 eV, which should result in dissolution kinetics that are several orders of magnitude enhanced relative to pH-neutral conditions. Also, diffusion coefficients can be calculated by molecular dynamics simulations and the impact of the nanostructure on ion mobility can be characterized.^[320] To investigate the microscopic mechanism of gas bubble nucleation and evolution, classical molecular dynamics is a suited tool.^[321,322] The critical size and geometry of bubble nuclei leading to stable bubbles can be determined^[323] and the importance of the double-layer surface charge for bubble stability was shown by this method.^[324] Also, the impact of flat versus grooved surfaced and local heterogeneities on bubble formation was studied,^[321,322,325–328] 2) Optical measurement techniques (particle image velocimetry and particle tracking velocimetry) can be utilized to evaluate the mass transfer around the bubbles close to the surface^[190,192] and to generate and observe bubbles for characterizing surface properties (wetting angle) as well as the bubble formation and interaction. As different time and length scales are involved in these processes, measurements are either limited to the bulk or the close vicinity of the evolving gas bubbles. Due to the large necessary magnification, micro- or nanoelectrodes are employed to fix the position of the evolving bubbles.^[329] However, this changes the electric field and the concentration gradients significantly and also does not allow to study the interaction between multiple bubbles. Therefore, further developments of advanced techniques and optically transparent electrodes are necessary in conjunction with simulations to complete the understanding of the relevant processes; and 3) In situ liquid AFM serves as a valuable tool for gathering useful information about the surface stability of the photoelectrode.^[146] A area-wide or local dissolution of photoactive or passivation layers can take place especially in the presence of hydrogen or OER, resulting in the degradation of the photoelectrodes.^[330] Therefore, utilizing in situ AFM^[146] to examine microscopic surface changes is crucial for understanding the corrosion

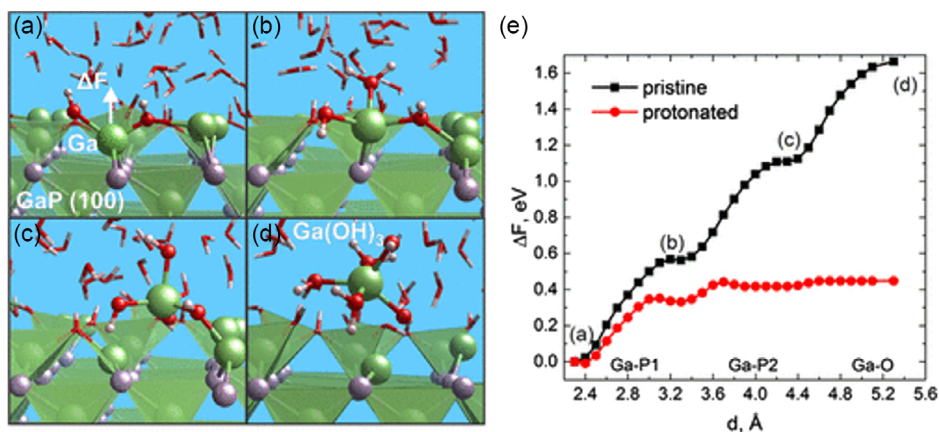


Figure 20. a–d) Scheme showing the mechanism of Ga dissolution from the GaP (100) surface in an aqueous solution (color scheme: Ga—green, P—gray, O—red, and H—white): (a) Ga–P bond breaking, (b) Ga– H_2O bond formation, (c) second Ga–P bond breaking and Ga release to the surface, (d) Ga–O bond breaking and desorption of a $Ga(OH)_3$ complex, e) corresponding free energy profiles for the pristine and protonated GaP (100) surfaces in contact with water. Reproduced with permission.^[319] Copyright 2021, American Chemical Society.

mechanism and developing strategies to improve the durability of the photoelectrode. In addition, employing EC methods such as EC EIS, open circuit, potential step, and linear polarization measurements enables further in-depth characterization for both the stability of the photoelectrode and the efficiency of the HER or OER.^[143]

A future goal should be to obtain a unified picture for mass transport in the boundary region close to the different interfaces (solid–liquid, liquid–gas, gas–solid). This requires a combined experimental/theoretical approach, which allows to study gas bubble kinetics and ion diffusion across multiple time and length scales, starting from the EC formation of H₂ and O₂ molecules from H and O atoms adsorbed on the electrode surface after ion oxidation or reduction to the removal of gas bubbles of millimetric size from the electrodes.

5.5. Challenge No 5: Design and Characterization of Complex Multifunctional Interfaces

The complexity of solid–liquid and solid–solid interfaces represents a major challenge in PEC devices with respect to controlling the rate- and stability-limiting processes for hydrogen and oxygen formation. The structural and physicochemical interplay between the photoabsorber passivation, protection, and/or contact layers and the catalyst layers strongly determines the overall STH efficiency of the multijunction tandem devices.^[18,32,53,331]

Ideally, the individual layers which have been optimized at first independently with respect to their primary function can be grown isostructurally and with retained properties on each other forming applicable junctions. However, the usually given structural diversity and their physicochemical interplay limit their compatibility. Especially, structural misfits as well as atomic intermixing at the various junctions can substantially change their mechanical, electronic, or catalytic properties. In addition, the specific processing and synthesis conditions needed and developed for obtaining the desired properties of the individual layers may not be compatible with each other.

For example, the semiconductor bandgap and the catalyst–adsorbate binding energy can be significantly altered by strain effects. Along this line, the charge transfer can be deteriorated by the interfacial/surface electronic structure. Even more severe are side reactions occurring during the synthesis of passivation and cocatalyst layers or during operations which may modify the interphase chemistry significantly and thus the electronic properties.

These undesired interfacial modifications with changed electronic properties can significantly limit the charge transfer properties and dynamics causing charge recombination and efficiency losses. Research aims to understand those processes under working conditions in synthesis and operation on a fundamental atomistic level which is a decisive challenge for realizing efficient devices. The involved research efforts starts from the bare semiconductor surface with the stepwise addition of the different functional layers, thus enabling a subsequent knowledge-driven optimization of the materials selection and used deposition process. To decrease the parameter space, one needs at first to find optimized combinations for a limited number of

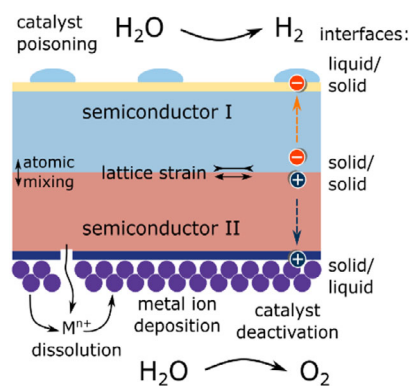


Figure 21. Illustration of the complexity of interfaces due to the combination of tandem absorbers functionalized with protection, contact, catalyst layers under PEC reaction conditions, and the main physicochemical interactions.

most promising tandem absorbers functionalized with protection/contact and catalyst layers, as displayed in **Figure 21**. In the long run, however, it can be expected that design rules from these studies for optimized interface engineering can also be transferred to other material combinations.

Long-term stability is a very crucial issue for the practical application of multijunction devices. In particular, the OER conditions can induce metal ion dissolution, interdiffusion of reaction intermediates as, for example, H atoms, and irreversible structural changes altering the catalytic activity and thus, the overall EC efficiency and stability.

Most of the experimental techniques to study the electronic structure, surface chemistry, and composition of the different layers and interfaces of multilayer PEC devices under working conditions are based on soft X-ray radiation. However, only hard X-ray radiation (>2 keV) provides enough kinetic energy for photoelectrons to travel through the solid and liquid and thus will preferentially be used to provide a precise characterization of the interfacial properties, within the EC environment. To tackle these challenges a variety of in situ and operando techniques can be applied (**Figure 22**), including methods available at synchrotron radiation facilities that allow obtaining comprehensive insights on the interfacial properties under working conditions (see, e.g.,^[332]).

Near-ambient pressure hard X-ray photoelectron and absorption spectroscopy (NAP-HAXPES/AP-HAXAS) are representative examples of techniques that can be applied to investigate electrified solid/liquid interfaces under working conditions.

In this context, the Berlin Joint Laboratory for Electrochemical Interfaces (BEIChem) operating at the BESSY II synchrotron facility has been set up to play a pivotal role: its primary focus lies in providing a detailed molecular-level understanding of PEC interfaces relevant to solar fuel production and renewable energy storage.^[218] BEIChem is a collaborative effort between the Fritz-Haber-Institute of the Max-Planck society and the Helmholtz-Zentrum Berlin.^[218] In BEIChem, NAP-XPS and ambient pressure, hard X-ray photoelectron and absorption spectroscopies are used for in situ and operando investigations of the electronic structure and chemical composition of catalytically active solid/gas and solid/liquid interfaces. This instrumentation

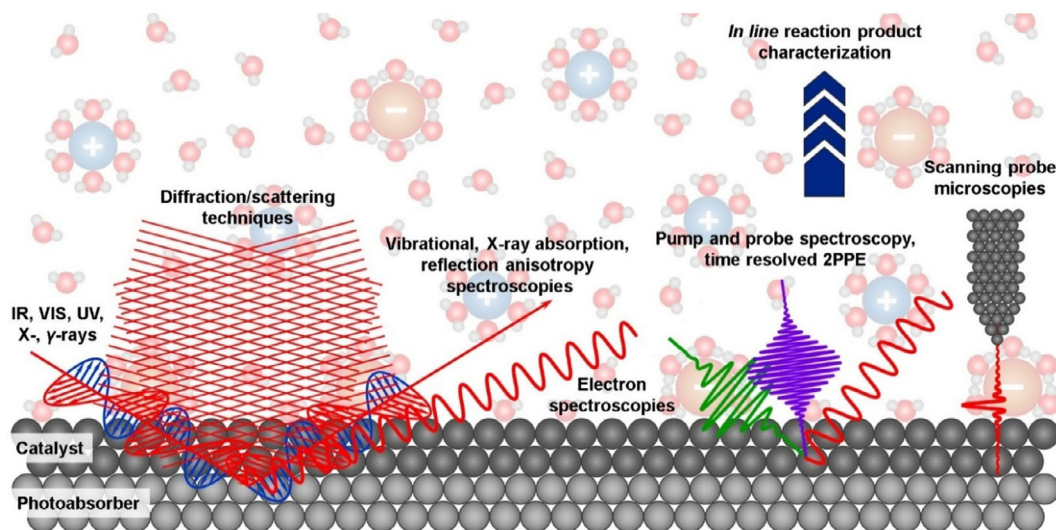


Figure 22. Schematic view of the different in situ/operando characterization methods for studying electrified solid/liquid interfaces. The goal is to achieve atomic-/molecular-level understanding of the key interfaces in (photo-)electrocatalytic systems.

has already provided fundamental insights on the chemical and electronic structure of the oxygen-evolving near surface of electrocatalysts. These studies highlight the importance of understanding oxygen chemistry under (photo)electrocatalytic conditions as the oxidative charge is apparently located at the oxygen ligand of the metal oxide surface. Adaptations of the near-surface oxygen chemistry have been shown for the most relevant Ir-, Ni-, and Co-based catalysts using operando and in situ photoelectron spectroscopy.^[333–335] It is an ongoing challenge to identify activity- and stability-determining properties of the oxygen-evolving surfaces under PEC conditions and these recent works are providing the basis for in-depth investigations of PEC devices. Within BELChem, the Institute for Solar Fuels of the Helmholtz-Zentrum Berlin recently developed the spectroscopic analysis using a tender X-rays (SpAnTeX) end-station.^[336] This end station is characterized by the capability to achieve high electron transmission and detection efficiency, even when operating under gas pressures of up to 30 mbar and photon energies ranging from 200 to 10 keV. By leveraging two specific features of the electron spectrometer equipping the end station, namely a new lateral resolution lens and a 3D delay line detector, a capability to collect the spatial distribution of photoelectrons under realistic working conditions (presence of liquid electrolytes and pressures ≥ 20 mbar) with a lateral resolution finer than $30 \mu\text{m}$ was developed. Moreover, this setup allows performing TR studies utilizing a continuous tender X-ray source, enabling the in situ characterization of interfacial processes potentially down to the ns timescale.^[336] At the SpAnTeX end-station, using the “dip-and-pull” method,^[336–338] researchers are able to generate liquid electrolyte layers with a thickness of tens of nanometers on various semiconducting surfaces relevant for photoelectrochemistry. Hence, the surface chemistry and energetics of these solid/liquid interfaces can be investigated with full EC control.^[336] With this set of technical capabilities, the light-induced formation of a 2 nm bismuth phosphate (BiPO_4) film at the interface between a BiVO_4 photoanode and a phosphate-containing electrolyte was recently observed.^[254]

Furthermore, evidence was found for the presence of intrabandgap states, most likely associated with small polaron formation, at the surface of BiVO_4 using resonant photoemission.^[339] In a recent follow-up study,^[340] it was found that the surface morphology and composition of BiVO_4 photoanodes strongly influences the formation of such BiPO_4 layer under illumination conditions, with potentially drastic consequences for the long-term stability of the corresponding devices. In addition, at the SpAnTeX end station, PEC device structures can be investigated under realistic working conditions. In a recent study, ion-exchange membranes were investigated in a hybrid liquid/gas (photo)electrolyzer, utilizing a combination of in situ NAP-HAXPES and finite-element analysis.^[341] The obtained results reveal that the preferential ion movement across the membrane which separates the liquid and gas compartments is predominantly governed by diffusion driven by the ionized functional groups embedded in the membranes, rather than electromigration. Moreover, the presence of undesired polarization fields at the interface between the liquid electrolyte and the polymer membrane was detected. The occurrence of these polarization fields is contingent upon the polarity of the applied bias and the electric charge of the ions rejected by the membranes.^[341] Consequently, these losses lead to an increase of the cell voltage, thereby negatively influencing the overall efficiency and reaction selectivity of hybrid liquid/gas (photo)electrolyzers. This comprehensive understanding aids in devising effective strategies to mitigate the effect of these phenomena, ultimately maximizing the device performance.

To study EC charge transfer at the solid–liquid interface, information about the electronic DOS close to the Fermi level as well as on the chemical speciation in the EC double layer is required. For this purpose, a novel X-ray/IR beamline endstation at the new enhanced liquid interface spectroscopy and analysis X-ray/IR beamline at BESSY II is under consideration in order to study the VB electronic structure of (photo)electrocatalytic systems. Key to this beamline end station and unique capability complementing to the BelChem infrastructure will be the

possibility of carrying out two-color experiments which couple (NAP) soft X-ray photoelectron and near-edge X-ray absorption fine structure spectroscopies with IR spectroscopy in order to gain specificity to molecular speciation.^[342] Relevant model systems which must be studied will be ultrathin, defined water adsorbate layers on photoelectrodes (bare, protected, catalytically functionalized), with specifically designed potential control schemes. Thus, the platform under consideration would dramatically improve spectroscopic characterization of the different absorber structures under controllable model conditions approaching realistic (i.e., wet) solid–liquid and gas–liquid interfaces.

In addition to the sample-averaging operando methods discussed above, it is also crucial to obtain spatially resolved information on the near-surface chemistry and electronic structure. Thus, in situ and operando conditions are essential to correlate parameters like local surface composition, local atomic structure, and morphology of complex catalysts with reaction intermediates and products. For this reason, a unique NAP-Low-energy electron microscopy (LEEM)/X-ray photoemission electron microscopy (XPEEM) spectromicroscope with operando capabilities is currently being developed at BESSY II. Equipped with a reaction chamber surrounding the sample stage and differential pumping of the electron optics, this worldwide unique instrument has already successfully shown chemical reactions on surfaces in real time under NAP gaseous conditions, with a demonstrated lateral resolution below 20 nm and an energy resolution better than 70 meV. The implementation of a versatile gas dosing system and a quadrupole mass spectrometer will allow to bridge the pressure gap in understanding surface processes. At present, the system can already be used for electrocatalysis in a quasi in situ mode thanks to an EC cell directly attached to the UHV system, allowing sample transfer without air exposure. Nonetheless, the development of a new EC cell compatible with the current NAP-LEEM/XPEEM design is currently being conducted inspired by graphene-sealed cells^[343] that are already used for EC XPS measurements. The latter will vastly extend the capabilities of the setup to the operando study of EC processes relevant in the field of (photo)electrocatalysis, providing simultaneous chemical and morphological information spatially resolved.

Such unique facilities, coupled with standard PEC techniques and product analysis capabilities, must be applied in the future to establish quantitative correlations between the composition/geometric/electronic structure and reactivity, selectivity, and degradation processes at and across the electrified solid/interlayer/electrolyte interfaces. These in situ/operando experimental results need to be linked with findings from computational investigations. In situ/operando characterizations will play a pivotal role in understanding the influence of the interactions between catalyst–catalyst and support–catalyst systems on the observed electrocatalytic properties. Hence, the synergistic cooperation between in situ/operando experiments and theoretical approaches will enable to achieve a detailed atomistic understanding of (photo-)electrocatalytic systems and will allow new light on the reaction mechanisms occurring at such interfaces. This knowledge can then be applied to the development/optimization of fabrication techniques and material research, thereby leading to improved, highly efficient (photo-)electrocatalytic systems with tailored properties.

6. Case Studies Summarizing Own Work to Achieve Efficient Device Structures

6.1. III–V Compounds

Efficient multijunction solar cells based on III–V compounds are composed from the 3- and 5-valent elements In, Al, or Ga and P, As, or Sb, with multiple options for reliably high n- and p-type doping with dopants such as Si or S (Se, Te) and C or Zn, respectively. To achieve desired electronic band structures and lattice constants, the semiconducting materials may be fabricated from multinary tunable III–V compositions, such as InP, GaInP, AlGaP, GaInAsP, etc. Because of their model-like tunable properties, monolithic III–V multi junction solar cells and PEC cells are the most efficient PV devices worldwide so far.^[252]

These cells comprise a plurality of individual semiconducting absorber layer structures connected in series and deposited on substrates such as Si, Ge, GaAs, or InP.^[344,345] They can be grown in a bandgap range between ≈ 0.15 and 2.2 eV, with (direct) transitions at the Γ -point of the band structure, low defect densities with reproducible preparation on atomic scales, as well as high minority charge carrier lifetimes and diffusion lengths.^[256,258,259] Also, the electronic alignment is tunable in a wide energetic range via the famous “principle of bandgap engineering” including tunable band discontinuities.^[346,347] With this, high-quality thin films of only a few μm are sufficient for almost complete sunlight absorption fabricated from crystalline materials with high perfection, and lattice constants, adjusted to the lattice constant of the substrate material. Alternatively, lattice constants can be changed with metamorphic, so-called graded material growth^[348,349] by a stepwise change of the atomic distances in the conventional unit cells in order to avoid severe crystalline defects detrimental with regard to nonradiative impurity recombination.^[45] To facilitate photocurrent flow, a plurality of tunnel junctions of low-resistivity materials are typically inserted between each adjacent semiconductor cell.^[350] Functional layers such as charge carrier-selective transport^[45] are available in order to control the direction of electron and hole photocurrents in the PV device structure and prevent interfacial electron–hole recombination at the contacts. A well-established heterocontact for efficient charge separation is the heterointerface consisting of n-GaInP (top absorber)/n-AlInP (electron-selective contact), which is an effective component of record cells for multijunction solar as well as PEC cells.^[17,31,252] Even at this model-like junction, characterization of the band alignment, band offsets, the influence of defects, interdiffusion, or the preparation of a well-defined, atomically abrupt interface is nevertheless a challenge.^[351]

Currently, monolithic solar cells with highest conversion efficiencies (47.6% under light concentration) have been achieved with a multijunction cell with four individual absorber structures connected in series:^[17,352,353] a GaAs(100)-based tandem solar cell ($\text{Ga}_{0.5}\text{In}_{0.49}\text{P}/\text{GaAs}$ with bandgaps of 1.88/1.42 eV) on top bonded to a bottom InP(100)-based tandem ($\text{Ga}_{0.16}\text{In}_{0.84}\text{As}_{0.31}\text{P}_{0.69}/\text{Ga}_{0.47}\text{In}_{0.53}\text{As}$ with 1.12/0.72 eV). This configuration is close to the perfect bandgap combination for a four-junction device.^[17] Accordingly, also in PEC tandem cells, absorber materials can be selected with appropriate bandgaps to most efficiently generate the suitable operational photovoltages

with a maximized utilization of the solar spectrum.^[20] Record tandems for water splitting are, presently, realized in two-junction configurations ($\text{Ga}_{0.89}\text{In}_{0.11}\text{As}/\text{Ga}_{0.41}\text{In}_{0.59}\text{P}$ with 1.26/1.78 eV) close to idealized bandgaps of about 1.1 and 1.7 eV (see Figure 2).^[30] For their preparation, metal–organic vapor phase epitaxy (MOVPE) is the method of choice due to reproducibility and opportunities for industrial upscaling.

Within the device structures, the heterointerfaces are the most critical components.^[352,354] However, only limited information is available on the interfacial atomic and electronic structure and processes, in particular, on chemically delicate interfaces due to, for example, dynamic interaction of different materials or phase transitions at the interface as at the solid–liquid interface.

In search for optimum material combinations for light-induced unassisted water splitting, both bulk and interface properties are crucial. In principle, III–V semiconductor compounds are capable of providing Fermi-level splitting alias photovoltage close to the theoretical limit,^[355,356] sufficient absorption coefficients in relation to the diffusion lengths,^[357] and selective charge carrier transport,^[45] whereas the interfaces need to exhibit proper energy band alignments,^[351] promote carrier transport to the adjacent materials as the liquid electrolyte, prohibit nonradiative recombination, and remain stable.^[7]

Challenges for a competitive application of III–V semiconductors are manifold: lowering production costs, deep understanding of the elementary processes, integration of Si with III–V epitaxy, new absorber structures such as MQW structures,^[84] stability of well-defined hetero-interfaces, etc. For the latter challenge, in situ control during the preparation and operation is desired, for example, with benchmarking of in situ signals via interfacial characterization.^[358,359] New III–V compounds involving nitrogen or boron for high-efficiency multijunction solar cell components may advance the portfolio of suitable materials.^[360–362] To prepare III–V compounds, less hazardous, nongaseous, and more efficient precursor molecules should be employed such as tertiarybutylphosphine (TBP) instead of phosphine (PH_3), ditertiarybutylsilane (DTBSi) instead of silane (SiH_4), and tertiarybutylarsine (TBAs) instead of arsine (AsH_3). Higher growth rates and new in-line processing procedures and equipment must be developed for industrial scale-up and competitiveness.

Equally important to the knowledge of the electronic and atomic structure of absorber materials, surfaces, and interfaces is the understanding of the behavior of electrons and holes on the microscopic scale. Charge carrier dynamics in the absorber materials and at interfaces in a wide range of timescales (see Section 5.4 on dynamics) is of critical importance for their efficient performance in solar energy conversion (but also for other thin-film devices such as high-speed switches, surface emitting lasers, or light-emitting diodes).

6.2. Silicon

Our results presented on silicon-based photoelectrodes have already been published in detail in a number of review articles^[12,48,128,363] and we will only refer to some fundamental insights in relation to the conceptual ideas of this review on the coupling of PV action to EC reactions. We will therefore also not

provide an extensive report of the numerous studies published in literature.

The application of Si as an absorber component for artificial leaf approaches using PEC arrangements has intensively been studied during the years (see some recent reviews and references therein).^[364–366] These studies are motivated by the fact that Si is the standard PV material reaching high solar cell (solar-to-electricity) efficiencies and a solid technology status.^[93,367–369] Si can be considered as prototype semiconductor material which is very well understood in its physical and materials bulk and device properties due to extensive research efforts over an extended period of time which also forms a solid basis for PV applications. Different device structures have been investigated over the years and conversion efficiencies of up to 25% have been reached applying single-crystalline absorber materials with typical values of open circuit and maximum power point voltages of $V_{oc} = 0.75$ V and $V_{mpp} < 0.65$ V, respectively, and of maximum power point photocurrents of up to 42 mA cm^{-2} (see, e.g.,^[93]). Please note that in PEC studies often the value of V_{oc} and of the short-circuit currents I_{sc} at the reversible redox potential of the HER or OER is presented which are not relevant values for defining the conversion efficiency. Due to its small bandgap of 1.12 eV, a single Si absorber cell will not provide a sufficient operational photovoltage for bias-free H_2O splitting. Therefore, tandem or multiabsorber structures are needed. These may be either realized using thin-film amorphous/multicrystalline tandem or even multilayer cells or by combining Si with other large-bandgap semiconductors in intimately or electrically coupled device arrangement. Otherwise also parallel internally connected Si cells can be applied for adding up the operational voltage to the needed minimum value needed for H_2O splitting of more than 1.8 V.^[370]

In any case, detailed research efforts on Si-based PEC cells are expected to provide benchmark results on how to couple a semiconducting absorber material to an electrolyte solution and which design and engineering strategies need to be developed for reaching efficient and stable devices. Research on single-crystalline Si electrodes will provide a detailed understanding which surface and interface engineering steps are needed to provide reasonable conversion efficiencies for light-driven HER and OER.^[364–366] These studies involve the application of optical surface conditioning, formation of charge separating junctions, surface passivation processing, and cocatalyst deposition steps. The development, testing, and characterization of the involved manufacturing steps will provide a detailed understanding of defect formation, electronic and chemical passivation strategies, as well as loss-free electronic coupling to the cocatalysts and the desired EC reactions needed for an efficient control of minority carriers. Thus, the obtained results will be of value for development of specific device structures applying Si-based selective half-cell photoelectrodes but also for developing general design strategies of PEC devices with other materials. p- as well as n-doped Si is available as material of high electronic quality, specifically the surface- and interface-related aspects of contact formation to solids, adsorbates, and electrolytes as well as the reactions within the electrolyte can be studied in very detail combining EC as well as surface science characterization techniques as suggested in this review. Comparing chemically passivated Si photoelectrodes with high light-to-electric conversion efficiencies

using reversible one-electron redox couples to Si photoelectrodes used, for example, as photocathodes for HER or photoanodes for OER, which do not provide high conversion efficiencies due to low operational photovoltages, even when the photocurrents in the saturation regime are high, show that the PV components lose photovoltage to the outer electrolyzer component of the PEC cell. Adding passivation and/or metal (e.g., Pt) cocatalyst layers does not completely avoid the losses involved, due to Fermi-level pinning and/or electronic states caused by dangling bond defect states on the Si surfaces close to midgap, which persist even after applying hydrogen, Si-Oxide, TiO₂, or other passivation layers. As a consequence of the pinning states available or possibly formed during operation and application of a bias voltage, a double-layer potential step builds up between the photoelectrode and the electrolyte, leading to the shift of Si band edges and with that to a nearly complete loss of photovoltage. Strongly improved results can be obtained when, for example, p-n⁺ or n-p⁺ homojunctions or even better a heterojunction between p- or n-doped crystalline Si and n⁺- or p⁺-doped amorphous Si-H is used, respectively.^[363] Other heterojunctions, for example, to strongly doped oxide layers usually do not provide perfect charge-selecting contacts as also in these cases pinning

effects usually will occur either in the Si absorber but also in the semiconducting oxide layer.

We have concentrated on our PEC studies using Si as absorber materials on the application of thin-film multijunction solar cells using microcrystalline and amorphous Si because these systems provide high photovoltages, which can be adjusted to the needs of PEC photosplitting cells.^[367] Some more information on the structural arrangement and performance of thin-film Si solar cells can also be obtained from literature.^[233,368] Summarizing these results (see **Figure 23**),^[363] it could be shown that promising results for unbiased water splitting can only be expected for device structures using multiabsorber cells, providing PV operating voltages of above 1.6 V or larger, which correspond to open-circuit voltages of more than 1.9 eV. Tandem cells of $\mu\text{c-Si}/\text{a-SiH}$, which will deliver only V_{oc} and V_{op} values of 1.6 and 1.2 V, respectively, will not provide sufficient driving force for the light-driven HER and OER combined in one device. Of course, the often observed losses in photovoltage from the open-circuit conditions to the maximum power point in PV devices to the PEC operational voltage in combined PEC devices are governed by different types of loss processes in the layer sequence. The coupling of the available photovoltage provided from the PV

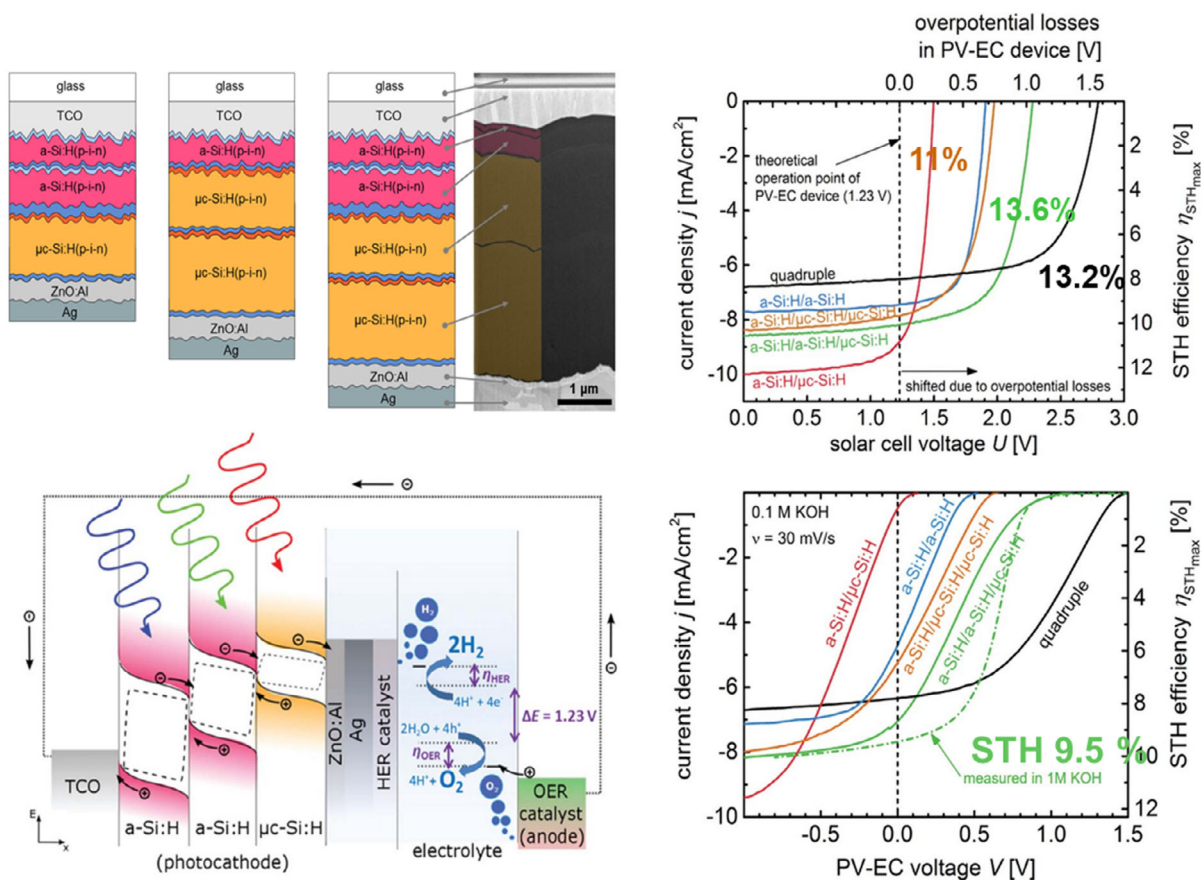


Figure 23. Different thin-film solar cell structures to be used as PV components for PEC devices (top left). Schematic energy diagrams of a buried triple-junction thin-film solar cell consisting of p-i-n cells of $\mu\text{c-Si}$ and a-Si and used as photocathode (left bottom). Photocurrent voltage curves and efficiency values of the different thin-film Si solar cells as indicated (top right).^[29] STH current voltage curves of different buried junction thin-film Si PEC cells used for water splitting and best STH efficiency obtained (right bottom).^[449] Reproduced with permission.^[29] Copyright 2016, Royal Society of Chemistry, and Adapted under terms of the CC-BY license.^[449] Copyright 2016, The Authors. Published by Forschungszentrum Jülich.

component and strongly defined by the absorber device properties to the electrolyzer components as represented by the cocatalysts and, finally, the overvoltage losses of the HER and OER play a dominant role. In contrast, the photocurrent will often be of similar values as reached for the PV component in many cases, when no light blocking layer is needed for the design of the PEC cell. Therefore, one may deduce simple selection criteria and design strategies from these results, which must be considered for all PEC structures under consideration. At first, a PV or PEC device for electric power generation must be developed and optimized in performance. Afterward, the needed engineering and processing steps must be transferred to the design of PEC cells for water splitting or other fuel formation processes. In the second step, the deposition of chemical passivation layers and cocatalysts must be realized in a way which will not degrade the performance reached before in the manufacturing of the buried PV junction. This could be realized by separating the surface exposed to solar light at a transparent back contact from the PEC junction directly exposed to the electrolyte for the HER. The OER was performed at a dark electrode electrically connected to the PV hole contact. An arrangement like this is shown in Figure 23 using a glass/TCO solid back contact substrate for the hole extraction and n-ZnO/Ag/HER catalyst as the photocathode in contact to the electrolyte.

Applying thin-film Si solar in photoelectrode arrangements for H₂O splitting, some promising results have been already published by Reece and Nocera et al. reaching 4.7%.^[28] In our approach, the maximum conversion efficiency of 9.5% STH efficiency was reached with a triple solar cell consisting of one μ c and two a-Si n-i-p cells coupled in series to a photocathode for HER.^[29] The overall performance is strongly influenced by pH and the type of catalyst selected, since these factors substantially affect the EC overvoltages required to get the desired photocurrents. The variations of performance for different processing steps and working conditions are described in detail in the given studies.^[29,48,128] Overall it is evident that the performance is strongly coupled to the PV performance of the multijunction cell and reduced by the additional inherent PEC-related losses. As for thin-film Si cells, a power conversion efficiency close to 14% is also the maximum reached so far, no more improvements beyond the 10% STH efficiency can be expected if no strong reductions in EC overvoltages are possible. It is also evident that higher voltages than needed for the operational voltage of the integrated water-splitting PEC cell close to V_{mpp} will not lead to STH improvements as the increase of photovoltage in multijunction cells is inherently coupled to a decrease of photocurrent.

6.3. Oxides

Over the past decade, several dozens of standalone (i.e., bias-free) multijunction water-splitting devices that feature at least one metal oxide absorber have been reported.^[371] The first demonstrations were based on nanostructured WO₃ or α -Fe₂O₃ (hematite) photoanodes placed in front of a dye-sensitized solar cell, reaching STH efficiencies of 1–3%.^[372,373] WO₃ is limited by its relatively large bandgap (\approx 2.7 eV),^[16] while α -Fe₂O₃ suffers from a short minority carrier diffusion length and a large contribution of localized d–d transitions that do not lead to mobile

charge carriers.^[374] Therefore, significant research efforts have been dedicated to finding alternative oxide absorbers. One of the more promising candidates is BiVO₄ (bandgap \approx 2.4 eV), which was identified by Kudo et al. as a good photocatalyst for oxygen evolution as early as 1998.^[375] In 2012, Abdi et al. reported the first BiVO₄-based multijunction device for bias-free water splitting. Using a double-junction amorphous silicon PV cell as a bottom absorber, they were able to demonstrate STH efficiency close to 5%.^[35] A collaboration with Lee et al. later improved this to 7.7% using a Si/ α -Fe₂O₃/BiVO₄ triple-junction device.^[36] Other groups have reported combinations of BiVO₄ with III–V and with HaP solar cells, reaching efficiencies up to \approx 8%.^[37,38] Although photocurrents up to 10 mA cm⁻² have been reported for nanostructured Cu₂O photocathodes,^[376] 8% remains, to the best of our knowledge, the highest STH efficiency reported thus far for bias-free PEC water-splitting devices with at least one metal oxide absorber.

One of the main challenges that has hampered the development of efficient PEC devices based on metal oxide absorbers is the incomplete understanding of how to make selective and energetically well-aligned contacts. For example, the Grätzel group developed ZnO/TiO₂ “overlayers” for Cu₂O photocathodes with the aim to offer protection against photocorrosion, but did not yet explicitly refer to these layers as being electron selective.^[377] This work inspired one of our first attempts to fabricate an all-oxide multijunction device by combining a BiVO₄ photoanode with a Cu₂O photocathode.^[378] This device showed STH efficiency of only 0.5% due to a combination of a modest photovoltage and poor FF. One reason for this was the poor band alignment of the Al-doped ZnO overlayer with the Cu₂O, which limited the Cu₂O photovoltage to \approx 0.5 V. Grätzel et al. later improved on this by switching to a Ga₂O₃ overlayer, resulting in an improved photovoltage of 1 V and STH efficiency of 3% for their Cu/Cu₂O/Ga₂O₃/TiO₂/NiMo photocathode.^[32]

Back contacts also need to be charge selective. For n-type metal oxide photoabsorbers, this can often be achieved by simply using commercially available F-doped SnO₂-coated glass (FTO). FTO glass is, however, not a good back contact for p-type oxides, such as CuBi₂O₄. Song et al. solved this by inserting a hole-selective Cu-doped NiO layer in between FTO and CuBi₂O₄.^[379] Making an electron-selective front contact for CuBi₂O₄ photocathodes is more challenging. Song et al. attempted this with a CdS/TiO₂ layer, but the presence of defect states at the CuBi₂O₄/CdS interface limited the photovoltage of \approx 0.65 V. As a result, their all-oxide CuBi₂O₄/BiVO₄ water-splitting device required an external bias of 0.4 V before any hydrogen could be detected.^[380] There are a handful of examples of truly integrated oxide-based tandem devices, in which the bottom absorber, typically silicon, serves as the back contact for the metal oxide top absorber. Here, it is interesting to note that obtaining a good silicon/ α -Fe₂O₃ junction seems trivial,^[381] whereas integration of silicon with BiVO₄ requires a more complicated Si/SiO_x/TiO₂/WO₃/BiVO₄ structure to avoid excessive photovoltage losses.^[382]

Another promising strategy to improve charge separation in metal oxides is to use doping. Abdi and van de Krol used a doping gradient to improve the charge separation efficiency in an n⁺n homojunction of BiVO₄, an approach that is analogous to the use of a BSF in PV.^[35] Their gradient doping strategy is especially suited for improving charge separation in highly doped

semiconductors, such as metal oxides. In contrast to conventional PV materials, metal oxides typically require high dopant concentrations to reach conductivities high enough to minimize Ohmic losses during charge transport. This is a direct consequence of the low charge carrier mobilities in most oxides.^[282] In some cases, doping can also be used to change a material from *n*- to *p*-type or vice versa. Abdi et al. used this to form a gradual *p*-*n* homojunction in BiVO₄ by calcium doping, resulting in a buried junction with improved charge carrier separation efficiency.^[383]

Although the STH efficiencies of multijunction oxide-based PEC devices are well behind those demonstrated for state-of-the-art III-V semiconductors, their low cost and relative ease of preparation render them well suited for scale-up studies. In their 50 cm² silicon/BiVO₄ multijunction PEC demonstrator, Ahmet et al. showed that ionic transport losses in the electrolyte can easily lead to a factor of 3 reduction in STH efficiency when scaling up from 1 to 50 cm²,^[384] illustrating the urgent need for creative PEC engineering solutions.^[39]

Most efforts on metal oxide absorbers in the past decades have focused on achieving high photocurrents. This has been invaluable for the initial selection of promising absorbers, the development of passivation strategies for bulk and surface defects, and the selection of suitable HER and OER cocatalysts. Further development of oxide absorbers for efficient PEC devices requires a shift in focus toward the photovoltage. This necessitates the design of selective contacts and smart (gradient) doping

strategies. Careful study of established design principles^[385] and close collaborations with colleagues from the field of PV will strongly benefit these efforts.

6.4. Halide Perovskites (HaP)

In recent years, HaPs have gained prominence as cost-effective, solution-processed semiconductor materials. Their high efficiency, processability, and tunability make them ideal candidates for constructing leaf-like structures. Nevertheless, their inherent ionic nature poses the primary challenge when implementing HaP in PEC devices, as they are prone to spontaneous dissolution in aqueous environments. In this section, we aim to highlight the benefits of HaP through examples applied to PEC devices that overcome the stability limitation. We recommend that readers refer to recent reviews for an in-depth exploration of developments in this field.^[386–388]

HaPs are ideally suited for fabricating tandem solar cells due to their ability to finely adjust bandgaps through compositional engineering. This allows them to serve as both the top and bottom cells in tandem solar cell architectures, leading to remarkable efficiencies. Notably, Si/HaP tandems have achieved a record-breaking efficiency of 33.9%,^[64] while all-perovskite tandem structures have demonstrated an impressive 28% efficiency.^[389] Fehr et al.^[62] uses the record Si/HaP from HZB as integrated photoelectrode. Here, a conductive adhesive barrier allows the integration of impermeable graphite sheets with

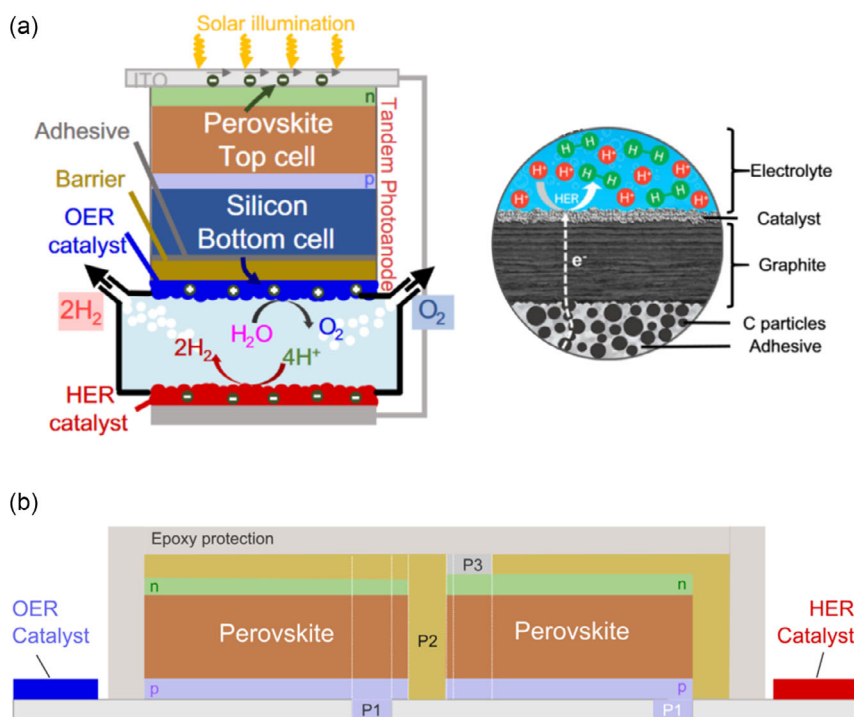


Figure 24. Different protection strategies for the integration of HaP in PEC devices. a) Silicon/Perovskite tandem structure utilizing a graphite/adhesive protection layer, effectively preventing direct contact between the absorber and the electrolyte without compromising PV performance. This configuration has achieved a noteworthy record STH efficiency of 20%. b) Interconnection scheme for HaP integration; through the sequential scribing process (P1, P2, P3), the incorporation of HaP is achieved with minimal impact on the active area. Notably, this approach enables the attainment of cell potentials exceeding 2 V, sufficient for driving unassisted water splitting. Reproduced under terms of the CC-BY license.^[62] Copyright 2023, The Authors. Published by Nature Communications, and Adapted with permission.^[393] Copyright 2023, Wiley.

minimum losses in the PV device, as shown in the panel (a) of **Figure 24**. This approach demonstrates an integrated device with STH of 13.4% for interconnected perovskite and 20.8% using Si/HaP tandem device with decrease of 60% of their efficiency in 100 h. This represents the first nonconcentrator PEC device to exceed 20% STH. In a similar approach, Song et al.^[390] used a conductive paste of carbon/silver to adhere a platinum foil to a perovskite/perovskite tandem device achieving STH of 15.1%. This design enables the continuous operation of the device for more than 120 h with less than 5% efficiency loss.

The high absorption coefficient of HaP and their low-temperature processability allow the fabrication of lightweight and flexible substrates. Virgil et al.^[391] exploited this concept fabricating a leaf structure using HaP and BiVO₄ to provide unassisted CO₂ reduction and hydrogen generation. The barrier protection was achieved using a mixture of epoxy adhesive and graphite powder, serving as a conductive encapsulant. Here efficiencies of solar-to-fuel of 0.58% (H₂) and 0.053% (CO) were achieved.

HaP offer a wide range of scalable processability routes ranging from inkjet printing and slot-die coating to coevaporation. Large-scale designs are required to validate the implementation of artificial leaf designs on practical applications. In an excellent example of the potential of perovskites for large-area, Li and Unger demonstrated a highly efficient and large-area HaP PV device with efficiency over 22% using slot die.^[392] These designs can be extrapolated into leaf architectures, as shown in the panel (b) of **Figure 24**.^[393] Here, a 16 cm² module with efficient sub-cells connection was used as monolithic PEC device and an epoxy encapsulation allows perovskite immersion in the electrolyte. STH efficiency of 11.56% was achieved with a stability of 85 h.

The interest toward halide-based semiconductors has greatly increased due to rediscovery of the HaP. The interest in environment friendly substitutes of lead-based perovskites and water-resistant materials has driven the research to a new set of materials with a wider range of stoichiometries and super-structures, for example, double perovskites, Ruddlesden-Popper phases, Aurivillius, and Dion-Jacobson phases.^[386] As an example, Romani et al.^[394] showed a water-resistant perovskite-inspired structure DMASnBr₃, which in conjunction with g-C₃N composite achieved a photocatalytic hydrogen generation of 1.7 mmol g⁻¹ h⁻¹. Novel combinatorial research studies would be critical to assess rapidly new perovskite-inspired materials and their viability on PEC devices.

In summary, HaPs have emerged as a transformative force in the landscape of artificial leaf applications. Their exceptional properties, such as high efficiency, tunability, and ease of fabrication, position them as game changers in the field of PEC devices. While addressing the challenge of stability of HaP in aqueous environments is an ongoing endeavor, innovative solutions are actively being pursued.^[395,396]

7. Long-Term Approaches and Their Perspectives

7.1. Nanostructuring, Patterning, and Improved Kinetics

For around two decades, nanowires have been considered as alternative building blocks with increased versatility for (opto-) electronic applications and, since recently, also for water

splitting.^[157,397–399] Wires of almost any semiconductor material can be grown as low-cost, nanoscale structures, largely independent of the substrate used, and they can uniquely absorb, convert, and emit light. Hence, structuring of light absorbers and catalysts of a photoelectrode is an alternative approach to enhance solar-driven water splitting performance. Structured light absorbers with precisely controlled morphologies and micro-/nanoscale dimensions enable the efficient coupling of sunlight into the photoelectrode for maximizing solar energy harvesting efficiency.^[400,401]

Compound semiconductor nanowires offer a versatile range of design options, including core-shell and/or axial multijunction heterostructures. Specifically, core-shell components of solar cells or PEC cells possess short transport paths for electrons and holes to reach interactive sites for performing electrocatalytic water-splitting reactions.

To reduce overvoltage losses, micro- and nanostructured catalysts can provide a much larger surface area compared to planar catalysts. This increases the number of active sites per geometric area at the catalyst/electrolyte interface. The geometries and dimensions of structured light absorbers and catalysts can be adjusted to optimize their interplay and improve performance. To enable possible future industrial implementation of nanowire applications, it is necessary to use the bottom-up layer growth approach, since this could lead to more cost-effective and efficient fabrication techniques in the future.

This section covers nanowire arrangements for solar energy conversion as well as selected catalyst nanostructures for efficient (photo-)electrochemistry.

Vertical semiconductor nanowires from materials such as III-V, Si, or ZnO have been prepared and studied as light absorber device structures to improve light-harvesting efficiency, shorten carrier collection pathways, and promote charge carrier transfer.^[402–404] The current status of nanowire devices, such as transistors,^[405] light-emitting diodes,^[406] solar cells,^[401] or PEC cells^[157] is reaching a high level of saturation for the most important classes of benchmarking applications. However, in all these cases, they have not yet outperformed their counterparts made of planar semiconductor layer structures.

Although significant progress has been made, research on nanowire devices is still in its early stages. It is at the intersection of physics and engineering, rather than on the subsequent transition from superior engineered performance to the success of commercial products. Even though theoretically superior to planar cell structures, in practice, the choice of suitable bandgaps, band alignment, well-defined doping, and in particular complementarily modulated doping structures (n- and p-type) of homo- and heterostructures to optimize the unique and the most important properties of semiconductor nanowires is a complicated endeavor. An important aspect of functionality is the use of charge-separating contacts surrounding the absorber materials with bandgap-engineered homo- and heterostructures. In planar layer stacks, this paved already the way to the success of (opto-)electronic devices such as transistors, light-emitting diodes (LEDs), LASERS, and efficient solar cells. The possible transfer of this success to nanowires requires well-defined, modulation-doped junctions with ultimate performance and properties not available in layered structures. Although there have been impressive advancements in nanowire growth and designs, the

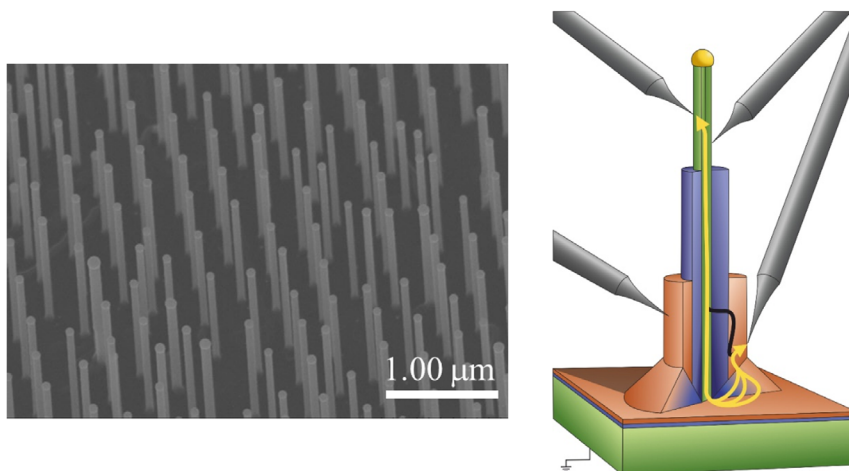


Figure 25. Each individual nanowires shown in the SEM image (left) is acting as a nano-antenna for light collection and concentration^[417] and can be analyzed in detail with regard to doping profiles, local resistance, current pathways, and (opto-)electronic response utilizing a UHV-based multi-tip STM (right). Here, the performance of a core-shell-shell *p-i-n*-structure for charge carrier separation is characterized. Adapted with permission.^[411] Copyright 2022, Wiley.

efficiency of light-to-current and current-to-light transformation in devices such as nanowire-based PEC and solar cells, light emitters, and detectors remains limited, clearly not superior to the planar counterparts, because of huge losses during electronic transport due to current leakage pathways.^[407–410] This can be due to inadvertent conductivity channels in the nanowire arrangement, as shown in **Figure 25**,^[411] when four-terminal probing was applied on free-standing, *p-i-n* (core-shell-shell) nanowires, or due to insufficient charge carrier separation due to defect-assisted tunneling. A similar problem holds for the bipolar heterojunction transistor that suffers from excessive leakage in the base-collector and base-emitter junction inhibiting a net current gain of the transistor.^[412] One hypothesis for the increased losses is that benchmarking nanowire devices with embedded *p-n* junctions is limited by leakage currents. Identifying leakage mechanisms and demonstrating low leakage as well as sufficiently charge-selective contacts are major issues in any case when benchmarking nanowire device components.

Even in the best available nanowire with III–V compound *p-n* junction, the saturation current density J_0 is substantially higher than in their layered counterparts. Possible reasons are manifold, among others. First, the growth direction in nanowires is (111) compared to (100) in layer growths. This results in complex growth mechanisms^[413] due to imperfect doping profile and the evolution of defects and modified and anisotropic charge transport. Second, doping during nanowire growth is physico-chemically different from layer doping^[411,414] and is taking place at substantially different growth parameters. Third, the surface-to-volume-ratio and contributions from surface transport in axial junctions are much increased in nanowires compared to layer structures.

The reverse saturation current density $J_{0,NW}$ in III–V nanowires could be reduced by physicochemical treatment of axial junction (passivation of surface states),^[415] including wide-bandgap shells for surface passivation of axial junctions,^[401] bandgap engineering of radial charge-selective junctions,^[243,412]

top-down processing of semiconductor layers to nanowires,^[400] or semiconductor layer growth for one of the contacts and nanowire growth for the other one.^[416]

Nanowire PV devices exhibit a significantly improved light absorption coefficient,^[400,401] exceeding the absorptivity of analogous layer structures and collecting light in a wide vicinity of the individual nanowire, virtually operating as optical nanoantennas.^[417,418] Hence, at a given photon current intensity I_{photo} , nanowire-based solar cells of the area A_{cell} can be assumed to concentrate light into the sum of all nanowire footprints ΣA_{NW} with a factor C smaller than $A_{\text{cell}} = C \times \Sigma A_{\text{NW}}$. Hence, the photocurrent density $J_{\text{photo,NW}}$ within each nanowire is enhanced by the factor C .

$$J_{\text{photo,NW}} = C \cdot J_{\text{cell}} = C \cdot \frac{J_{\text{photo}}}{A_{\text{cell}}} \quad (1)$$

The solar-generated splitting of quasi-Fermi levels in the nanowires causes an open-circuit voltage, V_{OC} , and the current I_{photo} directed internally via charge carrier separation in suitable hetero-(*p-n*)contacts. With the concentration factor C , at open-circuit conditions, the open circuit voltage $V_{\text{OC,NW}}$ amounts approximately to

$$V_{\text{OC,NW}} = n \cdot \frac{k_B T}{e} \cdot \ln \left(\frac{J_{\text{photo,NW}}}{J_{0,NW}} \right) = n \cdot \frac{k_B T}{e} \cdot \ln \left(C \frac{J_{\text{cell}}}{J_{0,NW}} \right) \quad (2)$$

with the ideality factor n of the diode. Therefore, $V_{\text{OC,NW}}$ should increase in nanowire-based solar cells with increasing $\ln C$. So far, nanowire-based solar cells suffer from an even lower open-circuit voltage^[419] compared to standard layer cells.^[420]

The limited number of nanowire-based PV device demonstrations with promising results have shown in general a reduced material consumption,^[399] reduced saturation current J_0 values by wide-gap surface passivation,^[401] or used top-down processes (e.g., for the record solar cell conversion efficiency of 17.6 %).^[400]

The latter approach avoids both the (111) growth direction and the low-temperature growth of nanowires, but does not provide any advantage compared to the layered devices. Wide-bandgap passivation of nanowires suppresses nonradiative minority charge carrier recombination at the nanowire surface such as AlGaAs reported by Åberg et al.^[401] Instead, the probability of radiative recombination is increased by many orders of magnitude and, correspondingly, the saturation current density J_0 is decreased. In core-shell nanowires, losses across the p-n junction can be reduced by inserting a well-designed radial charge carrier-selective contact instead.^[45]

Finally, the excessive reverse junction current in nanowire p-n junctions is attributed to a high defect density and a severely increased probability of reverse charge carrier transfer through a selective contact. The defect density originates from different sources, such as the huge surface and the various imperfections at the interfaces of crystal facets at the nanowire edges.

Ordered arrays of epitaxial nanowires can be grown by the industrial scalable process of MOVPE after applying a surface nanopatterning technique. Different surface nanopatterning techniques can be used here. For example, Si wafers with disordered nanograin structures have been used as templates for the fabrication of Ni nanorods-based hierarchical structures as excellent catalysts for both HER and OER.^[170,171,421] Moreover, a surface nanopatterning technique using ultrathin aluminum anodic oxide template (UTAM) as template is an efficient approach for large-scale surface nanopatterns of functional materials.^[422] These UTAM-prepared surface nanopatterns can be utilized as catalysts or shadowing masks for fabricating regular arrays of nanowires and nanotubes of different light absorber materials. Additionally, this UTAM-based nanopatterning technique can also be applied in order to fabricate HER/OER catalysts into regular nanopatterns on the surface of planar absorbers, aiming 1) to prepare well-defined catalyst adsorption sites for a controlled site and size distribution of the catalyst materials; and 2) to reduce the influence of the surface coating of catalysts on the light absorption of the absorber material. The interdependence between structural parameters, catalyst distribution, doping profiles, charge carrier dynamics, and HER/OER kinetics can be investigated by applying advanced in system, in situ, and

operando characterization techniques, as illustrated in **Figure 26** with some specific techniques, such as optical spectroscopy^[125] or advanced sample handling.^[423] Theoretical support regarding optical, structural, and electronic properties of nanostructures must be considered^[413] and nanostructured nanocomposites must be designed and fabricated to integrate absorbers and highly active catalysts in an adjusted composite design for HER and OER. As one promising approach, composites consisting of defect-engineered metal oxides (as cocatalysts) decorated with nanocluster catalysts may be considered.^[424,425]

These hierarchical nanostructures can be fabricated in different ways: 1) preparation of the metal oxide nanostructures on a planar absorber substrate; and 2) conformal coating of the metal oxide thin film on a nanostructured absorber substrate. The structural features and the combination of the composites shall be developed toward improved and efficient HER and OER, respectively. Highly ordered nanowire/nanopore arrays of conductive materials (e.g., metals and metal oxides/sulfides) can be designed and fabricated to serve as robust support for immobilizing HER/OER catalysts to increase the density of accessible active centers and the long-term durability. Furthermore, the HER and/or OER activity of catalysts can be optimized by manipulating the strong electronic interaction between the conductive materials and the supported catalysts. Moreover, the mass transfer process during the water-splitting reaction in the electrode can be tuned by optimizing the structural parameters of highly ordered nanowire/nanopore arrays to assure sufficient transport of reactants (e.g., OH^- , H_2O), favorable accessibility of the catalyst surface, and rapid release of gas bubbles (e.g., H_2 , O_2), aiming to promote HER and/or OER kinetics. Compared to the bulk electrolyte, the mobility of the protons and hydroxide ions (i.e., the mass transport) is affected by the interaction with the photoelectrodes and the gas bubbles. These phenomena are even more significant at the nanostructured electrolyte/photoelectrode interfaces. Ion diffusion is significantly impeded when the nanochannels are blocked by gas bubbles, and the desired increase in the active surface area through nanostructuring also increases the interactions of the ions with the electrode surface. The joint investigation of gas bubble dynamics and ion diffusion on different time and length scales offers a perspective for improvements to establish a comprehensive understanding of the mass transport in the nanostructured PEC devices and on gas-evolving electrodes in general. In particular, the information on the mobility of ions or proton transfer rates is crucial to adapt a multiscale approach for the simulation of ion conduction toward the systems used.

State-of-the-art multiphysics simulations of PEC cells use a single-diffusion coefficient to predict ion transport across the device and incorporate bubble flow and bubble scattering into a two-phase fluid flow model. This sophisticated model is already capable of simulating water splitting under concentrated irradiation.^[213]

However, the assumptions regarding mass transfer and bubble evolution and dynamics are quite strong, and a more realistic description, in particular the description of nanostructured electrode surfaces, requires considering many more phenomena. Nanostructuring is an important concept for the development of new PEC devices because it increases the catalytically active surface area. In these systems, the ion and bubble dynamics

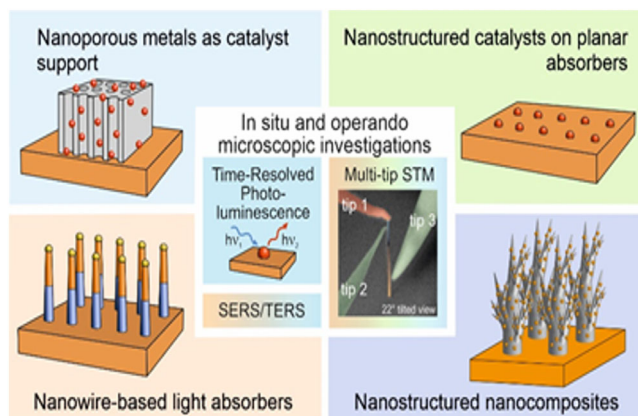


Figure 26. Possible nanostructural tuning of light absorbers and catalysts as well as the design and fabrication of nanostructured composites as highly active catalysts for HER and OER.

in the electrode/electrolyte region have to be explicitly studied with microscopic resolution (much larger resolution compared to multiphysics simulation).^[426] The ion diffusion coefficient depends on the spatial position within the interface and can no longer be described by a uniform value for the bulk phase.

The gas bubble dynamics and evolution depend on the wetting behavior and thus on the (nano)structure of the materials and the operating conditions (current density, pressure, temperature, pH, electrolyte, and concentration) and significantly affect the efficiency.^[194]

Gas bubble dynamics in nanostructured interfaces is related to ion diffusion because, for example, nanochannels can be blocked by gas bubbles. Therefore, the description of mass transfer in nanostructured interfaces must treat ion diffusion and gas bubble dynamics on the same footing. The development of these models is complicated because multiple time and length scales must be bridged even for simple nanostructured systems and reliable in situ in operando experimental techniques are necessary to provide data for the model validation. The effects of ion-electrode surface interactions on ion mobility and nucleation of bubbles at the electrode surface due to the combination of H and O atoms have to be modeled and studied with atomistic resolution, for example, using ab initio molecular dynamics simulations. In contrast, the further growth of the gas bubbles, their removal from the surface, and the influence of the topology of the nanostructure on ion diffusion must be simulated and studied on much larger time and length scales.

For the modeling of diffusion, Dreßler et al. already developed a model that can describe proton conduction in nanostructured fuel cell membrane materials by a combination of ab initio molecular dynamics and a Monte Carlo model.^[427–431] In the ab initio part, local proton transfer rates are sampled and in the Monte Carlo part, the actual propagation of protons on a dynamically evolving lattice is modeled. The development of a numerical model for the unified description of the dynamics of ions and bubbles with near-atomic resolution is an open and important task. Such a model could be coupled to the conventional multiphysics models in a further bottom-up step to include the effects of nanostructured electrodes.

7.2. Materials Selection and Criticality Issues

The innovations needed for efficient artificial leaf approaches (see Table 1) will only be possible and successful with an appropriate selection of noncritical materials. Considering the criticality aspects of materials, there are a number of criteria which must be maintained for technological applications on large scales. On a pure technological level, neglecting politically motivated supply vulnerabilities, these criteria include availability and related cost issues, stability and possible recycling perspectives, as well as environmental impact and health risks.^[432] The materials issues are of severe impact for PEC devices for solar fuel generation as different types and applications of materials must be considered as semiconductors for the PV component, catalysts for the EC reactions, and passivation layers for the contacts. For preparing integrated devices, the materials must be adjustable to each other, processable on each other, must be cost competitive, and durable at high-performance levels. As a mandatory

requirement for high-performance device structures, the selected materials must allow the transfer of the splitting of the EC potentials of electrons and holes as defined by the photovoltage induced in the light absorber (the PV component of the device) to the catalysts for HER and OER without severe potential losses. Also, the transfer of the light-induced minority charge carriers (photocurrents) must occur from the PV component to the EC reaction sites with minimized recombination losses approaching 100% quantum yields. For achieving these goals, the PV components, the catalysts, as well as the interfacial coupling layers required for the integration to devices must be selected to secure the efficiency as well as the materials criticality criteria. As one of the most relevant materials selection issues, we may consider at first the performance of the used materials either to be needed as PV absorbers, for example, considering the most efficient III–V semiconductors or the most efficient noble metal electrocatalysts for the HER and OER, for example, Pt and IrO₂ or RuO₂, or the selection of passivation and contact layers, for example, using In₂O₃. However in these cases, the criticality aspects of materials may fail in one or many different criticality aspects (Figure 27). In all these cases, alternative materials allowing similar performance would be welcome or minimized materials consumption or recycling strategies must be developed. In the search for non-critical elements used for PEC devices, the needed performance levels cannot be neglected. Alternative materials must have high-performance levels comparable to the best noncritical elements, as materials with low efficiency will not be beneficial.

There has been an ongoing discussion on which approach may be more promising in the selection of materials for the realization of competitive artificial leaf approaches: Concentrating on PEC devices, there are a fraction of scientists who argue that the most prominent perspective is to select stable and uncritical materials first and try to optimize the performance in a second step. Others like the authors of this conceptual review argue that the efficiency perspectives must be the first selection criteria and stability and recycling issues should be addressed in the second

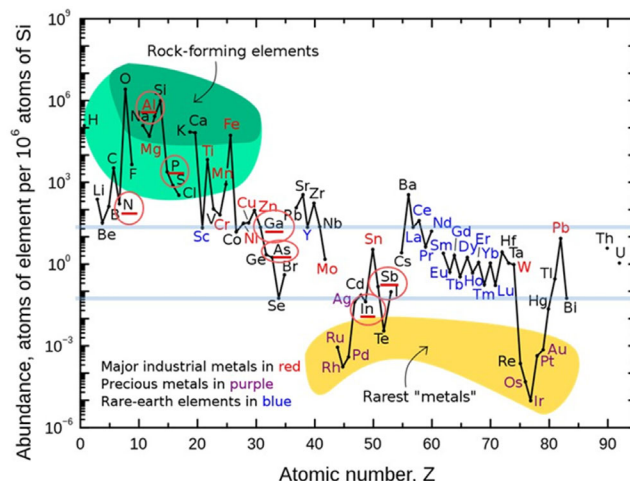


Figure 27. Abundance of different elements of the periodic table possibly of interest for the manufacturing of PEC devices for water splitting. As is evident from the presented data, many of the materials leading to high-performant PECs are composed of critical elements.^[450]

step. As already argued above within this review in very detail, the most promising approach is to first select the materials' properties which are relevant for achieving high performance. These must be investigated, understood, and implemented in benchmark devices. Afterward, either materials' criticality problems may be addressed by the minimization of the content of critical elements or by recycling strategies or using noncritical elements for stabilizing nonstable device structures. Most preferentially, of course, materials may be identified and chosen which provide similar performance-related physical and chemical properties or alternatively it must be clarified if and how these alternative materials can be modified to allow similar performance. As already mentioned earlier, there are also materials minimization and recycling strategies which may be implemented to use critical elements also in technological applications.

The central part of any artificial leaf approach is the absorber layer, where the conversion of solar radiation into free energy occurs and which must produce and separate the minority charge carriers efficiently, in order to approach the detailed balance limit.^[433] For this reason, the selection of proven tandem structures of using either III–V semiconductors and of Si/perovskite combinations should be investigated starting from efficient multiabsorber solar cells and using buried junction structures to be used in PEC cells.^[62,252,344,368] Additionally, novel promising chalcogenide absorbers may be of interest such as alloyed Zn(Cd)Te, Sb₂S₃, or BaZrS₃, which may provide cheaper and more stable thin-film wide-bandgap combinations in tandem architectures in the long term.^[72,73] Other chalcogenides such as chalcopyrites or kesterites do not provide promising solutions so far as their wide-band materials deliver only reduced photovoltages due the formation of inherent defects within the bulk and at the interfaces of these materials.^[434,435] For this reason, $\mu\text{c-Si/a-Si-H}$ tandem cells may not be of interest from a technological perspective as their maximum PV efficiency is limited to about 13%, which limits their STH efficiency to about 10%.^[12,29] Low-bandgap MOS may also not be in the focus as absorber layers; with reduced bandgaps related to the involvement of localized d-electron states, these materials inherently lead to limitation of photovoltage and photocurrent.^[436–438] However, they are of interest, utilized, and investigated as surface passivation, charge carrier-selective contacts, charge transfer, and most importantly as alternative cocatalyst layers.

So far, no efficient artificial leaf device was realized without the coupling of HER and OER (co-)catalyst materials to the absorbers. Hence, also the addition of well-known but also of novel (co-)catalyst materials should be investigated using different, soft deposition technologies matched to the absorber and passivation layers. In a first approach, established catalysts such as Pt and Ni will be used for HER and, for example, IrO₂ or RuO₂ for OER as a benchmark for the accessible efficiency values of the investigated absorber layer structures. This already provides an additional research area as the process- and preparation-dependent morphology and compositional structure of the interfacial coupling of the cocatalysts will determine the PEC and Faradaic efficiency.^[439–444] Additionally, reducing the materials consumption of the catalyst layers with 2D layer of reduced thickness or with 3D nanostructures or nanoporous morphologies may help to enhance the effective surface area with the amount of material. In parallel, new multinary oxide catalysts without or

with low noble metal content may be applied.^[147] However, as these oxides usually are electronic semiconductors, their doping and changes of doping induced during their EC exposure must be considered for their application on the PV components. Furthermore, their composition and related electronic and catalytic properties will strongly depend on the applied deposition technology. Successively, novel (co)catalysts arrangements and components have to be integrated with the components of the absorber layer structure toward working device structures.

Finally, the integration into complete artificial leaf structures/PEC cells with high performance leading to above 15% STH efficiency will only be possible if well-adapted chemical and electronic passivation and transfer layers can be realized using adapted soft processing and deposition recipes. The loss of bulk translational symmetry of the absorber surfaces and interfaces generally gives rise to unfavorable electronic defect states for nearly all semiconductors. Additionally, most of the considered absorber materials will not be stable in direct contact to the electrolyte solutions. Even stable originally existing passivation layers usually form new and detrimental electronic states on the absorber surfaces after the adsorption of chemical intermediates during multielectron transfer reactions. Thus, at first, contact layers must be designed securing the desired electronic and chemical passivation also during operational conditions. For this purpose, wide-bandgap metal oxides such as TiO₂ are often tested,^[140] but may be substituted with oxides of lower or higher work functions (e. g. ZrO₂, In₂O₃ or Ga₂O₃, NiO). The required chemical and electronic passivation may be either reached by chemical bond formation to the defect states at the surface or interfaces or may be induced by high doping concentrations within the passivation layers shifting the formation of the space charge layers into the interior of the absorbers. Either nondoped very thin passivation layers working as tunneling barriers or highly doped thicker interface layers working as carrier transporting contacts may be considered. In any case, these additional layers must be free of unfavorable electronic defects states leading to Fermi-level pinning within or at the interface of these (oxide) or passivation layers. These additional electronic defect related effects within the passivation or contact layer must not lead to a noticeable loss of photovoltage and photocurrent but must allow for an efficient selective contact for charge carrier transfer either of the electron for the HER or of holes for the OER) to the (co-)catalysts without Ohmic losses or charge carrier trapping. As it is immediately evident, these interfacial passivation, contact, and charge transfer layers may even be complex compositions of different materials, which must be specifically adjusted to the absorber in use. As a consequence, different materials must be investigated to secure high performance. Additionally, different soft deposition techniques must be tested and optimized to avoid a growth-related deterioration of predeposited layers. This is also true for the final integration with the catalyst layer by applying specific deposition techniques.

Summarizing the above presented considerations, it is evident that the selection of appropriate materials plays a dominant role for reaching high performance without running into materials related constraints. First, a broad range of materials and processing procedures need to be investigated which primarily should fulfill performance considerations before materials criticality aspects must also be considered.

8. Conclusion

There have been, and still are, large research centers in the USA that aim to produce chemical fuels from sunlight, such as the Joint Center for Artificial Photosynthesis (JCAP), the Liquid Sunlight Alliance (LISA), and the Center for Hybrid Approaches in Solar Energy to Liquid Fuels (CHASE), all funded by the US Department of Energy. With the exception of the initial phase of JCAP (2010–2015), these centers all tend to focus their actual research goals on solving fundamental research challenges related to photodriven conversion of CO₂ into higher-value hydrocarbon fuels, while also addressing the oxidation of H₂O to O₂.^[445] Due to the higher overvoltages expected for the CO₂ electroreduction, the demands for reaching higher photovoltages from the PV component are even enlarged. Therefore it seems a reasonable approach to solve the challenge of scalable, efficient, and durable production of green hydrogen from sunlight and water before addressing the more demanding photodriven CO₂-to-CH conversion. Considering the rather similar multidisciplinary challenges directed to the design of multiabsorber PEC cells, one needs to address, understand, and solve the open fundamental questions and challenges in solar water splitting at first that currently hamper implementation. For reaching this goal, the scientific community must identify and address the main performance limitations in individual absorbers and electrocatalysts. Additionally, we must develop a comprehensive understanding of how these materials interact with each other and what occurs at and across their different interfaces. Controlling both the bulk properties and the properties of solid/solid and solid/liquid interfaces is a key challenge that requires a holistic, interdisciplinary approach. Specific emphasis must be put on the development of materials integration strategies with regard to their respective functionality in the device, their electronic alignment, and their structural compatibility. Especially, the role and origin of possibly formed electronic defects must be analyzed and controlled to reach targets for the respective materials' properties. For that, we require innovative experimental techniques and a strong collaboration between theory and experiments to deduce promising materials and material structures. With the expected results on novel material compositions and their combinations, a scientific and industrial TRL can be possibly reached, where the bias-free STH efficiencies and the long-term stability of PEC water-splitting devices can be pushed to new limits.

Aside from multiabsorber cells, understanding the limitations of individual components under various conditions and operational environments poses a significant challenge for fundamental science that can be addressed only by systematic studies. This should be done using the comprehensive set of established experimental and theoretical methodology available today for the fabrication and characterization of semiconductor structures, PEC junctions, and electrocatalysis. Next to that, the challenge is to shift the borders of the established experimental and theoretical methodologies to novel specifically adopted and/or still missing experimental techniques, which have not been applied yet or are in development for the investigation of (P)EC interfaces. In combination with detailed theoretical studies on the electronic structure of involved materials and their interfaces, one needs to create new scientific knowledge and insights, using machine

learning approaches, DFT calculations, and data mining. The coupling of novel absorbers to highly efficient tandems needs to be guided by computational and experimental interface engineering, high-resolution X-ray, mid infrared (MIR)-NUV, and vibrational spectroscopy with high chemical specificity and sensitivity. A specific and unique aspect is the construction and application of novel spectroscopic liquid–solid interface studies utilizing synchrotron radiation and the use of a complementary tender X-ray spectroscopy allowing for comprehensive in situ core level and VB spectroscopy on model systems as well as photoelectrodes approaching technology readiness. The core-level and VB methods should be extended with TR techniques such as 2PPE/2PPE) experiments and TR operando spectroscopy. These techniques include absorption, emission (PL), and ellipsometry featuring highest temporal resolution to capture and understand the complete chain of events from charge carrier generation–separation–transport in the bulk and across interfaces to recombination. Additionally, the influence of interfacial chemical reactions at the photoelectrode, multielectron charge transfer reactions for HER and OER in competition to degradation effects and stability determining processes must be studied in PEC junctions. From this, design principles for improved PEC cells and full devices can be derived and implemented. The perspective to efficient artificial leaf devices can, therefore, be divided into three different but strongly interrelated research actions:

8.1. Research Action 1: Understanding

The main objective must address fundamental knowledge gaps on contact selectivity, electronic band alignment, charge carrier dynamics, and EC surface and interface reactivity. Charge-selective contacts and electronic passivation layers must be prepared and investigated for selected absorber materials, especially wide-bandgap top absorbers, to study their influence on the extractable photovoltage and photocurrent. A key challenge is the identification and adjustment of electronic surface and interfacial states across the different junctions under operation conditions. This must be complemented with experimental and theoretical charge carrier dynamics studies on model absorber materials for a wide range of timescales (fs–s). In parallel, HTP computational screening studies must be initiated to identify promising new absorber materials. To gain insight on (P)EC surface reactivity, the structure–property relationships of a first series of many thin-film and 2D layered electrocatalysts with their support need to be investigated and generally applicable design rules must be identified if possible. To this goal, the energetic alignment of selected absorber/passivation layer/catalyst interfaces, as well as selected solid/liquid interfaces, must be studied with a variety of (P)EC, photon-, and electron-based spectroscopy methods.

8.2. Research Action 2: Design

The novel insights and understanding generated in research action 1 must be used in designing increasingly efficient and robust photoelectrode assemblies and tandem devices. Here, novel top absorbers must be identified and paired with optimized

bottom absorbers and further improved with regard to the energetic alignment. Selected nanostructured absorber/catalyst assemblies need to be tuned to improve performance and stability and enable optimal integration in tandem devices. These efforts must be guided by (P)EC dynamics studies, which can be extended to 2D and 3D systems. These studies can then form the basis for more extended (P)EC engineering studies on charge and mass transport in the liquid phase. Furthermore, there is the need to expand the materials portfolio by synthesizing promising new materials predicted by HTP computational screening efforts. To address more complex device structures, the ultrafast studies on charge carrier dynamics must be extended to more complex absorber materials, such as ternary compounds, for example, composed from metal oxides or chalcogenides. Additionally, these studies, together with studies on electrocatalyst/support interactions, must be carried out in increasingly realistic and harsh environments to further develop our understanding of materials and interfaces under operating conditions, such as elevated temperature, prolonged solar irradiation, atmospheric pressures, and liquid environment. The results gained from the investigations or more complex materials artificial leaf configurations will lay the scientific basis for a knowledge-based design of improved and possibly competitive new generations of materials for absorbers, catalysts, and functional layers such as passivation layers.

8.3. Research Action 3: System and Technology Considerations Based on the 12 Principles of Green Engineering.

Finally, system considerations come into play following the principles of green engineering,^[446] which are essential for any technological implementation of artificial leaf devices. For large-scale systems, Ohmic losses as well as the formation of pH gradients will play an increasingly important role and can easily lead to large efficiency losses and materials degradation. (P)EC device and engineering investigations and development efforts should include multiscale modeling as early as possible to identify and minimize transport-related losses and guide efforts to select and further optimize the device and system design. In addition, machine learning algorithms for inverse design strategies can hopefully be developed to predict optimal device configurations and new material combinations. We are convinced that optimized tandem devices will provide the most promising systems for an efficient and competitive artificial leaf device. These devices must be subjected to extensive performance benchmarking, long-term stability testing, and industrial manufacturing studies. For any new technology, materials criticality and circularity have to be considered at an early stage. Here, integrated PEC systems, while more difficult to design, offer a compelling advantage over PV-powered electrolyzers, since their lower current densities offer the possibility to substitute Pt- and Ir-based catalysts with abundant, noncritical alternatives. The end of life of the device will be investigated with the goal of recovering as much of the raw materials as possible. Determining the technological applicability of monolithically integrated artificial leaves for a future sustainable energy economy, in comparison to electrically connected PV-electrolyzer combinations, depends also on various factors. These include system size and further environmental

parameters such as temperature and illumination conditions and understanding how these devices perform under realistic operating conditions. At this time, PV electrolyzer systems have the advantage due to their technological maturity. They benefit from their much higher current densities, show superior efficiencies and durability, and the components can be individually optimized. Integrated PEC systems offer a path toward the next generation of solar fuel technology that is more resource efficient (abundant catalysts, fewer system components) and potentially more efficient in terms of energy conversion due to the inherently easy thermal coupling between absorber and catalyst. Such systems are, however, more difficult to design and therefore still in a much earlier stage of development. Future areas of application for both technologies will depend on both technoeconomic and sustainability considerations, and trade-offs will have to be made. A full assessment requires concerted research efforts that address the following knowledge gaps: 1) incomplete understanding of fundamental aspects of contact selectivity, electronic band alignment, and charge dynamics in PEC systems; 2) lacking insights in materials compatibility and integration challenges to enable the design of efficient photoelectrode assemblies; and 3) missing expertise on PEC systems engineering and device fabrication technology for large-scale implementation of artificial leaf devices. Here, the ultimate aim is the development of optimized tandem devices with extensive performance testing and consideration of materials criticality for a sustainable energy economy.

Acknowledgements

The authors express gratitude for financial support provided by the German Federal Ministry of Education and Research (H2Demo project no. 03SF0619 and DEPECOR project no. 10033RC021) and German Research Foundation (DFG project PAK 981, project nos. HA3096/14-1, JA859/35-1, RU1383/6, KR4816/1-1; NSF-DFG project no. HA3096/19-1). W.J. acknowledges additionally the support by DFG priority programme 1613, Ja 859/26-1, and Ja 859/26-2, and Excellency graduate school DFG GSC 1070. The authors acknowledge Juliane Koch for providing the material used in Figure 25.

Conflict of Interest

The authors declare no conflict of interest.

Keywords

buried junctions, catalyst integrations, interface engineering, photoelectrochemistries, semiconductor tandem cells, solar hydrogen formations, water splitting

Received: December 17, 2023

Revised: March 4, 2024

Published online:

[1] *Stellungnahme: Künstliche Photosynthese. Forschungsstand, Wissenschaftlich-Technische Herausforderungen Und Perspektiven*, Acatech – Deutsche Akademie Der Technikwissenschaften E. V. (Federführung); Deutsche Akademie Der Naturforscher Leopoldina

- E. V. – Nationale Akademie Der Wissenschaften, Union Der Deutschen Akademien Der Wissenschaften E. V., München **2018**.
- [2] B. Tumas, J. Dempsey, T. Mollouk, S. Ardo, K. Bren, A. Rappe, W. Shaw, H. Abruna, H. Atwater, K. Ayers, C. Berlinguette, J. Concepcion, V. Cooper, D. Esposito, J. Gregorie, L. Hammarstrom, S. Haussener, F. Houle, S. Linic, H. Shafaat, Y. Shao-Horn, W. Smith, Y. Surendranath, D. Tiede, J. Yang, *Report of the Basic Energy Sciences Roundtable on Liquid Solar Fuels*, USDOE Office of Science (SC), Washington, DC **2019**.
- [3] S. Linic, *Chem. Eng. News* **2018**, 96, 2.
- [4] R. van de Krol, B. A. Parkinson, *MRS Energy Sustainability* **2017**, 4, E13.
- [5] J. Garcia-Navarro, M. A. Isaacs, M. Favaro, D. Ren, W. J. Ong, M. Grätzel, P. Jiménez-Calvo, *Global Challenges* **2023**, 7, 2300073.
- [6] M. M. May, D. Lackner, J. Ohlmann, F. Dimroth, R. van de Krol, T. Hannappel, K. Schwarzburg, *Sustainable Energy Fuels* **2017**, 1, 492.
- [7] M. T. Spitler, M. A. Modestino, T. G. Deutsch, C. X. Xiang, J. R. Durrant, D. V. Esposito, S. Haussener, S. Maldonado, I. D. Sharp, B. A. Parkinson, D. S. Ginley, F. A. Houle, T. Hannappel, N. R. Neale, D. G. Nocera, P. C. McIntyre, *Sustainable Energy Fuels* **2020**, 4, 985.
- [8] R. van de Krol, M. Grätzel, *Photoelectrochemical Hydrogen Production (Electronic Materials: Science & Technology)*, Springer, New York, IN **2012**.
- [9] *Photoelectrochemical Water Splitting: Materials, Processes and Architectures* (Eds: H.-J. Lewerenz, P. Laurie), Royal Society of Chemistry, Cambridge, UK **2013**.
- [10] M. G. Walter, E. L. Warren, J. R. McKone, S. W. Boettcher, Q. Mi, E. A. Santori, N. S. Lewis, *Chem. Rev.* **2010**, 110, 6446.
- [11] I. Holmes-Gentle, S. Tembhurne, C. Suter, S. Haussener, *Nat. Energy* **2023**, 8, 586.
- [12] F. Finger, K. Welter, F. Urbain, V. Smirnov, B. Kaiser, W. Jaegermann, *Z. Phys. Chem.* **2020**, 234, 1055.
- [13] E. Kemppainen, R. Bagacki, C. Schary, F. Bao, I. Dorbandt, S. Janke, Q. Emery, B. Stannowski, R. Schlattmann, S. Calnan, *Energy Technol.* **2023**, 11, 2201081.
- [14] S. Tembhurne, F. Nandjou, S. Haussener, *Nat. Energy* **2019**, 4, 399.
- [15] Z. Pan, R. Yanagi, Q. Wang, X. Shen, Q. Zhu, Y. Xue, J. A. Röhr, T. Hisatomi, K. Domen, S. Hu, *Energy Environ. Sci.* **2020**, 13, 162.
- [16] K. Sivula, R. van de Krol, *Nat. Rev. Mater.* **2016**, 1, 15010.
- [17] F. Dimroth, M. Grave, P. Beutel, U. Fiedeler, C. Karcher, T. N. D. Tibbitts, E. Oliva, G. Siefert, M. Schachtner, A. W. Wekkeli, A. W. Bett, R. Krause, M. Piccin, N. Blanc, C. Drazek, E. Guot, B. Ghyselen, T. Salvetat, A. Tauzin, T. Signamarcheix, A. Dobrich, T. Hannappel, K. Schwarzburg, *Prog. Photovoltaics* **2014**, 22, 277.
- [18] C. A. Nelson, N. R. Monahan, X. Y. Zhu, *Energy Environ. Sci.* **2013**, 6, 3508.
- [19] A. Al-Ashouri, E. Köhnen, B. Li, A. Magomedov, H. Hempel, P. Caprioglio, J. A. Márquez, A. B. M. Vilches, E. Kasparavicius, J. A. Smith, N. Phung, D. Menzel, M. Grischek, L. Kegelmann, D. Skroblin, C. Gollwitzer, T. Malinauskas, M. Jošt, G. Matič, B. Rech, R. Schlattmann, M. Topič, L. Korte, A. Abate, B. Stannowski, D. Neher, M. Stollerfoht, T. Unold, V. Getautis, S. Albrecht, *Science* **2020**, 370, 1300.
- [20] S. Hu, C. Xiang, S. Haussener, A. D. Berger, N. S. Lewis, *Energy Environ. Sci.* **2013**, 6, 2984.
- [21] L. Gao, Y. Cui, R. H. J. Vervuurt, D. Van Dam, R. P. J. Van Veldhoven, J. P. Hofmann, A. A. Bol, J. E. M. Haverkort, P. H. L. Notten, E. P. A. M. Bakkers, E. J. M. Hensen, *Adv. Funct. Mater.* **2016**, 26, 679.
- [22] A. E. Delahoy, S. C. Gau, O. J. Murphy, M. Kapur, J. O'M. Bockris, *Int. J. Hydrogen Energy* **1985**, 10, 113.
- [23] A. J. Nozik, *Appl. Phys. Lett.* **1976**, 29, 150.
- [24] O. Khaselev, J. A. Turner, *Science* **1998**, 280, 425.
- [25] J. Hu, F. Zhu, I. Matulionis, A. Kunrath, T. Deutsch, L. Kuritzky, E. Miller, A. Madan, in *Proc. European Photovoltaic Solar Energy Conf.*, Vol. 23, Valencia, Spain, August **2010**, p. 69.
- [26] I. Matulionis, J. Hu, F. Zhu, J. Gallon, N. Gaillard, T. Deutsch, E. Miller, A. Madan, in *Solar Hydrogen and Nanotechnology V*, Vol. 8, SPIE, Bellingham, Washington, USA **2010**.
- [27] R. E. Rocheleau, E. L. Miller, A. Misra, *Energy Fuels* **1998**, 12, 3.
- [28] S. Y. Reece, J. A. Hamel, K. Sung, T. D. Jarvi, A. J. Esswein, J. J. H. Pijpers, D. G. Nocera, *Science* **2011**, 334, 645.
- [29] F. Urbain, V. Smirnov, J. P. Becker, A. Lambertz, F. Yang, J. Ziegler, B. Kaiser, W. Jaegermann, U. Rau, F. Finger, *Energy Environ. Sci.* **2016**, 9, 145.
- [30] W. H. Cheng, M. H. Richter, M. M. May, J. Ohlmann, D. Lackner, F. Dimroth, T. Hannappel, H. A. Atwater, H. J. Lewerenz, *ACS Energy Lett.* **2018**, 3, 1795.
- [31] M. M. May, H. J. Lewerenz, D. Lackner, F. Dimroth, T. Hannappel, *Nat. Commun.* **2015**, 6, 8286.
- [32] L. Pan, J. H. Kim, M. T. Mayer, M. K. Son, A. Ummadisingu, J. S. Lee, A. Hagfeldt, J. Luo, M. Grätzel, *Nat. Catal.* **2018**, 1, 412.
- [33] Y. Kuang, Q. Jia, G. Ma, T. Hisatomi, T. Minegishi, H. Nishiyama, M. Nakabayashi, N. Shibata, T. Yamada, A. Kudo, K. Domen, *Nat. Energy* **2017**, 2, 16191.
- [34] D. K. Lee, K. S. Choi, *Nat. Energy* **2018**, 3, 53.
- [35] F. F. Abdi, L. Han, A. H. M. Smets, M. Zeman, B. Dam, R. van de Krol, *Nat. Commun.* **2013**, 4, 2195.
- [36] J. H. Kim, J. W. Jang, Y. H. Jo, F. F. Abdi, Y. H. Lee, R. van de Krol, J. S. Lee, *Nat. Commun.* **2016**, 7, 13380.
- [37] Y. Qiu, W. Liu, W. Chen, G. Zhou, P. C. Hsu, R. Zhang, Z. Liang, S. Fan, Y. Zhang, Y. Cui, *Sci. Adv.* **2016**, 2, 1501764.
- [38] Y. Pihosh, I. Turkevych, K. Mawatari, J. Uemura, Y. Kazoe, S. Kosar, K. Makita, T. Sugaya, T. Matsui, D. Fujita, M. Tosa, M. Kondo, T. Kitamori, *Sci. Rep.* **2015**, 5, 11141.
- [39] G. Segev, J. Kibsgaard, C. Hahn, Z. J. Xu, W. S. Cheng, T. G. Deutsch, C. Xiang, J. Z. Zhang, L. Hammarström, D. G. Nocera, A. Z. Weber, P. Agbo, T. Hisatomi, F. E. Osterloh, K. Domen, F. F. Abdi, S. Haussener, D. J. Miller, S. Ardo, P. C. McIntyre, T. Hannappel, S. Hu, H. Atwater, J. M. Gregoire, M. Z. Ertem, I. D. Sharp, K.-S. Choi, J. S. Lee, O. Ishitani, J. W. Ager, et al. *J. Phys. D: Appl. Phys.* **2022**, 55, 323003.
- [40] B. Turan, J. P. Becker, F. Urbain, F. Finger, U. Rau, S. Haas, *Nat. Commun.* **2016**, 7, 12681.
- [41] A. C. Nielander, M. R. Shaner, K. M. Papadantonakis, S. A. Francis, N. S. Lewis, *Energy Environ. Sci.* **2015**, 8, 16.
- [42] W. Jaegermann, in *Modern Aspects of Electrochemistry* (Eds: J. O. Bockris, B. E. Conway, R. E. White), Springer, USA **1996**.
- [43] R. Memming, *Semiconductor Electrochemistry*, John Wiley & Sons, Germany **2015**.
- [44] *Photoelectrochemical Solar Fuel Production from Basic Principles to Advanced Devices* (Eds: S. Giménez, J. Bisquert), Springer, Cham, Switzerland **2016**.
- [45] U. Würfel, A. Cuevas, P. Würfel, *IEEE J. Photovoltaics* **2014**, 5, 461.
- [46] L. Peter, *Curr. Opin. Green Sustainable Chem.* **2021**, 31, 100505.
- [47] L. Christian, K. Andreas, W. Jaegermann, *Nat. Commun.* **2018**, 9, 4309.
- [48] W. Jaegermann, B. Kaiser, J. Ziegler, J. Klett, in *Photoelectrochemical Solar Fuel Production: From Basic Principles to Advanced Devices* (Eds: S. Giménez, J. Bisquert), Springer International Publishing, Cham, Switzerland **2016**.
- [49] O. Romanyuk, A. Paszuk, I. Gordeev, R. G. Wilks, S. Ueda, C. Hartmann, R. Félix, M. Bär, C. Schlueter, A. Gloskovskii, I. Bartoš, M. Nandy, J. Houdková, P. Jiříček, W. Jaegermann, J. P. Hofmann, T. Hannappel, *Appl. Surf. Sci.* **2022**, 605, 154630.

- [50] W. Mönch, *Semiconductor Surfaces and Interfaces*, Springer Berlin, Heidelberg **2013**.
- [51] D. C. Moritz, I. A. Ruiz Alvarado, M. A. Zare Pour, A. Paszuk, T. Frieß, E. Runge, J. P. Hofmann, T. Hannappel, W. G. Schmidt, W. Jaegermann, *ACS Appl. Mater. Interfaces* **2022**, *14*, 47255.
- [52] B. W. Jaegermann, A. Klein, T. Mayer, *Adv. Mater.* **2009**, *21*, 4196.
- [53] B. A. Pinaud, J. D. Benck, L. C. Seitz, A. J. Forman, Z. Chen, T. G. Deutsch, B. D. James, K. N. Baum, G. N. Baum, S. Ardo, H. Wang, E. Miller, T. F. Jaramillo, *Energy Environ. Sci.* **2013**, *6*, 1983.
- [54] P. Zhai, S. Haussener, J. Ager, R. Sathre, K. Walczak, J. Greenblatt, T. McKone, *Energy Environ. Sci.* **2013**, *6*, 2380.
- [55] R. Sathre, C. D. Scown, W. R. Morrow, J. C. Stevens, I. D. Sharp, J. W. Ager, K. Walczak, F. A. Houle, J. B. Greenblatt, *Energy Environ. Sci.* **2014**, *7*, 3264.
- [56] A. K. Niaz, A. Akhtar, J. Y. Park, H. T. Lim, *J. Power Sources* **2021**, *481*, 229093.
- [57] R. A. Krivina, G. A. Lindquist, S. R. Beaudoin, T. N. Stovall, W. L. Thompson, L. P. Tigh, D. Marsh, J. Grzyb, K. Fabrizio, J. E. Hutchison, S. W. Boettcher, *Adv. Mater.* **2022**, *34*, 2203033.
- [58] J. Parrondo, C. G. Arges, M. Niedzwiecki, E. B. Anderson, K. E. Ayers, V. Ramani, *RSC Adv.* **2014**, *4*, 9875.
- [59] P. Würfel, *Physics of Solar Cells*, Wiley-VCH, Berlin, Germany **2005**.
- [60] J. W. Ager, M. R. Shaner, K. A. Walczak, I. D. Sharp, S. Ardo, *Energy Environ. Sci.* **2015**, *8*, 2811.
- [61] M. S. Prévot, K. Sivula, *J. Phys. Chem. C* **2013**, *117*, 17879.
- [62] A. M. K. Fehr, A. Agrawal, F. Mandani, C. L. Conrad, Q. Jiang, S. Y. Park, O. Alley, B. Li, S. Sidhik, I. Metcalf, C. Botello, J. L. Young, J. Even, J. C. Blancon, T. G. Deutsch, K. Zhu, S. Albrecht, F. M. Toma, M. Wong, A. D. Mohite, *Nat. Commun.* **2023**, *14*, 3797.
- [63] M. Wang, B. Shi, Q. Zhang, X. Li, S. Pan, Y. Zhao, X. Zhang, *Sol. RRL* **2022**, *6*, 2100748.
- [64] National Renewable Energy Laboratory, <https://www.nrel.gov/pv/cell-efficiency.html>, (accessed: 2023).
- [65] J. Klett, J. Ziegler, A. Radetnac, B. Kaiser, R. Schäfer, W. Jaegermann, F. Urbain, J. P. Becker, V. Smirnov, F. Finger, *Phys. Chem. Chem. Phys.* **2016**, *18*, 10751.
- [66] Y. W. Chen, J. D. Prange, S. Dühnen, Y. Park, M. Gunji, C. E. D. Chidsey, P. C. McIntyre, *Nat. Mater.* **2011**, *10*, 539.
- [67] J. Kamimura, M. Budde, P. Bogdanoff, C. Tschammer, F. F. Abdi, R. van de Krol, O. Bierwagen, H. Riechert, L. Geelhaar, *Sol. RRL* **2020**, *4*, 2000568.
- [68] Z. Tian, P. Zhang, P. Qin, D. Sun, S. Zhang, X. Guo, W. Zhao, D. Zhao, F. Huang, *Adv. Energy Mater.* **2019**, *9*, 1901287.
- [69] S. Hu, N. S. Lewis, J. W. Ager, J. Yang, J. R. McKone, N. C. Strandwitz, *J. Phys. Chem. C* **2015**, *119*, 24201.
- [70] A. G. Scheuermann, P. C. McIntyre, *J. Phys. Chem. Lett.* **2016**, *7*, 2867.
- [71] M. F. Lichterman, K. Sun, S. Hu, X. Zhou, M. T. McDowell, M. R. Shaner, M. H. Richter, E. J. Crumlin, A. I. Carim, F. H. Saadi, B. S. Brunschwig, N. S. Lewis, *Catal. Today* **2016**, *262*, 11.
- [72] Y. Sun, M. L. Agiorgousis, P. Zhang, S. Zhang, *Nano Lett.* **2015**, *15*, 581.
- [73] K. Kuhar, M. Pandey, K. S. Thygesen, K. W. Jacobsen, *ACS Energy Lett.* **2018**, *3*, 436.
- [74] J. A. Del Alamo, *Nature* **2011**, *479*, 317.
- [75] J. J. Williams, H. McFavilen, A. M. Fischer, D. Ding, S. R. Young, E. Vadiée, F. A. Ponce, C. Arena, C. B. Honsberg, S. M. Goodnick, in *Conf. Record of the IEEE Photovoltaic Specialists Conf.*, Vol. 6, IEEE, Portland, OR, November **2016**.
- [76] D. R. Baker, C. A. Lundgren, *J. Mater. Chem. A* **2017**, *5*, 20978.
- [77] L. A. Reichertz, I. Gherasoiu, K. M. Yu, V. M. Kao, W. Walukiewicz, J. W. Ager, *Appl. Phys. Express* **2009**, *2*, 4.
- [78] Y. Kuwahara, T. Fujii, Y. Fujiyama, T. Sugiyama, M. Iwaya, T. Takeuchi, S. Kamiyama, I. Akasaki, H. Amano, *Appl. Phys. Express* **2010**, *3*, 3.
- [79] H. Döscher, O. Supplie, M. M. May, P. Sippel, C. Heine, A. G. Muñoz, R. Eichberger, H.-J. Lewerenz, T. Hannappel, *ChemPhysChem* **2012**, *13*, 2899.
- [80] T. G. Deutsch, J. L. Head, J. A. Turner, *J. Electrochem. Soc.* **2008**, *155*, B903.
- [81] B. Seger, I. E. Castelli, P. C. K. Vesborg, K. W. Jacobsen, O. Hansen, I. Chorkendorff, *Energy Environ. Sci.* **2014**, *7*, 2397.
- [82] S. Kumar, K. Ojha, A. K. Ganguli, *Adv. Mater. Interfaces* **2017**, *4*, 1600981.
- [83] B. Kunert, Y. Mols, M. Baryshnikova, N. Waldron, A. Schulze, R. Langer, *Semicond. Sci. Technol.* **2018**, *33*, 093002.
- [84] B. Kim, K. Toprasertpong, A. Paszuk, O. Supplie, Y. Nakano, T. Hannappel, M. Sugiyama, *Sol. Energy Mater. Sol. Cells* **2018**, *180*, 303.
- [85] L. Gao, Y. Cui, J. Wang, A. Cavalli, A. Standing, T. T. T. Vu, M. A. Verheijen, J. E. M. Haverkort, E. P. A. M. Bakkers, P. H. L. Notten, *Nano Lett.* **2014**, *14*, 3715.
- [86] K. T. Butler, D. W. Davies, A. Walsh, *Computational Materials Discovery*, Royal Society of Chemistry, London, UK, October **2018**, p. 176.
- [87] T. Das, G. Di Liberto, G. Pacchioni, *J. Phys. Chem. C* **2022**, *126*, 2184.
- [88] L. Yu, A. Zunger, *Phys. Rev. Lett.* **2012**, *108*, 068701.
- [89] J. J. Zhou, J. Park, I. Te Lu, I. Maliyov, X. Tong, M. Bernardi, *Comput. Phys. Commun.* **2021**, *264*, 107970.
- [90] C. Freysoldt, B. Grabowski, T. Hickel, J. Neugebauer, G. Kresse, A. Janotti, C. G. van de Walle, *Rev. Mod. Phys.* **2014**, *86*, 253.
- [91] J.-S. Park, S. Kim, Z. Xie, A. Walsh, *Nat. Rev. Mater.* **2018**, *3*, 194.
- [92] D. Friedrich, P. Sippel, O. Supplie, T. Hannappel, R. Eichberger, *Phys. Status Solidi A* **2019**, *216*, 1800738.
- [93] C. Ballif, F. J. Haug, M. Boccard, P. J. Verlinden, G. Hahn, *Nat. Rev. Mater.* **2022**, *7*, 597.
- [94] A. Kojima, K. Teshima, Y. Shirai, T. Miyasaka, *J. Am. Chem. Soc.* **2009**, *131*, 6050.
- [95] J. Luo, J. H. Im, M. T. Mayer, M. Schreier, M. K. Nazeeruddin, N. G. Park, S. D. Tilley, H. J. Fan, M. Grätzel, *Science* **2014**, *345*, 1593.
- [96] J. Gao, F. Sahli, C. Liu, D. Ren, X. Guo, J. Werner, Q. Jeangros, S. M. Zakeeruddin, C. Ballif, M. Grätzel, J. Luo, *Joule* **2019**, *3*, 2930.
- [97] S. K. Karuturi, H. Shen, A. Sharma, F. J. Beck, P. Varadhan, T. Duong, P. R. Narangari, D. Zhang, Y. Wan, J. H. He, H. H. Tan, C. Jagadish, K. Catchpole, *Adv. Energy Mater.* **2020**, *10*, 2070122.
- [98] Y. Wang, A. Sharma, T. Duong, H. Arandiyani, T. Zhao, D. Zhang, Z. Su, M. Garbrecht, F. J. Beck, S. Karuturi, C. Zhao, K. Catchpole, *Adv. Energy Mater.* **2021**, *11*, 2101053.
- [99] J. P. Correa-Baena, M. Saliba, T. Buonassisi, M. Grätzel, A. Abate, W. Tress, A. Hagfeldt, *Science* **2017**, *358*, 739.
- [100] M. B. Faheem, B. Khan, C. Feng, M. U. Farooq, F. Raziq, Y. Xiao, Y. Li, *ACS Energy Lett.* **2020**, *5*, 290.
- [101] X. Yang, W. Wang, R. Ran, W. Zhou, Z. Shao, *Energy Fuels* **2020**, *34*, 10513.
- [102] J. W. Lee, S. Tan, S. Il Seok, Y. Yang, N. G. Park, *Science* **2022**, *375*, eabj1186.
- [103] C. Katan, N. Mercier, J. Even, *Chem. Rev.* **2019**, *119*, 3140.
- [104] B. Saporov, D. B. Mitzi, *Chem. Rev.* **2016**, *116*, 4558.
- [105] F. Jahanbakhshi, M. Mladenović, M. Dankl, A. Boziki, P. Ahlawat, U. Rothlisberger, *Helv. Chim. Acta* **2021**, *104*, e2000232.
- [106] R. Woods-Robinson, Y. Han, H. Zhang, T. Ablekim, I. Khan, K. A. Persson, A. Zakutayev, *Chem. Rev.* **2020**, *120*, 4007.
- [107] Q. Sun, W. J. Yin, S. H. Wei, *J. Mater. Chem. C* **2020**, *8*, 12012.

- [108] G. Volonakis, A. A. Haghighirad, R. L. Milot, W. H. Sio, M. R. Filip, B. Wenger, M. B. Johnston, L. M. Herz, H. J. Snaith, F. Giustino, *J. Phys. Chem. Lett.* **2017**, *8*, 772.
- [109] M. Ju, J. Dai, L. Ma, X. C. Zeng, *Adv. Energy Mater.* **2017**, *2*, 2.
- [110] Z. Huo, S. Wei, *J. Phys. D: Appl. Phys.* **2018**, *51*, 474003.
- [111] Q. Sun, J. Wang, W. Yin, Y. Yan, *Adv. Mater.* **2018**, *30*, 1705901.
- [112] Q. Sun, H. Chen, W. Yin, *Chem. Mater.* **2018**, *31*, 244.
- [113] M. Pandey, K. Kuhar, K. W. Jacobsen, *J. Phys. Chem. C* **2017**, *121*, 17780.
- [114] J. Wang, H. Chen, S. H. Wei, W. J. Yin, *Adv. Mater.* **2019**, *31*, 1806593.
- [115] T. Kirchartz, U. Rau, *Adv. Energy Mater.* **2018**, *8*, 1703385.
- [116] J. Heo, L. Yu, E. Altschul, B. E. Waters, J. F. Wager, A. Zunger, D. A. Keszler, *Chem. Mater.* **2017**, *29*, 2594.
- [117] M. Z. Rahman, *Joule* **2019**, *3*, 2290.
- [118] Y. Gan, N. Miao, P. Lan, J. Zhou, S. R. Elliott, Z. Sun, *J. Am. Chem. Soc.* **2022**, *144*, 5878.
- [119] C. Shen, T. Li, Y. Zhang, T. Long, N. M. Fortunato, F. Liang, M. Dai, J. Shen, C. Wolverton, H. Zhang, *J. Phys. D: Appl. Phys.* **2023**, *51*, 474003.
- [120] F. Mayr, M. Harth, I. Kouroudis, M. Rinderle, A. Gagliardi, *J. Phys. Chem. Lett.* **2022**, *13*, 1940.
- [121] S. Sun, A. Tiihonen, F. Oviedo, Z. Liu, J. Thapa, Y. Zhao, N. T. P. Hartono, A. Goyal, T. Heumueller, C. Batali, A. Encinas, J. J. Yoo, R. Li, Z. Ren, I. M. Peters, C. J. Brabec, M. G. Bawendi, V. Stevanovic, J. Fisher, T. Buonassisi, *Matter* **2021**, *4*, 1305.
- [122] R. E. Kumar, A. Tiihonen, S. Sun, D. P. Fenning, Z. Liu, T. Buonassisi, *Matter* **2022**, *5*, 1353.
- [123] P. Friederich, F. Häse, J. Proppe, A. Aspuru-guzik, *Nat. Mater.* **2021**, *20*, 750.
- [124] J. Ovčar, L. Grisanti, B. Mladineo, A. B. Djuričić, J. Popović, I. Lončarić, *Phys. Rev. B* **2022**, *107*, 174109.
- [125] M. M. May, H. J. Lewerenz, T. Hannappel, *J. Phys. Chem. C* **2014**, *118*, 19032.
- [126] M. Guidat, M. Löw, M. Kölbach, J. Kim, M. M. May, *ChemElectroChem* **2023**, *10*, e202300027.
- [127] E. A. Schmitt, M. Guidat, M. Nusshör, A. L. Renz, K. Möller, M. Flieg, D. Lörch, M. Kölbach, M. M. May, *Cell Rep. Phys. Sci.* **2023**, *4*, 101606.
- [128] W. Jaegermann, B. Kaiser, F. Finger, V. Smirnov, R. Schäfer, *Z. Phys. Chem.* **2020**, *234*, 549.
- [129] D. Guo, V. M. Caselli, E. M. Hutter, T. J. Savenije, *ACS Energy Lett.* **2019**, *4*, 855.
- [130] B. Seger, T. Pedersen, A. B. Laursen, P. C. K. Vesborg, O. Hansen, I. Chorkendorff, *J. Am. Chem. Soc.* **2013**, *135*, 1057.
- [131] Y. Liu, J. Li, W. Li, Q. Liu, Y. Yang, Y. Li, Q. Chen, *Int. J. Hydrogen Energy* **2015**, *40*, 8856.
- [132] K. Kim, *Results Phys.* **2020**, *16*, 102964.
- [133] X. Song, G. Wang, L. Zhou, H. Yang, X. Li, H. Yang, Y. Shen, G. Xu, Y. Luo, N. Wang, *ACS Appl. Energy Mater.* **2023**, *6*, 9756.
- [134] I. M. Huygens, K. Strubbe, W. P. Gomes, *J. Electrochem. Soc.* **2000**, *147*, 1797.
- [135] P. Lorenz, R. Gutt, T. Haensel, M. Himmerlich, J. A. Schaefer, S. Krischok, *Phys. Status Solidi C* **2010**, *7*, 169.
- [136] A. Eisenhardt, S. Reiß, M. Himmerlich, J. A. Schaefer, S. Krischok, *Phys. Status Solidi A* **2010**, *207*, 1037.
- [137] A. Eisenhardt, S. Krischok, M. Himmerlich, *Phys. Rev. B* **2015**, *91*, 245305.
- [138] L. Lymperakis, J. Neugebauer, M. Himmerlich, S. Krischok, M. Rink, J. Kröger, V. M. Polyakov, *Phys. Rev. B* **2017**, *95*, 195314.
- [139] V. Irkha, A. Himmerlich, S. Reiß, S. Krischok, M. Himmerlich, *J. Phys. Chem. C* **2018**, *122*, 4250.
- [140] R. Liu, Z. Zheng, J. Spurgeon, X. Yang, *Energy Environ. Sci.* **2014**, *7*, 2504.
- [141] H. Kim, H. Bae, S. W. Bang, S. Kim, S. H. Lee, S.-W. Ryu, J.-S. Ha, *Opt. Express* **2019**, *27*, A206.
- [142] S. Hu, M. R. Shaner, J. A. Beardslee, M. Lichterman, B. S. Brunschwig, N. S. Lewis, *Science* **2014**, *344*, 1005.
- [143] F. E. Bedoya-Lora, I. Holmes-Gentle, A. Hankin, *Curr. Opin. Green Sustainable Chem.* **2021**, *29*, 100463.
- [144] T. Lopes, L. Andrade, H. A. Ribeiro, A. Mendes, *Int. J. Hydrogen Energy* **2010**, *35*, 11601.
- [145] S. Vanka, G. Zeng, T. G. Deutsch, F. M. Toma, Z. Mi, *Front. Energy Res.* **2022**, *10*, 840140.
- [146] W. Yu, H. J. Fu, T. Mueller, B. S. Brunschwig, N. S. Lewis, *J. Chem. Phys.* **2020**, *153*, 020902.
- [147] C. C. L. Mccrory, S. Jung, J. C. Peters, T. F. Jaramillo, *J. Am. Chem. Soc.* **2013**, *135*, 16977.
- [148] B. M. Hunter, H. B. Gray, A. M. Müller, *Chem. Rev.* **2016**, *116*, 14120.
- [149] K. Park, Y. J. Kim, T. Yoon, S. David, Y. M. Song, *RSC Adv.* **2019**, *9*, 30112.
- [150] C. Gort, P. W. Buchheister, M. Klingenhof, S. D. Paul, F. Dionigi, R. van de Krol, U. I. Kramm, W. Jaegermann, J. P. Hofmann, P. Strasser, B. Kaiser, *ChemCatChem* **2023**, *15*, e202201670.
- [151] P. Cheng, Y. Liu, M. Ziegler, M. Klingenhof, D. Wang, Z. Zhang, P. Strasser, P. Schaaf, *ACS Appl. Energy Mater.* **2022**, *5*, 8222.
- [152] C. Gao, J. Wang, H. Xu, Y. Xiong, *Chem. Soc. Rev.* **2017**, *46*, 2799.
- [153] M. A. Marwat, M. Humayun, M. W. Afridi, H. Zhang, M. R. Abdul Karim, M. Ashtar, M. Usman, S. Waqar, H. Ullah, C. Wang, W. Luo, *ACS Appl. Energy Mater.* **2021**, *4*, 12007.
- [154] F. Niu, D. Wang, F. Li, Y. Liu, S. Shen, T. J. Meyer, *Adv. Energy Mater.* **2020**, *10*, 1900399.
- [155] Y. Hou, X. Zhuang, X. Feng, *Small Methods* **2017**, *1*, 1700090.
- [156] Y. Yan, C. Liu, H. Jian, X. Cheng, T. Hu, D. Wang, L. Shang, G. Chen, P. Schaaf, X. Wang, E. Kan, T. Zhang, *Adv. Funct. Mater.* **2021**, *31*, 2009610.
- [157] J. Liu, H. Zhao, Z. Wang, T. Hannappel, U. I. Kramm, B. J. M. Etzold, Y. Lei, *Sol. RRL* **2022**, *6*, 2200181.
- [158] F. Dionigi, P. Strasser, *Adv. Energy Mater.* **2016**, *6*, 1600621.
- [159] S. Yuan, J. Peng, B. Cai, Z. Huang, A. T. Garcia-Esparza, D. Sokaras, Y. Zhang, L. Giordano, K. Akkiraju, Y. G. Zhu, R. Hübner, X. Zou, Y. Román-Leshkov, Y. Shao-Horn, *Nat. Mater.* **2022**, *21*, 673.
- [160] R. Jacobs, J. Booske, D. Morgan, *Adv. Funct. Mater.* **2016**, *26*, 5471.
- [161] X. Li, H. Zhao, J. Liang, Y. Luo, G. Chen, X. Shi, S. Lu, S. Gao, J. Hu, Q. Liu, X. Sun, *J. Mater. Chem. A* **2021**, *9*, 6650.
- [162] J. Varignon, M. Bibes, A. Zunger, *Nat. Commun.* **2019**, *10*, 1658.
- [163] L. Mohapatra, K. Parida, *J. Mater. Chem. A* **2016**, *4*, 10744.
- [164] D. A. Kuznetsov, B. Han, Y. Yu, R. R. Rao, J. Hwang, Y. Román-Leshkov, Y. Shao-Horn, *Joule* **2018**, *2*, 225.
- [165] E. M. Miner, M. Dinca, *Nat. Energy* **2016**, *1*, 1.
- [166] M. Ko, L. Mendecki, K. A. Mirica, *Chem. Commun.* **2018**, *54*, 7873.
- [167] W. Da Zhang, Q. T. Hu, L. L. Wang, J. Gao, H. Y. Zhu, X. Yan, Z. G. Gu, *Appl. Catal., B* **2021**, *286*, 119906.
- [168] Y. H. Xiao, Z. G. Gu, J. Zhang, *Nanoscale* **2020**, *12*, 12712.
- [169] M. Ziegler, S. Thamm, H. L. K. S. Stolle, J. Dellith, U. Hübner, D. Wang, P. Schaaf, *Appl. Surf. Sci.* **2020**, *514*, 1600621.
- [170] Q. Wang, H. Wang, X. Cheng, M. Fritz, D. Wang, H. Li, A. Bund, G. Chen, P. Schaaf, *Mater. Today Energy* **2020**, *17*, 100490.
- [171] H. Wang, J. Xiong, X. Cheng, M. Fritz, A. Ispas, A. Bund, G. Chen, D. Wang, P. Schaaf, *ACS Appl. Nano Mater.* **2020**, *3*, 10986.
- [172] Y. Yan, X. Cheng, W. Zhang, G. Chen, H. Li, A. Konkin, Z. Sun, S. Sun, D. Wang, P. Schaaf, *ACS Sustainable Chem. Eng.* **2019**, *7*, 885.
- [173] M. R. Singh, S. Haussener, A. Z. Weber, in *Integrated Solar Fuel Generators* (Eds: I. D. Sharp, H. A. Atwater, H.-J. Lewerenz), Royal Society of Chemistry, London, UK **2018**.

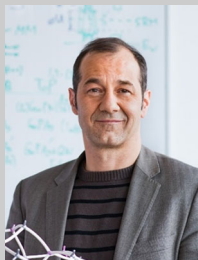
- [174] C. Xiang, A. Z. Weber, S. Ardo, A. Berger, Y. Chen, R. Coridan, K. T. Fountaine, S. Haussener, S. Hu, R. Liu, N. S. Lewis, M. A. Modestino, M. M. Shaner, M. R. Singh, J. C. Stevens, K. Sun, K. Walczak, *Angew. Chem.* **2016**, *128*, 13168.
- [175] L. Meier, W. G. Schmidt, *Phys. Status Solidi B* **2022**, *259*, 2100462.
- [176] L. Meier, C. Braun, T. Hannappel, W. G. Schmidt, *Phys. Status Solidi B* **2021**, *258*, 2000463.
- [177] K. Lauer, K. Peh, D. Schulze, T. Orltapp, E. Runge, S. Krischok, *Phys. Status Solidi A* **2022**, *219*, 2200099.
- [178] A. Lücke, W. G. Schmidt, E. Rauls, F. Ortmann, U. Gerstmann, *J. Phys. Chem. B* **2015**, *119*, 6481.
- [179] A. Lücke, F. Ortmann, M. Panhans, S. Sanna, E. Rauls, U. Gerstmann, W. G. Schmidt, *J. Phys. Chem. B* **2016**, *120*, 5572.
- [180] O. Pankratov, M. Scheffler, *Phys. Rev. Lett* **1995**, *75*, 701.
- [181] T. Frigge, B. Hafke, T. Witte, B. Krenzer, C. Streubühr, A. Samad Syed, V. Mikšić Trontl, I. Avigo, P. Zhou, M. Ligges, D. Von Der Linde, U. Bovensiepen, M. Horn-Von Hoegen, S. Wippermann, A. Lücke, S. Sanna, U. Gerstmann, W. G. Schmidt, *Nature* **2017**, *544*, 207.
- [182] C. W. Nicholson, A. Lücke, W. G. Schmidt, M. Puppig, L. Rettig, R. Ernstorfer, M. Wolf, *Science* **2018**, *362*, 821.
- [183] M. Krenz, U. Gerstmann, W. G. Schmidt, *Appl. Phys. A: Mater. Sci. Process.* **2022**, *128*, 480.
- [184] M. A. Modestino, S. M. H. Hashemi, S. Haussener, *Energy Environ. Sci.* **2016**, *9*, 1533.
- [185] M. Kölbach, K. Rehfeld, M. M. May, *Energy Environ. Sci.* **2021**, *14*, 4410.
- [186] A. Angulo, P. Van Der Linde, H. Gardeniers, M. Modestino, D. Ferna, *Joule* **2020**, *4*, 555.
- [187] S. Park, L. Liu, Ç. Demirkir, O. Van Der Heijden, D. Lohse, D. Krug, M. T. M. Koper, *Nat. Chem.* **2023**, *15*, 1532.
- [188] X. Yang, D. Baczymalski, C. Cierpka, G. Mutschke, K. Eckert, *Phys. Chem. Chem. Phys.* **2018**, *20*, 11542.
- [189] P. Repository, G. C. Law, *Electrochim. Acta* **2019**, *297*, 929.
- [190] T. Weier, D. Baczymalski, J. Massing, S. Landgraf, C. Cierpka, *Int. J. Hydrogen Energy* **2017**, *42*, 20923.
- [191] K. Obata, F. F. Abdi, *Sustainable Energy Fuels* **2021**, *5*, 3791.
- [192] D. Baczymalski, T. Weier, C. J. Kähler, C. Cierpka, *Exp. Fluids* **2015**, *56*, 1.
- [193] D. Baczymalski, M. Schürer, C. Neubert, G. Mutschke, M. Uhlemann, K. Eckert, C. Cierpka, *J. Electrochem. Soc.* **2016**, *163*, E248.
- [194] L. Krause, K. Skibińska, H. Rox, R. Baumann, M. M. Marzec, X. Yang, G. Mutschke, P. Żabiński, A. F. Lasagni, K. Eckert, *ACS Appl. Mater. Interfaces* **2023**, *15*, 18290.
- [195] D. Henkensmeier, M. Najibah, C. Harms, J. Žitka, J. Hnát, K. Bouzek, *J. Electrochem. Energy Convers. Storage* **2021**, *18*, 024001.
- [196] J. R. Varcoe, P. Atanassov, D. R. Dekel, A. M. Herring, M. A. Hickner, P. A. Kohl, A. R. Kucernak, W. E. Mustain, K. Nijmeijer, K. Scott, T. Xu, L. Zhuang, *Energy Environ. Sci.* **2014**, *7*, 3135.
- [197] M. A. Hickner, A. M. Herring, E. B. Coughlin, *J. Polym. Sci., Part B: Polym. Phys.* **2013**, *51*, 1727.
- [198] G. Couture, A. Alaaeddine, F. Boschet, B. Ameduri, *Prog. Polym. Sci.* **2011**, *36*, 1521.
- [199] S. S. Kumar, H. Lim, *Sustainable Energy Fuels* **2023**, *7*, 3560.
- [200] T. D. Gierke, G. E. Munn, F. C. Wilson, E. I. Du Pont, *J. Polym. Sci., Part B: Polym. Phys.* **1981**, *11*, 1687.
- [201] K. Schmidt-Rohr, Q. Chen, *Nat. Mater.* **2008**, *7*, 75.
- [202] K. A. Mauritz, R. B. Moore, *Chem. Rev.* **2004**, *104*, 4535.
- [203] H. Zhang, P. K. Shen, *Chem. Rev.* **2012**, *112*, 2780.
- [204] M. A. Hickner, H. Ghassemi, Y. S. Kim, B. R. Einsla, J. E. McGrath, *Chem. Rev.* **2004**, *104*, 4587.
- [205] C. E. Diesendruck, D. R. Dekel, *Curr. Opin. Electrochem.* **2018**, *9*, 173.
- [206] J. Miyake, K. Miyatake, *Sustainable Energy Fuels* **2019**, *3*, 1916.
- [207] J. Wang, C. Zhao, Z. Liu, X. Lan, S. Huang, J. Zhou, H. Liang, *Int. J. Hydrogen Energy* **2024**, *58*, 514.
- [208] F. Liu, I. S. Kim, K. Miyatake, *Sci. Adv.* **2023**, *9*, eadg9057.
- [209] S. M. Ahn, J. E. Park, G. Y. Jang, H. Y. Jeong, D. M. Yu, J. K. Jang, J. C. Lee, Y. H. Cho, T. H. Kim, *ACS Energy Lett.* **2022**, *7*, 4427.
- [210] C. M. Evans, M. R. Singh, N. A. Lynd, R. A. Segalman, *Macromolecules* **2015**, *48*, 3303.
- [211] K. Sun, R. Liu, Y. Chen, E. Verlage, N. S. Lewis, C. Xiang, *Adv. Energy Mater.* **2016**, *6*, 1600379.
- [212] S. Thiele, B. Mayerhöfer, D. McLaughlin, T. Böhm, M. Hegelheimer, D. Seeberger, *ACS Appl. Energy Mater.* **2020**, *3*, 9635.
- [213] F. E. Bedoya-Lora, I. Holmes-Gentle, S. Haussener, *Electrochim. Acta* **2023**, *462*, 142703.
- [214] S. Haussener, C. Xiang, J. M. Spurgeon, S. Ardo, N. S. Lewis, A. Z. Weber, *Energy Environ. Sci.* **2012**, *5*, 9922.
- [215] C. A. Mesa, E. Pastor, L. Francàs, *Curr. Opin. Electrochem.* **2022**, *35*, 101098.
- [216] E. A. Carbonio, J.-J. Velasco-Velez, R. Schlögl, A. Knop-Gericke, *J. Electrochem. Soc.* **2020**, *167*, 54509.
- [217] C. Baeumer, *J. Appl. Phys.* **2021**, *129*, 170901.
- [218] D. E. Starr, M. Hävecker, A. Knop-gericke, M. Favaro, M. Mertin, G. Reichardt, J. Schmidt, F. Siewert, R. Schulz, J. Vieffhaus, C. Jung, R. van de Krol, *Synchrotron Radiat. News* **2022**, *35*, 54.
- [219] G. S. Harlow, E. Lundgren, M. Escudero-escribano, *Curr. Opin. Electrochem.* **2020**, *23*, 162.
- [220] O. M. Magnussen, J. Drnec, C. Qiu, I. Martens, J. J. Huang, R. Chattot, A. Singer, *Chem. Rev.* **2024**, *124*, 629.
- [221] C. S. Santos, B. N. Jaato, I. Sanju, W. Schuhmann, C. Andronescu, *Chem. Rev.* **2023**, *123*, 4972.
- [222] T. O. Schmidt, R. W. Haid, E. L. Gubanova, R. M. Kluge, A. S. Bandarenka, *Top. Catal.* **2023**, *66*, 1270.
- [223] M. Borgwardt, S. T. Omelchenko, M. Favaro, P. Plate, C. Höhn, D. Abou-Ras, K. Schwarzburg, R. van de Krol, H. A. Atwater, N. S. Lewis, R. Eichberger, D. Friedrich, *Nat. Commun.* **2019**, *10*, 1803951.
- [224] D. Lyu, J. Xu, Z. Wang, *Front. Chem.* **2023**, *11*, 1231886.
- [225] F. E. Oropeza, B. T. Feleki, K. H. L. Zhang, E. J. M. Hensen, J. P. Hofmann, *ACS Appl. Energy Mater.* **2019**, *2*, 6866.
- [226] L. J. Glahn, I. A. Ruiz Alvarado, S. Neufeld, M. A. Zare Pour, A. Paszuk, D. Ostheimer, S. Shekarabi, O. Romanyuk, D. C. Moritz, J. P. Hofmann, W. Jaegermann, T. Hannappel, W. G. Schmidt, *Phys. Status Solidi B* **2022**, *259*, 2200308.
- [227] D. C. Moritz, W. Calvet, M. A. Zare Pour, A. Paszuk, T. Mayer, T. Hannappel, J. P. Hofmann, W. Jaegermann, *Sol. RRL* **2023**, *7*, 2201063.
- [228] S. Abayzeed, T. Anwar, A. Barnaveli, M. Z. Bazant, L. Bocquet, A. Donev, R. A. W. Dryfe, S. Faez, A. Janardanan, F. Jiménez-Ángeles, T. M. Kamsma, F. Kanoufi, A. A. Kornyshev, S. G. Lemay, Y. Levin, S. Marbach, J. Montes de Oca, P. Robin, Z. S. Siwy, D. Stein, R. van Rooij, T. Vidaković-Koch, G. Yossifon, Y. Zhang, *Faraday Discuss.* **2023**, *246*, 157.
- [229] M. Z. Bazant, *Faraday Discuss.* **2023**, *246*, 60.
- [230] S. Zhang, I. Ahmet, S. H. Kim, O. Kasian, A. M. Mingers, P. Schnell, M. Kölbach, J. Lim, A. Fischer, K. J. J. Mayrhofer, S. Cherevko, B. Gault, R. van de Krol, C. Scheu, *ACS Appl. Energy Mater.* **2020**, *3*, 9523.
- [231] Q. Meng, B. Zhang, L. Fan, H. Liu, M. Valvo, K. Edström, M. Cuartero, R. de Marco, G. A. Crespo, L. Sun, *Angew. Chem.* **2019**, *131*, 19203.
- [232] S. M. Sze, Y. Li, K. K. Ng, *Physics of Semiconductor Devices*, John Wiley & Sons, Hsinchu, Taiwan **2021**.

- [233] S. H. A. Luque, *Handbook of Photovoltaic Science and Engineering*, John Wiley & Sons, Hoboken, NJ **2011**.
- [234] B. J. Trześniewski, W. A. Smith, *J. Mater. Chem. A* **2016**, *4*, 2919.
- [235] F. Lin, S. W. Boettcher, *Nat. Mater.* **2014**, *13*, 81.
- [236] W. A. Smith, I. D. Sharp, N. C. Strandwitz, J. Bisquert, *Energy Environ. Sci.* **2015**, *8*, 2851.
- [237] R. Hurt, *J. Am. Chem. Soc.* **2001**, *123*, 10141.
- [238] H. M. Kühne, H. Tributsch, *J. Electroanal. Chem.* **1986**, *201*, 263.
- [239] H. Tributsch, in *Proc. of the Eighth Inter. Conf. on Photochemical Conversion and Storage of Solar Energy*, Springer Netherlands, Palermo, Italy, July **1990**.
- [240] P. C. Vesborg, B. Seger, *Chem. Mater.* **2016**, *28*, 8844.
- [241] F. Feldmann, M. Simon, M. Bivour, C. Reichel, M. Hermle, S. W. Glunz, *Appl. Phys. Lett.* **2014**, *104*, 181105.
- [242] C. Gutsche, R. Niepelt, M. Gnauck, A. Lysov, W. Prost, C. Ronning, F. J. Tegude, *Nano Lett.* **2012**, *12*, 1453.
- [243] C. Gutsche, A. Lysov, D. Braam, I. Regolin, G. Keller, Z. Li, M. Geller, M. Spasova, W. Prost, F. Tegude, *Adv. Funct. Mater.* **2012**, *22*, 929.
- [244] A. Neubauer, J. M. Szarko, A. F. Bartelt, R. Eichberger, T. Hannappel, *J. Phys. Chem. C* **2011**, *115*, 5683.
- [245] R. Brendel, R. Peibst, *IEEE J. Photovoltaics* **2016**, *6*, 1413.
- [246] E. T. Roe, K. E. Egelhofer, M. C. Lonergan, *ACS Appl. Energy Mater.* **2018**, *1*, 1037.
- [247] M. Schleuning, I. Y. Ahmet, R. van de Krol, M. M. May, *Sustainable Energy Fuels* **2022**, *6*, 3701.
- [248] D. E. Pulfrey, *IEEE Trans. Electron Devices* **1978**, *25*, 1308.
- [249] C. Zachäus, F. F. Abdi, L. M. Peter, R. van de Krol, *Chem. Sci.* **2017**, *8*, 3712.
- [250] D. K. Zhong, S. Choi, D. R. Gamelin, *J. Am. Chem. Soc.* **2011**, *133*, 18370.
- [251] A. Heller, E. Aharon-Shalom, W. A. Bonner, B. Miller, *J. Am. Chem. Soc.* **1982**, *104*, 6942.
- [252] J. L. Young, M. A. Steiner, H. Döscher, R. M. France, J. A. Turner, T. G. Deutsch, *Nat. Energy* **2017**, *2*, 1.
- [253] M. M. May, W. Jaegermann, *Curr. Opin. Electrochem.* **2022**, *34*, 100968.
- [254] M. Favaro, F. F. Abdi, M. Lamers, E. J. Crumlin, Z. Liu, R. van de Krol, D. E. Starr, *J. Phys. Chem. B* **2018**, *122*, 801.
- [255] S. Haussener, S. Hu, C. Xiang, A. Z. Weber, N. S. Lewis, *Energy Environ. Sci.* **2013**, *6*, 3605.
- [256] M. Niemeyer, P. Kleinschmidt, A. W. Walker, L. E. Mundt, C. Timm, R. Lang, T. Hannappel, D. Lackner, *AIP Adv.* **2019**, *9*, 045034.
- [257] M. Ziwrtsch, S. Müller, H. Hempel, T. Unold, F. F. Abdi, R. van de Krol, D. Friedrich, R. Eichberger, *ACS Energy Lett.* **2016**, *1*, 888.
- [258] M. Großmann, S. Bohm, S. Heyder, K. Schwarzburg, P. Kleinschmidt, E. Runge, T. Hannappel, *Phys. Status Solidi B* **2023**, *260*, 2200339.
- [259] M. Niemeyer, J. Ohlmann, A. W. Walker, P. Kleinschmidt, R. Lang, T. Hannappel, F. Dimroth, D. Lackner, *J. Appl. Phys.* **2017**, *122*, 115702.
- [260] C. Strothkämper, A. Bartelt, P. Sippel, T. Hannappel, R. Schütz, R. Eichberger, *J. Phys. Chem. C* **2013**, *117*, 17901.
- [261] T. Hannappel, B. Burfeindt, W. Storck, F. Willig, *J. Phys. Chem. B* **1997**, *101*, 6799.
- [262] A. J. Cowan, J. R. Durrant, *Chem. Soc. Rev.* **2013**, *42*, 2281.
- [263] R. Godin, Y. Wang, M. A. Zwiijnenburg, J. Tang, J. R. Durrant, *J. Am. Chem. Soc.* **2017**, *139*, 5216.
- [264] A. Litke, Y. Su, I. Tranca, T. Weber, E. J. M. Hensen, J. P. Hofmann, *J. Phys. Chem. C* **2017**, *121*, 7514.
- [265] P. Sippel, J. M. Szarko, T. Hannappel, R. Eichberger, *Phys. Rev. B* **2015**, *91*, 115312.
- [266] L. Töben, L. Gundlach, R. Ernstorfer, R. Eichberger, T. Hannappel, F. Willig, A. Zeiser, J. Förstner, A. Knorr, P. H. Hahn, W. G. Schmidt, *Phys. Rev. Lett.* **2005**, *94*, 067601.
- [267] R. K. Ahrenkiel, M. S. Lundstrom, *Minority Carriers in III-V Semiconductors: Physics and Applications*, Academic Press, Boston **1993**.
- [268] M. W. Gerber, R. N. Kleiman, *J. Appl. Phys.* **2017**, *122*, 095705.
- [269] D. Ren, A. C. Scofield, A. C. Farrell, Z. Rong, M. A. Haddad, R. B. Laghumavarapu, B. Liang, D. L. Huffaker, *Nanoscale* **2018**, *10*, 7792.
- [270] S. Münch, S. Reitzenstein, M. Borgström, C. Thelander, L. Samuelson, L. Worschech, A. Forchel, *Nanotechnology* **2010**, *21*, 105711.
- [271] C. T. Plass, V. Bonino, M. Ritzer, L. R. Jäger, V. Rey-Bakaikoa, M. Hafermann, J. Segura-Ruiz, G. Martínez-Criado, C. Ronning, *Adv. Sci.* **2023**, *10*, 2205304.
- [272] S. Nussbaum, E. Socie, G. C. Fish, N. J. Diercks, H. Hempel, D. Friedrich, J. E. Moser, J. H. Yum, K. Sivula, *Chem. Sci.* **2023**, *14*, 6052.
- [273] F. F. Abdi, T. J. Savenije, M. M. May, B. Dam, R. van de Krol, *J. Phys. Chem. Lett.* **2013**, *4*, 2752.
- [274] M. Schleuning, M. Kölbach, F. F. Abdi, K. Schwarzburg, M. Stolterfoht, R. Eichberger, R. van de Krol, D. Friedrich, *PRX Energy* **2022**, *10*, 023008.
- [275] P. P. Infelta, M. P. De Haas, J. M. Warman, *Radiat. Phys. Chem.* **1977**, *10*, 353.
- [276] H. Hempel, T. J. Savenije, M. Stolterfoht, J. Neu, M. Failla, V. C. Paingad, P. Kužel, E. J. Heilweil, J. A. Spies, M. Schleuning, J. Zhao, D. Friedrich, K. Schwarzburg, L. D. A. Siebbeles, P. Dörflinger, V. Dyakonov, R. Katoh, M. J. Hong, J. G. Labram, M. Monti, E. Butler-Caddle, J. Lloyd-Hughes, M. M. Taheri, J. B. Baxter, T. J. Magnanelli, S. Luo, J. M. Cardon, S. Ardo, T. Unold, *Adv. Energy Mater.* **2022**, *12*, 2102776.
- [277] T. J. Savenije, A. J. Ferguson, N. Kopidakis, G. Rumbles, *J. Phys. Chem. C* **2013**, *117*, 24085.
- [278] A. Nagelein, L. Liborius, M. Steidl, C. Blumberg, P. Kleinschmidt, A. Poloczek, T. Hannappel, *J. Phys.: Condens. Matter* **2017**, *29*, 394007.
- [279] J. A. Spies, J. Neu, U. T. Tayvah, M. D. Capobianco, B. Pattengale, S. Ostresh, C. A. Schmuttenmaer, *J. Phys. Chem. C* **2020**, *124*, 22335.
- [280] J. Neu, C. A. Schmuttenmaer, *J. Appl. Phys.* **2018**, *124*, 231101.
- [281] C. Wehrenfennig, C. M. Palumbiny, H. J. Snaith, M. B. Johnston, L. Schmidt-Mende, L. M. Herz, *J. Phys. Chem. C* **2015**, *119*, 9159.
- [282] M. Schleuning, M. Kölbach, I. Ahmet, R. Präg, R. Gottesman, R. Gunder, M. Zhang, D. R. Wargulski, D. Abou-ras, D. A. Grave, F. F. Abdi, R. van de Krol, K. Schwarzburg, R. Eichberger, D. Friedrich, H. Hempel, *Adv. Funct. Mater.* **2023**, *33*, 2300065.
- [283] M. M. Taheri, T. M. Truong, S. Li, W. N. Shafarman, B. E. McCandless, J. B. Baxter, *J. Appl. Phys.* **2021**, *130*, 163104.
- [284] H. Hempel, R. Eichberger, I. Repins, T. Unold, *Thin Solid Films* **2018**, *666*, 40.
- [285] M. C. Beard, G. M. Turner, C. A. Schmuttenmaer, *Phys. Rev. B* **2000**, *62*, 15764.
- [286] S. Richter, O. Herrfurth, S. Espinoza, M. Rebarz, *New J. Phys.* **2020**, *22*, 083066.
- [287] A. Ashoka, R. R. Tamming, A. V. Girija, H. Bretscher, S. D. Verma, S. Da Yang, C. H. Lu, J. M. Hodgkiss, D. Ritchie, C. Chen, C. G. Smith, C. Schnedermann, M. B. Price, K. Chen, A. Rao, *Nat. Commun.* **2022**, *13*, 083066.
- [288] S. Richter, M. Rebarz, O. Herrfurth, S. Espinoza, R. Schmidt-Grund, J. Andreasson, *Rev. Sci. Instrum.* **2021**, *92*, 033104.
- [289] O. Herrfurth, T. Pflug, M. Olbrich, M. Grundmann, A. Horn, R. Schmidt-Grund, *Appl. Phys. Lett.* **2019**, *115*, 212103.

- [290] C. Emminger, S. Espinoza, S. Richter, M. Rebarz, O. Herrfurth, M. Zahradník, R. Schmidt-Grund, J. Andreasson, S. Zollner, *Phys. Status Solidi RRL* **2022**, *16*, 2200058.
- [291] S. Espinoza, S. Richter, M. Rebarz, O. Herrfurth, R. Schmidt-Grund, J. Andreasson, S. Zollner, *Appl. Phys. Lett.* **2021**, *115*, 052105.
- [292] O. Herrfurth, S. Richter, M. Rebarz, S. Espinoza, C. Deparis, J. Leveillee, A. Schleife, M. Grundmann, J. Andreasson, *Phys. Rev. Res.* **2021**, *013246*, 21.
- [293] M. Zahradník, M. Kiaba, S. Espinoza, M. Rebarz, J. Andreasson, O. Caha, F. Abadizaman, D. Munzar, A. Dubroka, *Phys. Rev. B* **2022**, *105*, 235113.
- [294] A. Schleife, C. Rödl, F. Fuchs, K. Hannewald, F. Bechstedt, *Phys. Rev. Lett.* **2011**, *107*, 236405.
- [295] C. Cobet, K. Oppelt, K. Hingerl, H. Neugebauer, G. Knör, N. S. Sariciftci, J. Gasiorowski, *J. Phys. Chem. C* **2018**, *122*, 24309.
- [296] R. D. Webster, D. Beaglehole, *Phys. Chem. Chem. Phys.* **2000**, *2*, 5660.
- [297] M. A. McArthur, S. Trussler, J. R. Dahn, *J. Electrochem. Soc.* **2011**, *159*, A198.
- [298] R. Sachse, M. Sahre, M. Bernicke, V.-D. Hodoroba, P. Strasser, R. Kraehnert, A. Hertwig, Research Square, Vol. 10, version 1 **2021**, <https://doi.org/10.21203/rs.3.rs-934130/v1>.
- [299] L. C. Seitz, Z. Chen, A. J. Forman, B. A. Pinaud, J. D. Benck, T. F. Jaramillo, *ChemSusChem* **2014**, *7*, 1372.
- [300] H. Döscher, J. F. Geisz, T. G. Deutsch, J. A. Turner, *Energy Environ. Sci.* **2014**, *7*, 2951.
- [301] Y. Chen, S. Hu, C. Xiang, N. S. Lewis, *Energy Environ. Sci.* **2015**, *8*, 876.
- [302] A. Berger, R. A. Segalman, J. Newman, *Energy Environ. Sci.* **2014**, *7*, 1468.
- [303] M. R. Singh, K. Papadantonakis, C. Xiang, N. S. Lewis, *Energy Environ. Sci.* **2015**, *8*, 2760.
- [304] J. Jin, K. Walczak, M. R. Singh, C. Karp, N. S. Lewis, C. Xiang, *Energy Environ. Sci.* **2014**, *7*, 3371.
- [305] K. Walczak, Y. Chen, C. Karp, J. W. Beeman, M. Shaner, J. Spurgeon, I. D. Sharp, X. Amashukeli, W. West, J. Jin, N. S. Lewis, C. Xiang, *ChemSusChem* **2015**, *8*, 544.
- [306] Y. Chen, C. Xiang, S. Hu, N. S. Lewis, *J. Electrochem. Soc.* **2014**, *161*, F1101.
- [307] C. Xiang, Y. Chen, N. S. Lewis, *Energy Environ. Sci.* **2013**, *6*, 3713.
- [308] Y. Chen, N. S. Lewis, *J. Electrochem. Soc.* **2022**, *169*, 066510.
- [309] J. Newman, *J. Electrochem. Soc.* **2013**, *160*, F309.
- [310] B. C. Wood, E. Schwegler, W. I. Choi, T. Ogitsu, *J. Am. Chem. Soc.* **2013**, *135*, 15774.
- [311] B. C. Wood, E. Schwegler, W. I. Choi, T. Ogitsu, *J. Phys. Chem. C* **2014**, *118*, 1062.
- [312] X. Shen, Y. A. Small, J. Wang, P. B. Allen, M. V. Fernandez-Serra, M. S. Hybertsen, J. T. Muckerman, *J. Phys. Chem. C* **2010**, *114*, 13695.
- [313] J. Wang, L. S. Pedroza, A. Poissier, M. V. Fernández-Serra, *J. Phys. Chem. C* **2012**, *116*, 14382.
- [314] N. Kharche, J. T. Muckerman, M. S. Hybertsen, *Phys. Rev. Lett.* **2014**, *113*, 176802.
- [315] N. Kumar, P. R. C. Kent, D. J. Wesolowski, J. D. Kubicki, *J. Phys. Chem. C* **2013**, *117*, 23638.
- [316] L. M. Liu, C. Zhang, G. Thornton, A. Michaelides, *Phys. Rev. B* **2010**, *82*, 161415.
- [317] D. A. Duncan, F. Allegretti, D. P. Woodruff, *Phys. Rev. B* **2012**, *86*, 045411.
- [318] T. A. Pham, Y. Ping, G. Galli, *Nat. Mater.* **2017**, *16*, 401.
- [319] N. V. Ryzhkov, O. Ledovich, L. Eggert, A. Bund, A. Paszuk, T. Hannappel, K. Klyukin, V. Alexandrov, E. V. Skorb, *ACS Appl. Nano Mater.* **2021**, *4*, 425.
- [320] J. Ma, K. Li, Z. Li, Y. Qiu, W. Si, Y. Ge, J. Sha, L. Liu, X. Xie, H. Yi, Z. Ni, D. Li, Y. Chen, *J. Am. Chem. Soc.* **2019**, *141*, 4264.
- [321] Y. J. Chen, X. J. Chen, B. Yu, Y. Zou, W. Q. Tao, *Langmuir* **2020**, *36*, 13725.
- [322] Y. J. Chen, B. Yu, Y. Zou, B. N. Chen, W. Q. Tao, *Int. J. Heat Mass Transfer* **2020**, *158*, 119850.
- [323] S. R. German, M. A. Edwards, H. Ren, H. S. White, *J. Am. Chem. Soc.* **2018**, *140*, 4047.
- [324] Z. Gao, W. Wu, W. Sun, B. Wang, *Langmuir* **2021**, *37*, 11281.
- [325] L. Pizzagalli, M. L. David, M. Bertolus, *Modell. Simul. Mater. Sci. Eng.* **2013**, *21*, 065002.
- [326] Z. Wang, Z. Cui, W. Shao, Q. Cao, *Numer. Heat Transfer, Part A* **2023**, *1*, 1.
- [327] S. A. Hewage, J. N. Meegoda, *Colloids Surf., A* **2022**, *650*, 129565.
- [328] L. Yi, L. Yang, Y. Kuang, Y. Song, J. Zhao, A. K. Sum, *Phys. Chem. Chem. Phys.* **2021**, *23*, 27533.
- [329] D. Baczyszalski, F. Karnbach, G. Mutschke, X. Yang, K. Eckert, M. Uhlemann, C. Cierpka, *Phys. Rev. Fluids* **2017**, *2*, 093701.
- [330] F. M. Toma, J. K. Cooper, V. Kunzelmann, M. T. McDowell, J. Yu, D. M. Larson, N. J. Borys, C. Abeyan, J. W. Beeman, K. M. Yu, J. Yang, L. Chen, M. R. Shaner, J. Spurgeon, F. A. Houle, K. A. Persson, I. D. Sharp, *Nat. Commun.* **2016**, *7*, 12012.
- [331] N. Gaillard, Y. Chang, J. Kaneshiro, A. Deangelis, E. L. Miller, *Solar Hydrogen and Nanotechnology V*, Vol. 8, San Diego, CA **2010**.
- [332] J. Guo, W. Jaegermann, *J. Electron Spectrosc. Relat. Phenom.* **2017**, *221*, 1.
- [333] M. Favaro, J. Yang, S. Nappini, E. Magnano, F. M. Toma, E. J. Crumlin, J. Yano, I. D. Sharp, *J. Am. Chem. Soc.* **2017**, *139*, 8960.
- [334] F. T. Haase, A. Bergmann, T. E. Jones, J. Timoshenko, A. Herzog, H. S. Jeon, C. Rettenmaier, B. R. Cuenya, *Nat. Energy* **2022**, *7*, 765.
- [335] H. N. Nong, L. J. Falling, A. Bergmann, M. Klingenhof, H. P. Tran, C. Spöri, R. Mom, J. Timoshenko, G. Zichittella, A. Knop-Gericke, S. Piccinin, J. Pérez-Ramírez, B. R. Cuenya, R. Schlögl, P. Strasser, D. Teschner, T. E. Jones, *Nature* **2020**, *587*, 408.
- [336] M. Favaro, P. C. J. Clark, M. J. Sear, M. Johansson, S. Maehl, R. Van De Krol, D. E. Starr, *Surf. Sci.* **2021**, *713*, 121903.
- [337] M. Favaro, *Surfaces* **2020**, *3*, 392.
- [338] M. Favaro, F. F. Abdi, E. J. Crumlin, Z. Liu, R. van de Krol, D. E. Starr, *Surfaces* **2019**, *2*, 78.
- [339] M. Favaro, R. Uecker, S. Nappini, P. Igor, E. Magnano, H. Bluhm, R. van de Krol, D. E. Starr, *J. Phys. Chem. C* **2019**, *123*, 8347.
- [340] M. Favaro, I. Y. Ahmet, P. C. J. Clark, F. F. Abdi, M. J. Sear, R. van de Krol, D. E. Starr, *J. Phys. D: Appl. Phys.* **2021**, *54*, 164001.
- [341] M. Ralaiarisoa, S. S. Krishnamurti, W. Gu, C. Ampelli, R. van de Krol, F. F. Abdi, M. Favaro, *J. Mater. Chem. A* **2023**, *11*, 13570.
- [342] S. Vadilonga, P. Dumas, U. Schade, K. Holldack, G. Reichardt, T. Gerber, A. Vollmer, J. P. Hofmann, H. Oertel, B. Rech, R. Schlögl, J. Viehhaus, H. Bluhm, S. Vadilonga, P. Dumas, U. Schade, K. Holldack, K. Hinrichs, G. Reichardt, T. Gerber, A. Vollmer, J. P. Hofmann, *Synchrotron Radiat. News* **2022**, *35*, 67.
- [343] E. Betz-Güttner, S. D. Zilio, M. Lazzarino, *Micro Nano Eng.* **2022**, *15*, 100120.
- [344] J. F. Geisz, R. M. France, K. L. Schulte, M. A. Steiner, A. G. Norman, H. L. Guthrey, M. R. Young, T. Song, T. Moriarty, *Nat. Energy* **2020**, *5*, 326.
- [345] C. C. Ahia, E. L. Meyer, *Phys. Status Solidi A* **2023**, *221*, 2300293.
- [346] H. Kroemer, *RCA Rev.* **1957**, *18*, 332.
- [347] F. Capasso, *Science* **1987**, *235*, 172.
- [348] N. H. Karam, C. M. Fetzer, X.-Q. Liu, M. A. Steiner, K. L. Schulte, in *Metalorganic Vapor Phase Epitaxy (MOVPE): Growth, Materials Properties, and Applications* (Eds: S. Irvine, P. Capper), John Wiley & Sons, Hoboken, NJ **2020**.

- [349] J. F. Geisz, M. A. Steiner, N. Jain, K. L. Schulte, R. M. France, W. E. McMahon, E. E. Perl, D. J. Friedman, *IEEE J. Photovoltaics* **2018**, *8*, 626.
- [350] L. Esaki, *IEEE Trans. Electron Devices* **1976**, *23*, 644.
- [351] M. A. Zare Pour, O. Romanyuk, D. C. Moritz, A. Paszuk, C. Maheu, S. Shekarabi, K. D. Hanke, D. Ostheimer, T. Mayer, J. P. Hofmann, W. Jaegermann, T. Hannappel, *Surf. Interfaces* **2022**, *34*, 102384.
- [352] B. Erol Sağol, U. Seidel, N. Szabó, K. Schwarzburg, T. Hannappel, *Chimia* **2007**, *61*, 775.
- [353] M. A. Green, E. D. Dunlop, G. Siefert, M. Yoshita, N. Kopidakis, K. Bothe, X. Hao, *Prog. Photovoltaics* **2023**, *31*, 3.
- [354] H. Kroemer, *Surf. Sci.* **1983**, *132*, 543.
- [355] B. Vermang, H. Coverde, A. Lorenz, A. Uruena, G. Vereecke, J. Meersschaut, E. Cornagliotti, A. Rothschild, J. John, J. Poortmans, R. Mertens, in *37th IEEE Photovoltaic Specialists Conf.*, Vol. 6, New York, NY, June **2011**.
- [356] M. Yamaguchi, in *Post-Transition Metals* (Eds: M. Muzibur Rahman, A.M. Asiri, T.A. Tabbakh, A. Khan, Inamuddin), Intechopen, London, UK **2020**, Ch. 7.
- [357] U. W. Peter Würfel, *Physics of Solar Cells: From Basic Principles to Advanced Concepts*, John Wiley & Sons, Germany **2016**.
- [358] O. Maßmeyer, J. Haust, T. Hepp, R. Günkel, J. Glowatzki, C. Von Hänisch, W. Stolz, K. Volz, *ACS Omega* **2021**, *6*, 28229.
- [359] O. Supplie, M. M. May, S. Brückner, N. Brezhneva, T. Hannappel, E. V. Skorb, *Adv. Mater. Interfaces* **2017**, *4*, 1601118.
- [360] B. Kunert, K. Volz, in *Metalorganic Vapor Phase Epitaxy (MOVPE): Growth, Materials Properties, and Applications* (Eds: S. Irvine, P. Capper), John Wiley & Sons, London, UK **2019**.
- [361] L. Ostheim, P. J. Klar, S. Liebich, P. Ludewig, K. Volz, W. Stolz, *Semicond. Sci. Technol.* **2016**, *31*, 07LT01.
- [362] O. Supplie, M. M. May, H. Stange, C. Höhn, H. J. Lewerenz, T. Hannappel, *J. Appl. Phys.* **2014**, *115*, 113509.
- [363] D. C. Moritz, W. Calvet, M. A. Zare Pour, A. Paszuk, T. Mayer, T. Hannappel, J. P. Hofmann, W. Jaegermann, *Encycl. Solid-Liq. Interfaces* **2024**, *3*, 93.
- [364] Z. Luo, T. Wang, J. Gong, *Chem. Soc. Rev.* **2019**, *48*, 2158.
- [365] R. Fan, Z. Mi, M. Shen, *Opt. Express* **2019**, *27*, A51.
- [366] C. Cheng, W. Zhang, X. Chen, S. Peng, Y. Li, *Energy Sci Eng* **2022**, *10*, 1526.
- [367] B. Rech, O. Kluth, T. Repmann, T. Roschek, J. Springer, J. M. Uller, F. Finger, H. Stiebig, H. Wagner, *Sol. Energy Mater. Sol. Cells* **2002**, *74*, 439.
- [368] K. Elkhamisy, H. Abdelhamid, E. S. M. El-Rabaie, N. Abdel-Salam, *Plasmonics* **2023**, *18*, 1.
- [369] M. Sui, Y. Chu, R. Zhang, in *J. Phys.: Conf. Ser.*, Vol. 1907, IOP Science, München, Germany, May **2021**, Ch. 1.
- [370] H. C. Fu, P. Varadhan, C. H. Lin, J. H. He, *Nat. Commun.* **2020**, *11*, 3930.
- [371] J. H. Kim, D. Hansora, P. Sharma, J. W. Jang, J. S. Lee, *Chem. Soc. Rev.* **2019**, *48*, 1908.
- [372] W. J. Lee, P. S. Shinde, G. H. Go, E. Ramasamy, *Int. J. Hydrogen Energy* **2011**, *36*, 5262.
- [373] J. Brilllet, J. H. Yum, M. Cornuz, T. Hisatomi, R. Solarska, J. Augustynski, M. Graetzel, K. Sivula, *Nat. Photonics* **2012**, *6*, 824.
- [374] D. A. Grave, D. S. Ellis, Y. Piekner, M. Kölbach, H. Dotan, A. Kay, P. Schnell, R. van de Krol, F. F. Abdi, D. Friedrich, A. Rothschild, *Nat. Mater.* **2021**, *20*, 833.
- [375] A. Kudo, K. Ueda, H. Kato, I. Mikami, *Catal. Lett.* **1998**, *53*, 229.
- [376] J. Luo, L. Steier, M. K. Son, M. Schreier, M. T. Mayer, M. Grätzel, *Nano Lett.* **2016**, *16*, 1848.
- [377] A. Paracchino, V. Laporte, K. Sivula, M. Grätzel, E. Thimsen, *Nat. Mater.* **2011**, *10*, 456.
- [378] P. Borno, F. F. Abdi, S. D. Tilley, B. Dam, R. van de Krol, M. Graetzel, K. Sivula, *J. Phys. Chem. C* **2014**, *118*, 16959.
- [379] A. Song, P. Plate, A. Chemseddine, F. Wang, F. F. Abdi, M. Wollgarten, R. van de Krol, S. P. Berglund, *J. Mater. Chem. A* **2019**, *7*, 9183.
- [380] A. Song, P. Bogdanoff, A. Esau, I. Y. Ahmet, I. Levine, T. Dittrich, T. Unold, R. van de Krol, S. P. Berglund, *ACS Appl. Mater. Interfaces* **2020**, *12*, 13959.
- [381] M. T. Mayer, C. Du, D. Wang, *J. Am. Chem. Soc.* **2012**, *134*, 12406.
- [382] I. Y. Ahmet, S. Berglund, A. Chemseddine, P. Bogdanoff, R. F. Präg, F. F. Abdi, R. van de Krol, *Adv. Energy Sustainability Res.* **2020**, *1*, 2000037.
- [383] F. F. Abdi, D. E. Starr, I. Y. Ahmet, R. van de Krol, *Chempluschem* **2018**, *83*, 941.
- [384] I. Y. Ahmet, Y. Ma, J. W. Jang, T. Henschel, B. Stannowski, T. Lopes, A. Vilanova, A. Mendes, F. F. Abdi, R. van de Krol, *Sustainable Energy Fuels* **2019**, *3*, 2366.
- [385] A. G. Scheuermann, J. P. Lawrence, K. W. Kemp, T. Ito, A. Walsh, C. E. D. Chidsey, P. K. Hurley, P. C. McIntyre, *Nat. Mater.* **2016**, *15*, 99.
- [386] S. Klejna, T. Mazur, E. Wlazlak, P. Zawal, H. Sen Soo, K. Szaciowski, *Coord. Chem. Rev.* **2020**, *415*, 213316.
- [387] G. F. Samu, C. Janáky, *J. Am. Chem. Soc.* **2020**, *142*, 21595.
- [388] G. Yang, W. Yang, H. Gu, Y. Fu, B. Wang, H. Cai, J. Xia, N. Zhang, C. Liang, G. Xing, S. Yang, Y. Chen, W. Huang, *Adv. Mater.* **2023**, *35*, 2300383.
- [389] R. Lin, Y. Wang, Q. Lu, B. Tang, J. Li, H. Gao, Y. Gao, H. Li, C. Ding, J. Wen, P. Wu, C. Liu, S. Zhao, K. Xiao, Z. Liu, C. Ma, Y. Deng, L. Li, F. Fan, H. Tan, *Nature* **2023**, *620*, 994.
- [390] Z. Song, C. Li, L. Chen, K. Dolia, S. Fu, N. Sun, Y. Li, K. Wyatt, J. L. Young, T. G. Deutsch, Y. Yan, *ACS Energy Lett.* **2023**, *8*, 2611.
- [391] V. Andrei, G. M. Ucoski, C. Pornrungraj, C. Uswachoke, Q. Wang, D. S. Achilleos, H. Kasap, K. P. Sokol, R. A. Jagt, H. Lu, T. Lawson, A. Wagner, S. D. Pike, D. S. Wright, R. L. Z. Hoyer, J. L. MacManus-Driscoll, H. J. Joyce, R. H. Friend, E. Reisman, *Nature* **2022**, *608*, 518.
- [392] J. Li, J. Dagar, O. Shargaieva, O. Maus, M. Remec, Q. Emery, M. Khenkin, C. Ulbrich, F. Akhundova, J. A. Márquez, T. Unold, M. Fenske, C. Schultz, B. Stegemann, A. Al-Ashouri, S. Albrecht, A. T. Esteves, L. Korte, H. Köbler, A. Abate, D. M. Többsen, I. Zizak, E. J. W. List-Kratochvil, R. Schlattmann, E. Unger, *Adv. Energy Mater.* **2023**, *13*, 2203898.
- [393] J. Park, J. Lee, H. Lee, H. Im, S. Moon, C. S. Jeong, W. Yang, J. Moon, *Small* **2023**, *19*, 2300174.
- [394] L. Romani, L. Malavasi, *ACS Omega* **2020**, *5*, 25511.
- [395] S. Pan, J. Li, Z. Wen, R. Lu, Q. Zhang, H. Jin, L. Zhang, Y. Chen, S. Wang, *Adv. Energy Mater.* **2022**, *12*, 2004002.
- [396] S. Chen, H. Yin, P. Liu, Y. Wang, H. Zhao, *Adv. Mater.* **2023**, *35*, 2203836.
- [397] K. M. Kennedy, P. A. Kempler, M. Cabán-Acevedo, K. M. Papadantonakis, N. S. Lewis, *Nano Lett.* **2021**, *21*, 1056.
- [398] S. Hu, C. Y. Chi, K. T. Fontaine, M. Yao, H. A. Atwater, P. D. Dapkus, N. S. Lewis, C. Zhou, *Energy Environ. Sci.* **2013**, *6*, 1879.
- [399] A. Standing, S. Assali, L. Gao, M. A. Verheijen, D. Van Dam, Y. Cui, P. H. L. Notten, J. E. M. Haverkort, E. P. A. M. Bakkers, *Nat. Commun.* **2015**, *6*, 7824.
- [400] D. Van Dam, N. J. J. Van Hoof, Y. Cui, P. J. Van Veldhoven, E. P. A. M. Bakkers, J. Gómez Rivas, J. E. M. Haverkort, *ACS Nano* **2016**, *10*, 11414.
- [401] I. Aberg, G. Vescovi, D. Asoli, U. Naseem, J. P. Gilboy, C. Sundvall, A. Dahlgren, K. E. Svensson, N. Anttu, M. T. Bjork, L. Samuelson, *IEEE J. Photovoltaics* **2016**, *6*, 185.

- [402] A. Fitch, N. C. Strandwitz, B. S. Brunshwig, N. S. Lewis, *J. Phys. Chem. C* **2013**, *117*, 2008.
- [403] C. Gutsche, A. Lysov, D. Braam, I. Regolin, G. Keller, Z. A. Li, M. Geller, M. Spasova, W. Prost, F. J. Tegude, *Adv. Funct. Mater.* **2012**, *22*, 929.
- [404] M. D. Kelzenberg, D. B. Turner-Evans, B. M. Kayes, M. A. Filier, M. C. Putnam, N. S. Lewis, H. A. Atwater, *Nano Lett.* **2008**, *8*, 710.
- [405] K. Jansson, E. Lind, L. E. Wernersson, *IEEE Trans. Electron Devices* **2012**, *59*, 2375.
- [406] M. Mandl, X. Wang, T. Schimpke, C. Kölper, M. Binder, J. Ledig, A. Waag, X. Kong, A. Trampert, F. Bertram, J. Christen, F. Barbagini, E. Calleja, M. Strassburg, *Phys. Status Solidi RRL* **2013**, *7*, 800.
- [407] D. Saxena, S. Mokkapatil, P. Parkinson, N. Jiang, Q. Gao, H. H. Tan, C. Jagadish, *Nat. Photonics* **2013**, *7*, 963.
- [408] G. Koblmüller, B. Mayer, T. Stettner, G. Abstreiter, J. J. Finley, *Semicond. Sci. Technol.* **2017**, *32*, 053001.
- [409] B. Mayer, D. Rudolph, J. Schnell, S. Morkötter, J. Winnerl, J. Treu, K. Müller, G. Bracher, G. Abstreiter, G. Koblmüller, J. J. Finley, *Nat. Commun.* **2013**, *4*, 2931.
- [410] S. W. Eaton, A. Fu, A. B. Wong, C. Z. Ning, P. Yang, *Nat. Rev. Mater.* **2016**, *6*, 1.
- [411] J. Koch, L. Liborius, P. Kleinschmidt, N. Weimann, W. Prost, T. Hannappel, *Adv. Mater. Interfaces* **2022**, *9*, 2200948.
- [412] L. Liborius, F. Heyer, K. Arzi, C. Speich, W. Prost, F. J. Tegude, N. Weimann, A. Poloczek, *Phys. Status Solidi A* **2019**, *216*, 1800562.
- [413] M. Steidl, C. Koppka, L. Winterfeld, K. Peh, B. Galiana, O. Supplie, P. Kleinschmidt, E. Runge, T. Hannappel, *ACS Nano* **2017**, *11*, 8679.
- [414] S. Korte, M. Steidl, W. Prost, V. Cherepanov, B. Voigtländer, W. Zhao, P. Kleinschmidt, T. Hannappel, *Appl. Phys. Lett.* **2013**, *103*, 143104.
- [415] Y. Cui, J. Wang, S. R. Plissard, A. Cavalli, T. T. Vu, R. P. J. Van Veldhoven, L. Gao, M. Trainor, M. A. Verheijen, J. E. M. Haverkort, E. P. A. M. Bakkers, *Nano Lett.* **2013**, *13*, 4113.
- [416] A. C. Farrell, P. Senanayake, X. Meng, N. Y. Hsieh, D. L. Huffaker, *Nano Lett.* **2017**, *17*, 2420.
- [417] S. Mokkapatil, C. Jagadish, *Opt. Express* **2016**, *24*, 17345.
- [418] Y. Zeng, Q. Ye, W. Shen, *Sci. Rep.* **2014**, *4*, 4915.
- [419] R. R. Lapierre, A. C. E. Chia, S. J. Gibson, C. M. Haapamaki, J. Boulanger, R. Yee, P. Kuyanov, J. Zhang, N. Tajik, N. Jewell, K. M. A. Rahman, *Phys. Status Solidi* **2013**, *7*, 815.
- [420] M. Green, E. Dunlop, J. Hohl-Ebinger, M. Yoshita, N. Kopydakis, X. Hao, *Prog. Photovoltaics* **2021**, *29*, 3.
- [421] F. Li, M. Oliva-Ramirez, D. Wang, P. Schaaf, *Mater. Des.* **2021**, *209*, 109956.
- [422] M. Wu, L. Wen, Y. Lei, S. Ostendorp, K. Chen, G. Wilde, *Small* **2010**, *6*, 695.
- [423] T. Hannappel, S. Visbeck, L. Töben, F. Willig, *Rev. Sci. Instrum.* **2004**, *75*, 1297.
- [424] P. Raizada, V. Soni, A. Kumar, P. Singh, A. A. Parwaz Khan, A. M. Asiri, V. K. Thakur, V. H. Nguyen, *J. Materiomics* **2021**, *7*, 388.
- [425] H. Wang, X. Cheng, T. Kups, S. Sun, G. Chen, D. Wang, P. Schaaf, *Energy Technol.* **2022**, *10*, 2200085.
- [426] H. Rox, A. Bashkatov, X. Yang, S. Loos, F. Dynamics, *Int. J. Hydrogen Energy* **2023**, *48*, 2892.
- [427] C. Dreßler, G. Kabbe, D. Sebastiani, *J. Phys. Chem. C* **2016**, *120*, 19913.
- [428] C. Dreßler, G. Kabbe, M. Brehm, D. Sebastiani, *J. Chem. Phys.* **2020**, *152*, 114114.
- [429] C. Dreßler, G. Kabbe, M. Brehm, D. Sebastiani, *J. Chem. Phys.* **2020**, *152*, 164110.
- [430] G. Kabbe, C. Dreßler, D. Sebastiani, *J. Phys. Chem. C* **2016**, *120*, 19905.
- [431] G. Kabbe, C. Dreßler, D. Sebastiani, *Phys. Chem. Chem. Phys.* **2017**, *19*, 28604.
- [432] D. Schrijvers, A. Hool, G. A. Blengini, W. Q. Chen, J. Dewulf, R. Eggert, L. van Ellen, R. Gauss, J. Goddin, K. Habib, C. Hagelüken, A. Hirohata, M. Hofmann-Amttenbrink, J. Kosmol, M. Le Gleuher, M. Grohol, A. Ku, M. H. Lee, G. Liu, K. Nansai, P. Nuss, D. Peck, A. Reller, G. Sonnemann, L. Tercero, A. Thorenz, P. A. Wäger, *Resour. Conserv. Recycl.* **2020**, *155*, 104617.
- [433] W. Shockley, H. J. Queisser, *Renewable Energy*, Routledge, London **2018**, Ch.4.
- [434] X. Liu, Y. Feng, H. Cui, F. Liu, X. Hao, G. Conibeer, D. B. Mitzi, M. Green, *Prog. Photovoltaics* **2016**, *24*, 879.
- [435] R. Scheer, H.-W. Schock, *Chalcogenide Photovoltaics Physics, Technologies, and Thin Film Devices*, John Wiley & Sons, Berlin, Germany **2011**.
- [436] S. Li, J. Morasch, A. Klein, C. Chirila, L. Pintilie, L. Jia, K. Ellmer, M. Naderer, K. Reichmann, M. Gröting, K. Albe, *Phys. Rev. B* **2013**, *88*, 045428.
- [437] C. Lohaus, J. Morasch, J. Brötz, A. Klein, W. Jaegermann, *J. Phys. D: Appl. Phys.* **2016**, *49*, 155306.
- [438] J. Morasch, *PhD Thesis*, Technische Universität Darmstadt **2017**, p. 9.
- [439] T. Reier, Z. Pawolek, S. Cherevko, M. Bruns, T. Jones, D. Teschner, S. Selve, A. Bergmann, H. N. Nong, R. Schlögl, K. J. J. Mayrhofer, P. Strasser, *J. Am. Chem. Soc.* **2015**, *137*, 13031.
- [440] H. N. Nong, H. P. Tran, C. Spöri, M. Klingenhof, L. Frevel, T. E. Jones, T. Cottre, B. Kaiser, W. Jaegermann, R. Schlögl, D. Teschner, P. Strasser, *Z. Phys. Chem.* **2020**, *234*, 787.
- [441] T. Reier, H. N. Nong, D. Teschner, R. Schlögl, P. Strasser, *Adv. Energy Mater.* **2017**, *7*, 1601275.
- [442] L. Wang, F. Dionigi, N. T. Nguyen, R. Kirchgeorg, M. Gliech, S. Grigorescu, P. Strasser, P. Schmuki, *Chem. Mater.* **2015**, *27*, 2360.
- [443] M. Bernicke, D. Bernsmeier, B. Paul, R. Schmack, A. Bergmann, P. Strasser, E. Ortel, R. Kraehnert, *J. Catal.* **2019**, *376*, 209.
- [444] H. N. Nong, T. Reier, H. S. Oh, M. Gliech, P. Paciok, T. H. T. Vu, D. Teschner, M. Heggen, V. Petkov, R. Schlögl, T. Jones, P. Strasser, *Nat. Catal.* **2018**, *1*, 841.
- [445] W. H. Cheng, M. H. Richter, R. Müller, M. Kelzenberg, S. Yalamanchili, P. R. Jähelka, A. N. Perry, P. C. Wu, R. Saive, F. Dimroth, B. S. Brunshwig, T. Hannappel, H. A. Atwater, *Adv. Energy Mater.* **2022**, *12*, 2201062.
- [446] P. T. Anastas, J. B. Zimmerman, *Environ. Sci. Technol.* **2003**, *37*, 94A.
- [447] K. W. A. Chee, B. K. Ghosh, I. Saad, Y. Hong, Q. H. Xia, P. Gao, J. Ye, Z. J. Ding, *Nano Energy* **2022**, *95*, 106899.
- [448] A. Hajduk, M. Amin, Z. Pour, A. Paszuk, M. Guidat, M. Löw, F. Ullmann, D. C. Moritz, J. P. Hofmann, S. Krischok, E. Runge, W. G. Schmidt, W. Jaegermann, M. M. May, T. Hannappel, *Encycl. Solid-Liq. Interfaces* **2023**, *3*, 120.
- [449] F. Urbain, PhD Thesis, Lehrstuhl Für Photovoltaik (FZ Jülich), Jülich, **2016**.
- [450] G. B. Haxe, S. Boore, S. Mayfiel, https://en.wikipedia.org/wiki/Abundance_of_the_chemical_elements, (accessed: December 2023).



Thomas Hannappel is full professor, Head of the department “Fundamentals of Energy Materials,” and Dean of the master’s course “Renewable Energy Techniques” at the Institute of Physics, Technische Universität Ilmenau. He received his Ph.D. with studies on photoinduced charge carrier dynamics performed in Professor Gerhard Ertl’s Department “Physical Chemistry” at the Fritz-Haber-Institute Berlin. He established original analysis of semiconductor growth processes to scrutinize high-performance optoelectronic materials and complex physicochemical interfacial reactions for the development of highly efficient device structures achieving world record values for the conversion efficiency of solar cells and solar fuels production.



Sahar Shekarabi is a physics Ph.D. student in Professor Hannappel’s research group at TU Ilmenau, Germany. She holds a master’s degree in catalytic chemistry with a specialization in electrochemical water splitting. Her focus lies in the exploration of critical solid–solid and solid–liquid heterointerfaces that exist between the photoabsorber and the electrolyte or passivation layers. Through her investigations, she aims to study the impact of these heterointerfaces on electronic structures using spectroscopy methods in the context of photoelectrochemical water splitting.



Wolfram Jaegermann, born 1954, is a retired full professor of surface science at TU Darmstadt. His main research fields are surface science and thin-film synthesis of photovoltaic and (photo) electrochemical converters, intercalation batteries, and inorganic/organic composites. He was initiator, coordinator, and speaker of the Excellency Graduate School “Energy Science and Engineering” and of the DFG priority programme “Solar H2” and was the scientific coordinator of many energy-related collaborative research projects including EC doctoral schools. He was Dean of the Materials Science Department and coinitiator and Vice Dean of the new master degree course of Energy Science at TU Darmstadt.



Erich Runge is a broadly interested German solid-state theorist whose career path led him from fundamental questions of time-dependent density functional theory (Frankfurt University) via electronically highly correlated heavy-fermion metals (MPI FKF, Stuttgart) and nonequilibrium transport (Harvard University, Cambridge, Mass.) to optical properties of disordered systems (Humboldt University, Berlin) and geometrically frustrated systems (MPI PKS, Dresden) to energy science and ultrafast optics at the TU Ilmenau as head of the department “Theoretical Physics I.” He served in several boards of the German Physical Society DPG, the European Physical Society EPS, the Thuringian State Science Conference, and the German Research Foundation DFG.



Jan Philipp Hofmann has been a chemist and full professor of surface science at the Technical University of Darmstadt, Germany, since 2020. He received his academic education and Dr. rer. nat. from Justus-Liebig-University Giessen, Germany, followed by a postdoctoral stay at the Debye Institute of Nanomaterials Science at Utrecht University, The Netherlands. Between 2013 and 2020, he has been an assistant professor for solar fuel catalysis and inorganic materials chemistry at Eindhoven University of Technology, The Netherlands. His current research focuses on the investigation of interface chemistry, energetics and dynamics of renewable energy conversion and storage devices and materials using surface science and in situ/operando approaches.



Roel van de Krol is Head of the Institute for Solar Fuels at the Helmholtz-Zentrum Berlin (HZB) and full professor at the Chemistry Department of TU Berlin. His group focuses on the development of materials and devices for the photoelectrochemical conversion of sunlight into chemical fuels. This includes the development of deposition processes for thin-film photoelectrodes and catalysts and scale-up of solar fuel devices up to 100 cm. The group specializes in metal oxides and aims to understand charge generation, separation, and transfer processes in the bulk and at solid/liquid interfaces using advanced spectroscopy methods.



Matthias M. May studied physics in Stuttgart, Grenoble, and Berlin, with a focus on condensed matter and computational physics. His Ph.D. studies at Humboldt-Universität zu Berlin and Helmholtz-Zentrum Berlin targeted III–V semiconductors for solar water splitting. He spent two years as a postdoctoral fellow at the Chemistry Department of the University of Cambridge, funded by the German Academy of Sciences Leopoldina. He leads an Emmy-Noether group at the Institute of Physical and Theoretical Chemistry at Tübingen University. His scientific interests lie in the area of photoelectrochemical energy conversion and solid–liquid interfaces.



Agnieszka Paszuk is postdoc at the department “Fundamentals of Energy Materials” at the Technische Universität Ilmenau, Germany. She received her master’s degree at Wrocław University of Science and Technology in Poland and joined Professor’s Hannappel group in 2012. In 2017, she obtained her Ph.D. in experimental physics for work on “controlling Si(111) and Si(100) surfaces for subsequent GaP heteroepitaxy in CVD ambient.” Her research focuses on solar energy conversion, heteroepitaxy targeting growth control at the atomic scale, and surface science, which includes characterization of surfaces and (buried)heterointerfaces by optical in situ spectroscopy combined with UHV-based surface analysis techniques.



Franziska Hess earned her doctoral degree in 2015 from Justus-Liebig University Giessen, Germany, specializing in computational modeling of surface science and catalysis by Kinetic Monte Carlo Simulations. Following her doctoral studies, she conducted postdoctoral research at the Massachusetts Institute of Technology and RWTH Aachen, where she explored near-surface defect chemistry in solid oxide fuel cell cathodes. She established her own research group as an assistant professor at Technical University Berlin. Her current focus revolves around gaining a deeper understanding of catalyst degradation under operating conditions and developing computational models for efficiently screening large materials databases for stability.